Epigenetic and neurodevelopmental consequences of early life experience

Joshua Scott Danoff
Reisterstown, MD

B.A., University of Virginia, 2017

A Dissertation Presented to the Faculty of the University of Virginia in Candidacy for the Degree of Doctor of Philosophy

Department of Psychology
University of Virginia
May, 2023

Jessica J. Connelly, Ph.D.
Alev Erisir, Ph.D.
Joseph P. Allen, Ph.D.
Christopher D. Deppmann, Ph.D.
Ukpong B. Eyo, Ph.D.

Abstract

Individual development is influenced by both genetic processes and environmental factors, which interact throughout the lifespan. In mammals, early life parental care is particularly important in setting up developmental trajectories with long lasting consequences for physiology and behavior. In humans, early life stress which is often in the form of reduced parental care is associated with accelerated developmental outcomes and increased risk of mood disorders later in life. Research on neurobiological mechanisms mediating the impacts of early life parental care on these outcomes is generally completed in mice and rats, species which typically only provide maternal care in laboratory settings. Prairie voles are a laboratory rodent species which serve as a model of human-like social behaviors: they form monogamous pair bonds, and critically, both mothers and fathers provide parental care to the pups. In prairie voles and other rodents, animals raised with higher parental care are more social later in life. Prairie voles raised with high parental care are display more alloparental behavior as juveniles and have increased propensity to form a pair bond and provide high parental care to their own pups as adults.

One well studied mechanism which partially mediates the effects of early life parental care on social behavior later in life is the oxytocin system. Oxytocin is a neuropeptide hormone which regulates social behavior throughout the lifespan. Oxytocin acts primarily by binding to its one known receptor, the oxytocin receptor. In voles, the distribution of the oxytocin receptors in the brain differentiates between monogamous and non-monogamous species, and within prairie voles, the amount of oxytocin receptors in key brain regions is associated with species-typical social behaviors including pair bonding and parental care. While much work is done on the oxytocin system in prairie voles, many other neurobiological systems are involved in such complex behaviors.

This dissertation investigates how early life social experiences impact neurodevelopmental outcomes, in part by examining epigenetic regulation of gene expression. In Chapter 2, I examine how early life experience in the form of parental care impacts gene regulation of the oxytocin receptor. I examine two regions of the oxytocin receptor gene (*Oxtr*) promoter, a region termed MT2 and a region within exon 3. I find that while early nurture is associated with reduced DNA methylation in both MT2 and exon 3, only DNA methylation in MT2 is strongly associated with oxytocin receptor gene expression. Further, I identify a novel isoform of *Oxtr* which is under genetic control and is coregulated with the main transcript.

In Chapter 3, I use RNA-seq to identify genome-wide transcriptional changes associated with early nurture, which reveals differential gene expression in male offspring but not female offspring. I also examine neuroanatomical outcomes and find that in male offspring only, higher care by fathers leads to more excitatory synapses characterized by small-area terminals and shorter synaptic zones. I also find that in both sexes higher total parental care is associated with higher density of microglia. I then examine social behavior and find that male prairie voles raised with higher care by fathers is display more pup retrieval behavior as juveniles, while female offspring appear to display fewer pup retrievals. Finally, I show that high total parental care slows development, as indexed by epigenetic age.

In Chapter 4, I study the impact of adolescent social experiences on epigenetic age, a blood-derived metric for biological aging and healthspan, in humans. Using samples from the longitudinal KLIFF/VIDA study, I find that adolescents that experience peer struggles (i.e. lack of social connectedness, insecure attachments, etc.) have higher epigenetic age in midlife, indicating that positive social experiences are protective against biological aging and poor health outcomes. Further, the effect size of poor peer relationships on epigenetic age is comparable to that of lifetime history of cigarette smoking, suggesting that individual and public health outcomes are as highly influenced by social relationships as other environmental factors with known impacts on healthspan.

For my grandfathers, Stanley Silverstein and Jerome Danoff, two scientists in their own right who taught me the importance of education, hard work, and doing the right thing.

Acknowledgements

This dissertation would not have been possible without the vast amount of support I am lucky enough to have. I cannot express enough gratitude to my incredible mentor Jessica Connelly for allowing me to explore my ideas and pushing me to do rigorous and important science. I have benefitted from the help of all those in the Connelly Lab. A very special thank you goes to Allison Perkeybile, who generously took on the leg work of many of the projects in this dissertation and for the thoughtful discussions of these results. I also want to thank Alev Erisir for mentorship and assistance with all the neuroanatomy projects I've been involved in. Thank you to members of my committee for insightful discussions of my results: Joe Allen, Chris Deppmann, and Ukpong Eyo.

The projects in this dissertation focus on how early life experience impact development and health. With this in mind, I want to thank my parents Claudia and Michael Danoff for always providing me with everything I needed to excel. Thank you to all the alloparents in my life, including my sister Emma. Lastly, I want to thank my partner and best friend, Megan Carpenter, for the immense support she's given me throughout and for making me happy in even the most stressful times.

Table of Contents

Chapter 1: Introduction

Early life experience and psychosocial development

Early life experiences interact with an individual's genetic architecture to influence developmental processes and phenotypes. For example, early life stress can accelerate the onset of developmental markers including molar eruption[1] and puberty[2,3]. Early life stress also alters the developmental timing of neurological processes. Seminal work using fMRI showed that in typically developing children, there is a developmental shift in amygdala-prefrontal cortex functional connectivity[4]. However, this shift occurs earlier in children raised in institutions, suggesting accelerated development of this circuit[5]. Development of other circuits are also altered by extreme early life stress[6]. This change in the pace of development is thought to be adaptive at the time, but increases allostatic load later in life, leading to health problems and psychological distress[7] (though it should be noted that early life stress may also lead to "hidden talents")[8].

Though much research in early life experience in humans has focused on extreme early life stressors, more subtle variations in early life experience also impact psychosocial development. For example, both maternal and paternal warmth are associated with increased prosociality in preschool aged children[9], and both environmental stimulation and parental nurturance are associated with cognitive abilities in childhood[10]. Effects of early life experience last throughout the lifespan: kangaroo care, or increased skin-to-skin contact early in life, increases maternal-child behavioral synchrony from infancy through young adulthood[11]. These studies indicate that subtle variations in parental care impact offspring throughout the lifespan.

The oxytocin receptor as a candidate gene for studying the impacts of early life experience on the epigenome

The oxytocin system is critically involved in regulation of social behaviors throughout the lifespan[12]. Oxytocin is a neuropeptide hormone which acts both in the brain and periphery to regulate many psychological and physiological processes[13]. Oxytocin signaling is dependent on its binding to its one known receptor, the oxytocin receptor[14]. The oxytocin receptor is expressed in many brain regions associated with social behaviors[15]. The oxytocin system is sensitive to early life experience. Levels of oxytocin in blood plasma[16] and urine are reduced in adults who experience early life stressors[17]. However, peripheral concentrations of oxytocin may not reflect central oxytocin levels, particularly under basal conditions (i.e. no oxytocin administration or other paradigm such as acute stress)[18]. Additionally, measuring oxytocin peptide is challenging and interpretation may vary based on methodology used[19,20]. Further, because oxytocin must signal via its receptor the availability of the oxytocin receptor must be considered, though oxytocin receptor expression cannot be assayed from central tissues in living participants. For this reason, a biomarker of the oxytocin receptor may be the most reliable indicator of one's ability to access their endogenous oxytocin system.

Epigenetic modifications are chemical modifications to DNA and the histone proteins which package DNA into chromatin which modify gene expression. Epigenetic regulation of gene expression can be sensitive to the environment, particularly during periods of rapid development such as early life[21]. Work from our lab has shown that DNA methylation of the oxytocin receptor gene (*OXTR*) is sensitive to early life experience, related to gene expression, and correlated in blood and brain tissues[22]. In both humans and animal models, early life parental care leads to reduced DNA methylation at *OXTR*, which may be related to increased social behavior later on[23]. For example, our lab has shown that maternal engagement during infancy reduces *OXTR* methylation, which is related to infant temperament and the infant's brain response to emotional faces[24,25]. Thus, *OXTR* is a good candidate gene for examining how experience regulations the epigenome.

Prairie voles: a translational model of human social behaviors

Mechanistic understanding of how early life experience impacts social behaviors requires accessing brain tissue throughout development, which is not possible in human studies. Rodents have long been used to study neurobiology, and much of what is known about the neurobiology of maternal behavior is from studies completed in mice and rats. Early studies in rats and mice also led to discoveries about how early maternal care influences physical and psychosocial development[26,27]. However, mice and rats do not fully model human caregiving as they are not biparental; that is, only mothers provide care to pups in these species. Paternal care is only robustly present in socially monogamous species, comprising 3-5% of all mammalian species[28,29]. Studying the effects of early life experience in a biparental species allows for higher variability in early life experiences. Prairie voles are well suited for these studies since they are a socially monogamous, biparental species with much literature supporting the role of oxytocin in mediating affiliative and parental behaviors[30]. Further, their genome is sequenced and reasonably well annotated, allowing for transcriptomic studies. Studies in prairie voles have made use of RNA-sequencing techniques to understand gene regulation of monogamous pair bonds[31,32].

There is abundant literature studying the impact of early life experience in prairie voles. A study of natural parenting behaviors found that high contact care is associated with slower development and more social behavior as juveniles[33]. Manipulations of early life parental behaviors support this result, though specific behavioral alterations may be dependent on the kind of manipulation. Studies using a handling paradigm, which increases parental behavior, find a sex-specific effect on behavioral outcomes. Males raised in the high-care (handled) condition display more alloparenting behavior (parental behavior towards a novel infant pup) than males raised in the low care condition while there is no difference in female offspring[34,35]. However, female offspring raised in the high-care condition had a higher propensity to form a pair bond than those raised in the low care condition, while there was no difference among parenting conditions in male offspring[34].

Other studies have used a different manipulation: removing fathers. This leads to a general reduction in care but also the loss of what may be a specific type of care. In one study with no other manipulation than removal of paternal care, female alloparental behavior was impacted: females raised in the single-mother condition displayed less alloparental behavior than females raised in the biparental condition, while there was no effect on male offspring[36]. However, there was no sex difference in the effect of parenting condition on pair bonding, where both male and female offspring raised in the single-mother condition displayed less propensity to form a pair bond[36]. A second study combined this manipulation with a foraging tradeoff condition where food was placed at the top of an incline, making it harder to retrieve. This study found that male offspring's social investigation behavior was sensitive to the foraging tradeoff condition (which led to reduced paternal huddling in the biparental-raised pups but did not impact duration of maternal huddling) such that males raised in the tradeoff condition spent less time investigating a novel conspecific[37]. A third study again used paternal deprivation but included a third group where the father was replaced with an older sister, who provided an equivalent duration of care[38]. This study found that while paternal deprivation reduces the propensity to form a pair bond in both male and female offspring, this deficit can be rescued in female offspring only by the presence of an older sister[38]. These studies indicate that there are sex-specific impacts of early life parental care on social behaviors later in life, and there may be a specific role for fathers in species-typical social development in male offspring. However, the role of natural variation in paternal behavior has not yet been studied, and while behavioral studies are abundant, few studies have investigated the underlying genetic and neurodevelopmental processes mediating the effects of early life biparental care on social behavior in this species beyond the role of oxytocin and the closely related neuropeptide vasopressin.

Specific Studies

This dissertation is comprised of three studies which will examine the developmental consequences of early life social experiences using three unique but complementary approaches. The first two studies will use prairie voles as a model system to understand how early life parental care impacts neurodevelopment underpinning social behaviors. The third study is a translational aim which examines how adolescent social experience impacts biological indicators of aging.

Chapter 2: Examine the impact of early nurture on epigenetic regulation of the oxytocin receptor gene. In this chapter, I show that early nurture 1) is associated with decreased DNA methylation across *Oxtr* which is related to increased expression of the canonical transcript and 2) is not associated with expression of a novel transcript, which is instead related to genetic variation in *Oxtr*. These results further establish prairie voles as an excellent model organism to examine epigenetic regulation of the oxytocin receptor and provide evidence that epigenetic processes observed in human peripheral tissue also occur in brain tissue.

Chapter 3: Explore transcriptomic, neurodevelopmental, and behavioral consequences of early nurture. In this chapter, I show that 1) epigenetic aging is decelerated by high care parenting, 2) early nurture is associated with widespread transcriptomic changes in male offspring but not female offspring, 3) genes upregulated in male offspring are related to glutamatergic circuitry, 4) parental care composition impacts excitatory synapse density in male offspring only, 5) total parental care is moderately associated with microglia density in both sexes, and 6) parental care composition has sex-specific impacts on pup retrieval behaviors. These results build on Chapter 2 by examining genome-wide gene regulation. The results of these studies dissociate the impact of two distinct features of parental care in prairie voles. Specifically, I find that higher total parental care is associated with both reduced epigenetic age and increase microglia cell density in both male and female offspring. Further, I find that more care by fathers is specifically associated with increased excitatory synapse density in male offspring only and has opposing effects on pup retrieval behavior in male and female offspring.

Chapter 4: Determine the impact of adolescent social experience on epigenetic age at midlife. In this chapter, I show that 1) adolescents that struggle with social integration have increased epigenetic age at midlife, and 2) impacts of adolescent social experience on epigenetic age are comparable to lifetime history of cigarette smoking. These results provide translational evidence that similar epigenetic aging processes to those described in Chapter 3 are present in humans as well, which has large individual and public health implications. Furthermore, these results, combined with epigenetic aging results in Chapter 3, indicate that prairie voles are a suitable model for examining physiological impacts of social behavior on aging.

Chapter 5: Discussion and Overall Significance. In this chapter, I synthesize results from each of the studies to develop an overarching interpretation of the impact of early life social experience on neurobehavioral and physiological outcomes throughout the lifespan.

References

1. McDermott, C. L. *et al.* Early life stress is associated with earlier emergence of permanent molars. *Proceedings of the National Academy of Sciences* **118**, e2105304118 (2021).
2. Webster, G. D., Graber, J. A., Gesselman, A. N., Crosier, B. S. & Schember, T. O. A Life History Theory of Father Absence and Menarche: A Meta-Analysis. *Evol Psychol* **12**, 147470491401200200 (2014).

3. Lei, M.-K., Beach, S. R. H. & Simons, R. L. Childhood trauma, pubertal timing, and cardiovascular risk in adulthood. *Health Psychology* **37**, 613–617 (2018).
4. Gee, D. G. *et al.* A developmental shift from positive to negative connectivity in human amygdala-prefrontal circuitry. *Journal of Neuroscience* **33**, 4584–4593 (2013).
5. Gee, D. G. *et al.* Early developmental emergence of human amygdala-prefrontal connectivity after maternal deprivation. *Proceedings of the National Academy of Sciences of the United States of America* **110**, 15638–15643 (2013).
6. Smith, K. E. & Pollak, S. D. Early life stress and development: potential mechanisms for adverse outcomes. *Journal of Neurodevelopmental Disorders* **12**, 34 (2020).
7. McEwen, B. S. Stress, Adaptation, and Disease: Allostasis and Allostatic Load. *Annals of the New York Academy of Sciences* **840**, 33–44 (1998).
8. Ellis, B. J. *et al.* Hidden talents in harsh environments. *Development and Psychopathology* **34**, 95–113 (2022).
9. Daniel, E., Madigan, S. & Jenkins, J. Paternal and maternal warmth and the development of prosociality among preschoolers. *Journal of Family Psychology* **30**, 114–124 (2016).
10. Farah, M. J. *et al.* Environmental stimulation, parental nurturance and cognitive development in humans. *Developmental Science* **11**, 793–801 (2008).
11. Ulmer Yaniv, A. *et al.* Synchronous caregiving from birth to adulthood tunes humans' social brain. *Proceedings of the National Academy of Sciences* **118**, e2012900118 (2021).
12. Lee, H. J., Macbeth, A. H., Pagani, J. H. & Scott Young, W. Oxytocin: The great facilitator of life. *Progress in Neurobiology* (2009) doi:10.1016/j.pneurobio.2009.04.001.
13. Carter, C. S. *et al.* Is Oxytocin "Nature's Medicine"? *Pharmacological Reviews* **72**, 829–861 (2020).
14. Jurek, B. & Neumann, I. D. The Oxytocin Receptor: From Intracellular Signaling to Behavior. *Physiological Reviews* **98**, 1805–1908 (2018).
15. Quintana, D. S. *et al.* Oxytocin pathway gene networks in the human brain. *Nature Communications* **10**, (2019).
16. Opacka-Juffry, J. & Mohiyeddini, C. Experience of stress in childhood negatively correlates with plasma oxytocin concentration in adult men. *Stress* **15**, 1–10 (2012).
17. Fries, A. B. W., Ziegler, T. E., Kurian, J. R., Jacoris, S. & Pollak, S. D. Early experience in humans is associated with changes in neuropeptides critical for regulating social behavior. *Proceedings of the National Academy of Sciences* **102**, 17237–17240 (2005).
18. Valstad, M. *et al.* The correlation between central and peripheral oxytocin concentrations: A systematic review and meta-analysis. *Neuroscience and Biobehavioral Reviews* **78**, 117–124 (2017).
19. MacLean, E. L. *et al.* Challenges for measuring oxytocin: The blind men and the elephant? *Psychoneuroendocrinology* **107**, 225–231 (2019).
20. Gnanadesikan, G. E., Hammock, E. A. D., Tecot, S. R., Carter, C. S. & MacLean, E. L. Specificity of plasma oxytocin immunoassays: A comparison of commercial assays and sample preparation techniques using oxytocin knockout and wildtype mice. *Psychoneuroendocrinology* **132**, 105368 (2021).
21. Kundakovic, M. & Champagne, F. A. Early-life experience, Epigenetics, and the developing brain. *Neuropsychopharmacology* (2015) doi:10.1038/npp.2014.140.
22. Perkeybile, A. M. *et al.* Early nurture epigenetically tunes the oxytocin receptor. *Psychoneuroendocrinology* **99**, 128–136 (2019).
23. Danoff, J. S., Connelly, J. J., Morris, J. P. & Perkeybile, A. M. An epigenetic rheostat of experience: DNA methylation of OXTR as a mechanism of early life allostasis. *Comprehensive Psychoneuroendocrinology* **8**, 100098 (2021).
24. Krol, K. M., Moulder, R. G., Lillard, T. S., Grossmann, T. & Connelly, J. J. Epigenetic dynamics in infancy and the impact of maternal engagement. *Science Advances* **5**, (2019).

25. Krol, K. M., Puglia, M. H., Morris, J. P., Connelly, J. J. & Grossmann, T. Epigenetic modification of the oxytocin receptor gene is associated with emotion processing in the infant brain. *Developmental Cognitive Neuroscience* **37**, 100648 (2019).
26. Levine, S., Haltmeyer, G. C., Karas, G. G. & Denenberg, V. H. Physiological and behavioral effects of infantile stimulation. **2**, 55–59 (1967).
27. Francis, D., Diorio, J., Liu, D. & Meaney, M. J. Nongenomic transmission across generations of maternal behavior and stress responses in the rat. *Science* **286**, 1155–1158 (1999).
28. Kleiman, D. G. Monogamy in mammals. *The Quarterly review of biology* (1977) doi:10.1086/409721.
29. Lukas, D. & Clutton-Brock, T. H. The evolution of social monogamy in mammals. *Science* **341**, 526–530 (2013).
30. Tabbaa, M., Paedae, B., Liu, Y. & Wang, Z. Neuropeptide regulation of social attachment: The prairie vole model. *Comprehensive Physiology* **7**, 81–104 (2017).
31. Young, R. L. *et al.* Conserved transcriptomic profiles underpin monogamy across vertebrates. *Proceedings of the National Academy of Sciences* (2019) doi:10.1073/pnas.1813775116.
32. Duclot, F., Sailer, L., Koutakis, P., Wang, Z. & Kabbaj, M. Transcriptomic Regulations Underlying Pair-bond Formation and Maintenance in the Socially Monogamous Male and Female Prairie Vole. *Biol Psychiatry* **91**, 141–151 (2022).
33. Perkeybile, A. M., Griffin, L. L. & Bales, K. L. Natural variation in early parental care correlates with social behaviors in adolescent prairie voles (Microtus ochrogaster). *Frontiers in Behavioral Neuroscience* (2013) doi:10.3389/fnbeh.2013.00021.
34. Bales, K. L., Lewis-Reese, A. D., Pfeifer, L. A., Kramer, K. M. & Sue Carter, C. Early experience affects the traits of monogamy in a sexually dimorphic manner. *Developmental Psychobiology* **49**, 335–342 (2007).
35. Bales, K. L. *et al.* Are behavioral effects of early experience mediated by oxytocin? *Article* **2**, (2011).
36. Ahern, T. & Young, L. The impact of early life family structure on adult social attachment, alloparental behavior, and the neuropeptide systems regulating affiliative behaviors in the monogamous prairie vole (Microtus ochrogaster). *Frontiers in Behavioral Neuroscience* **3**, (2009).
37. Kelly, A. M., Ong, J. Y., Witmer, R. A. & Ophir, A. G. Paternal deprivation impairs social behavior putatively via epigenetic modification to lateral septum vasopressin receptor. *Science Advances* **6**, eabb9116 (2020).
38. Rogers, F. D. & Bales, K. L. Revisiting paternal absence: Female alloparental replacement of fathers recovers partner preference formation in female, but not male prairie voles (Microtus ochrogaster). *Developmental Psychobiology* **62**, 573–590 (2020).

Chapter 2: Determine the effect of early nurture on epigenetic regulation of *Oxtr* in prairie voles

This chapter is published in *Clinical Epigenetics*

Danoff, J.S., Wroblewski, K.L., Graves, A.J. *et al.* Genetic, epigenetic, and environmental factors controlling oxytocin receptor gene expression. *Clin Epigenet* **13**, 23 (2021). https://doi.org/10.1186/s13148-021-01017-5

Introduction

A major goal of translational neuroscience is to identify biomarkers of psychiatric disorders which can be used to inform diagnosis, predict possible courses of disease progression, or predict likelihood of response to a particular treatment[1]. A common target of efforts to identify biomarkers of psychiatric disorders is the oxytocin system[2]. The oxytocin system is an attractive target for biomarkers because of its involvement in many psychiatric disorders[3], modulation of a wide range of physiological processes[4], and potential use as medication via intranasal administration[5–7]. While many studies use serum oxytocin levels as a biomarker, proper collection and measurement of oxytocin is challenging, and interpretation may vary based on methodology[8].

Epigenetic modifications are promising biomarkers for disease since they are easily measured, variable in the population, and can be influenced by the environment[9]. A prominent epigenetic biomarker is DNA methylation, which is the addition of a methyl group to cytosine residues. DNA methylation typically occurs when cytosine is followed by guanine and generally leads to decreased gene expression[10]. One epigenetic biomarker for the oxytocin system is DNA methylation of the oxytocin receptor gene, *OXTR*. *OXTR* structurally consists of four exons and three introns in humans[11]. DNA methylation in MT2, a 405 bp region overlapping exon 1 and intron 1 of *OXTR*, regulates transcription both *in vivo* and *in vitro*[12]. *OXTR* is expressed throughout the human brain, with highest levels of expression in striatum, thalamus, and olfactory regions[13]. Reduced expression of *OXTR* has been documented in the superior temporal gyrus in autism[14] and in the posterior medial temporal cortex in schizophrenia[15]. Increased expression of *OXTR* was reported in the prefrontal cortex of patients with depression and bipolar disorder[16].

Dysregulation of *OXTR* expression in multiple psychopathologies has led many to study the epigenetic state of *OXTR* in both typical and clinical groups. These studies have generally focused on two regions of the *OXTR* gene: MT2 (covering much of exon 1 and some of intron 1) and exon 3. For example, dysregulated DNA methylation in MT2 has been associated with autism[14], callous-unemotional traits[17,18], anorexia nervosa[19,20], schizoaffective disorders[21,22], post-partum depression[23], attachment anxiety[24], obsessive compulsive disorder[25], and anxiety and depression[26]. DNA methylation in MT2 is associated with neural endophenotypes in typical populations: DNA methylation is positively correlated with brain activity during animacy perception[27], emotion perception[28,29], and social attention[30]. DNA methylation in exon 3 has also been associated with several psychopathologies, including anxiety and depression[26,31], social anxiety disorder[32], obsessive compulsive disorder[25,33], post-traumatic stress disorder[34], callous unemotional traits[17], and social communication deficits[35]. Despite the many studies connecting epigenetic markers at *OXTR* and psychological outcomes, several questions remain. Most studies measure DNA methylation in peripheral tissues such as blood or saliva, and the association between DNA methylation in these tissues and the brain is not established for all CpG sites. Furthermore, even if DNA methylation is measured in the brain, it is not yet known what the relative contributions of DNA methylation in the MT2 region and exon 3 region are in controlling *OXTR* expression.

In order to investigate epigenetic mechanisms controlling *OXTR* expression in the brain we use prairie voles as an animal model. Prairie voles are highly social rodents with characteristics resembling human social behavior including pair bonding and biparental care of

offspring[36]. We have previously shown that prairie voles are also a good model for studies of *OXTR*: the region of MT2 containing CpG sites -901, -924, and -934 is highly conserved in prairie voles and humans, but not in mice or rats[37]. We have also shown that DNA methylation in this region is malleable to early life experience, which ultimately leads to changes in gene expression in the juvenile period[37] and adulthood[38]. In this study, we clarify the genetic structure of *Oxtr* in prairie voles and compare the gene structure to human *OXTR*. We then investigate the relationships between DNA methylation in MT2, DNA methylation in exon 3, and *Oxtr* expression in the prairie vole brain. Finally, we describe novel findings related to prairie vole *Oxtr* including previously unidentified SNPs in exon 3 and a novel alternative transcript present in the nucleus accumbens.

Material and Methods

Human brain DNA and RNA samples

Genomic DNA and RNA isolated from the temporal cortex (BA 41/42) was obtained from the Maryland National Institute of Child Health and Human Development Brain Tissue Center and the Harvard Brain Tissue Resource Center (n= 11, male, 11-30yrs). Genomic DNA was analyzed for *OXTR* DNA methylation at CpG sites in the MT2 region of the promoter and gene expression was evaluated as previously described (Gregory *et al*., 2009).

Animal model

Subjects were laboratory-bred prairie voles (*Microtus ochrogaster*), descendants of a wild-caught stock captured near Champaign, Illinois. Breeding pairs were housed in large polycarbonate cages (44cm x 22cm x 16 cm) and same sex offspring pairs were housed in smaller polycarbonate cages (27cm x 16 cm x 16 cm) after weaning on postnatal day (PND) 20 (date of birth=PND0). Animals were given food (high-fiber Purina rabbit chow) and water *ad libitum*, cotton nestlets for nesting material in breeding cages, and were maintained on a 14:10 light:dark cycle. All procedures involved in generating tissue for the analysis of DNA methylation and gene expression following handling were reviewed and approved by the IACUC at the University of California, Davis.

Handling manipulation

Within 24 hours of giving birth, breeding pairs underwent a single handling manipulation as previously described[37,55]. Following this manipulation, parental care is heightened in the MAN1 group compared to the MAN0 group[37]. On PND24 offspring were anesthetized with isoflurane and euthanized via cervical dislocation and rapid decapitation for tissue collection. Brains were extracted and flash frozen in liquid nitrogen and stored at -80 °C. One male and one female from each litter were included in the analysis of *Oxtr* DNA methylation and *Oxtr* expression (MAN0: n= 7 per sex; MAN1: n= 6 per sex). An additional 5 sibling pairs were included in the EGA analysis in order to achieve adequate sample size such that the correlation matrix was full rank. These animals did not undergo MAN0 or MAN1 manipulations.

Sectioning of the nucleus accumbens

Whole brains were stored at -80 °C and equilibrated to -20°C for two hours prior to sectioning. Following sectioning, nucleus accumbens tissue was placed in a DNAse/RNAse free

microcentrifuge tube and flashed frozen with liquid nitrogen. Brain tissue was crushed using a mortar and pestle in preparation for DNA/RNA isolation.

Identifying conserved MT2 and exonic regions in prairie voles

The structure of *Oxtr* in prairie voles was determined by viewing RNA-sequencing reads near *Oxtr*. The sequence was taken for the whole region where reads were mapped and used to determine conserved regions of the gene. The MT2 region of *OXTR* in humans as identified by Kusui *et al.*, 2001 (GRCh38, chr3:8,769,033-8,769,438) was compared to the *Oxtr* sequence in prairie voles and with the NCBI BLASTn program, and a region in prairie voles was identified as having a highly similar sequence of DNA. To assess the significance of this similarity of the MT2 region between human and prairie vole we used the UVa FASTA server (http://fasta.bioch.virginia.edu/) and PRSS (DNA: DNA) to shuffle the prairie vole sequence 200 times and estimate the statistical significance of the shuffled scores.

Oxtr DNA methylation analysis

Extraction of DNA from nucleus accumbens tissue was done using the Qiagen AllPrep DNA/RNA Mini Kit (Qiagen, Valencia, CA) following manufacturer instructions. Two hundred nanograms of DNA was subject to bisulfite treatment (Kit MECOV50, Invitrogen, Carlsbad, CA), which allows for the detection of methylated cytosines by sequencing. Twelve nanograms of bisulfite converted DNA were used as template for PCR reactions. PCR was performed using a Pyromark PCR kit (Qiagen, Valencia, CA), and each PCR reaction was amplified in triplicate on three identical PCR machines (S1000 Thermal Cycler, Bio-Rad, Hercules, CA.). PCR primers, PCR cycling conditions, and pyrosequencing primers are reported in Table S2.4. All reactions were completed according to manufacturer instructions, except for the following which all included 3.5 nM $MgCl_2$ (provide in the Pyromark PCR kit): MT2, exon 3 sections 2-4, exon 3 sections 6-8. Standard controls of 0% and 100% methylated DNA, as well as a no DNA control standard were included for each PCR plate. The median DNA methylation value of the 0% control was 2% (interquartile range: 1%-2%). The median DNA methylation value of the 100% control was 88% (interquartile range: 85%-90%). Following PCR of exon 3 section 1, all samples were run on a 2% agarose gel and a 375 bp product was extracted using the QIAquick Gel Extraction Kit (Qiagen, Valencia, CA) which was subsequently used for pyrosequencing. All samples were randomized for pyrosequencing to account for plate and run variability. Pyrosequencing was performed on a Pyromark Q24 using Pyromark Gold Q24 Reagents (Qiagen, Valencia, CA) per the manufacturer's protocol. Epigenotypes reported are an average of three replicates. The mean deviation from the average ranged from 0.93% (MT2 CpG 7) to 2.29% (MT2 CpG 14).

Oxtr sequencing and SNP analysis

Ten nanograms of DNA was used as a template for PCR using a Pyromark PCR kit (Qiagen, Valencia, CA). In order to determine the alleles at polymorphic sites, pyrosequencing was completed using unknown base calling on a subset of samples using a Pyromark Q24 with PyroMark Gold Q24 Reagents (Qiagen, Valencia, CA) per the manufacturer protocol. Once alleles were identified, pyrosequencing was performed to measure genotypes of each sample. PCR primers, PCR cycling conditions, and pyrosequencing primers are reported in Table S2.4. The same primers were used for both unknown base calling and genotyping assays. SNPs KLW1 and KLW2 were tested for Hardy-Weinberg equilibrium using the HWExact function in the HardyWeinberg R package[39]. Linkage disequilibrium statistics for KLW1, KLW2, and NT213739 were determined using the LD function in the genetics R package[40].

Oxtr expression analysis

Extraction of RNA was done using the Qiagen AllPrep DNA/RNA Mini Kit (Qiagen, Valencia, CA) following manufacturer instructions. RNA was processed for cDNA synthesis following the protocol provided in the iScript cDNA Synthesis kit (Bio-Rad, Hercules, CA). Real-time PCR for the *Oxtr* main transcript was conducted using a 7500 Fast Real-Time PCR System (Applied Biosystems) using *Power* SYBR Green (Applied Biosystems No. 4367659). Real-time PCR for the *Oxtr* alternative transcript was conducted using the CFX96 System (Bio-Rad) using *Power* SYBR Green (Applied Biosystems). Real-time PCR for *Pgk1* was completed on both Real-time PCR systems. See Table S2.5 for all RT-PCR primers and cycling conditions. All reactions were run in triplicate (replicate standard deviation was <0.05) and their specificity verified by melting curve analysis and separation on a 2% agarose gel. Primer performance was evaluated using standard serial dilution and all primer sets performed within acceptable range for efficiency (See Table S2.5). Relative gene expression is presented using the comparative Ct method, $2^{-\Delta Ct}$, comparing target expression to *Pgk1* expression measured on the same Real-time PCR system. *Pgk1* was chosen as a reference based on data in mouse brain showing its reliability across brain regions and developmental time points[41].

RNA-sequencing and alignment

To identify the structure of *Oxtr* in prairie voles, we performed transcriptome analysis using RNA-sequencing on a single RNA sample derived from the nucleus accumbens of a female MAN1 vole in our cohort. RNA quality was assessed using an Agilent Tape Station. The RIN score was 9.0. The library was generated from 500 ng RNA using the NEBNext Ultra Directional RNA Library Prep Kit with mRNA magnetic isolation. The UVA Genome Analysis and Technology Core performed paired-end sequencing (2 X 75 bp paired-end run) on the Illumina NextSeq 500 platform. A total of 125 million reads were generated. The raw sequencing data was subjected to pre-processing steps of adapter removal and quality-based trimming using TrimGalore[42] with removal of auto-detected Illumina adapters and trimming of low-quality ends up to a threshold of Q20. Reads that became shorter than 35 bp due to either adapter removal or quality trimming were discarded. Quality control was completed with MultiQC[43]. Novel transcript identification and quantification was performed using a standard analysis approach outlined elsewhere[44]. Briefly, sequencing data was aligned to the *Microtus ochrogaster* genome using a splice-aware aligner STAR2[45], followed by assembly and quantification using Stringtie[46]. Alignments were viewed in the Integrated Genomics Viewer[47].

Statistical analysis

Statistical computing and graphics were generated with R statistical software[48]. Graphics were generated using the ggplot2 and ggpubr packages unless otherwise stated[49,50]. For each analysis, $p < 0.05$ was regarded as statistically significant with respect to multiple comparison procedures as appropriate. The effect of handling on DNA methylation in MT2 and exon 3 was determined using a mixed effects model with fixed effect of handling condition and random effects of intercepts for individual and CpG site using the lme4 package[51]. The type II Wald F test in the car package was used to determine significance of fixed effects[52]. The effect of handling condition on DNA methylation at individual CpG sites was determined using t tests followed by Bonferroni correction. In both humans and in prairie voles, Spearman's rank correlation was used to determine the relationship between DNA methylation and gene expression and uncorrected p-values are reported because the distribution of DNA methylation at some CpG sites in human

MT2, prairie vole MT2, and prairie vole exon 3 are non-normal. For visualization purposes, we plotted trend lines from linear regression models predicting DNA methylation from expression. The community structure of the MT2 region was determined using exploratory graph analysis (EGA) implemented in the EGAnet package[53]. We estimated the EGA network using the Triangulated Maximally Filtered Graph (TMFG) model[54] as opposed to the graphical LASSO (GLASSO) model, because the GLASSO procedure typically requires n (sample size) >> p (CpG sites) to accurately compute partial correlations for each site. TMFG skirts this issue by modeling the zero-order correlation matrix, rather than the partial correlation matrix. The effect of handling condition on standardized network community score was determined using a 2 way community x handling condition ANOVA, followed by t tests within each community and Bonferroni correction. Spearman's rho was used to determine the relationship between standardized network community score and *Oxtr* expression because the distribution of standardized network community scores is non-normal. The impact of *Oxtr* polymorphisms KLW1 and KLW2 (both A/G SNPs) on gene expression was determined using a t test comparing A carriers (A/A and A/G) to G/G homozygotes. The impact of sex, handling condition, and *Oxtr* polymorphisms KLW1, KLW2, and NT213739 on expression of the alternative transcript were determined using the Wilcoxon Rank Sum test as expression of the alternative transcript was non-normal.

Results

Oxtr gene structure in prairie voles resembles human OXTR gene structure with high homology in CpG-rich regions

Previously, the structure of the *Oxtr* gene in prairie voles was reported to have two exons which are homologous to exons 3 and 4 in humans (MicOch1.0, GCA_000317375.1, Ensembl release 100). However, this gene in other rodents has four exons, similar to humans, including two exons at the 5' end of the gene which are not translated [39]. In order to determine the full structure of *Oxtr* in prairie voles, we completed RNA-sequencing on RNA from the nucleus accumbens. Viewing the read alignment in the Integrated Genomes Viewer (IGV) reveals that this gene has four exons and three introns, much like the human gene (Figures 2.1A,B). In addition, the 3' UTR extends further than previously reported.

We assessed the homology between prairie voles and human for two CpG-rich regions in *OXTR* where many human studies associated DNA methylation and neuropsychological outcomes, MT2 and exon 3. Homology was determined using PRSS (DNA:DNA). For the MT2 region, this analysis identified a conserved region between human and prairie voles with 64.3% shared identity (Figure S2.1A; Smith-Waterman score: 566; 64.3% similar; Z-score: 120.2; bits: 120.2; E(1000): $1x10^{-31}$). For the exon 3 region, this analysis identified a conserved region between human and prairie voles with 88.4% identity (Fig. S2.1B, Smith-Waterman score: 2275; 88.4% similar; Z-score: 1966.2; bits: 373.7; E(1000): $1x10^{-107}$).

DNA methylation in MT2 is sensitive to early life experience and associated with Oxtr gene expression in prairie vole and human brains

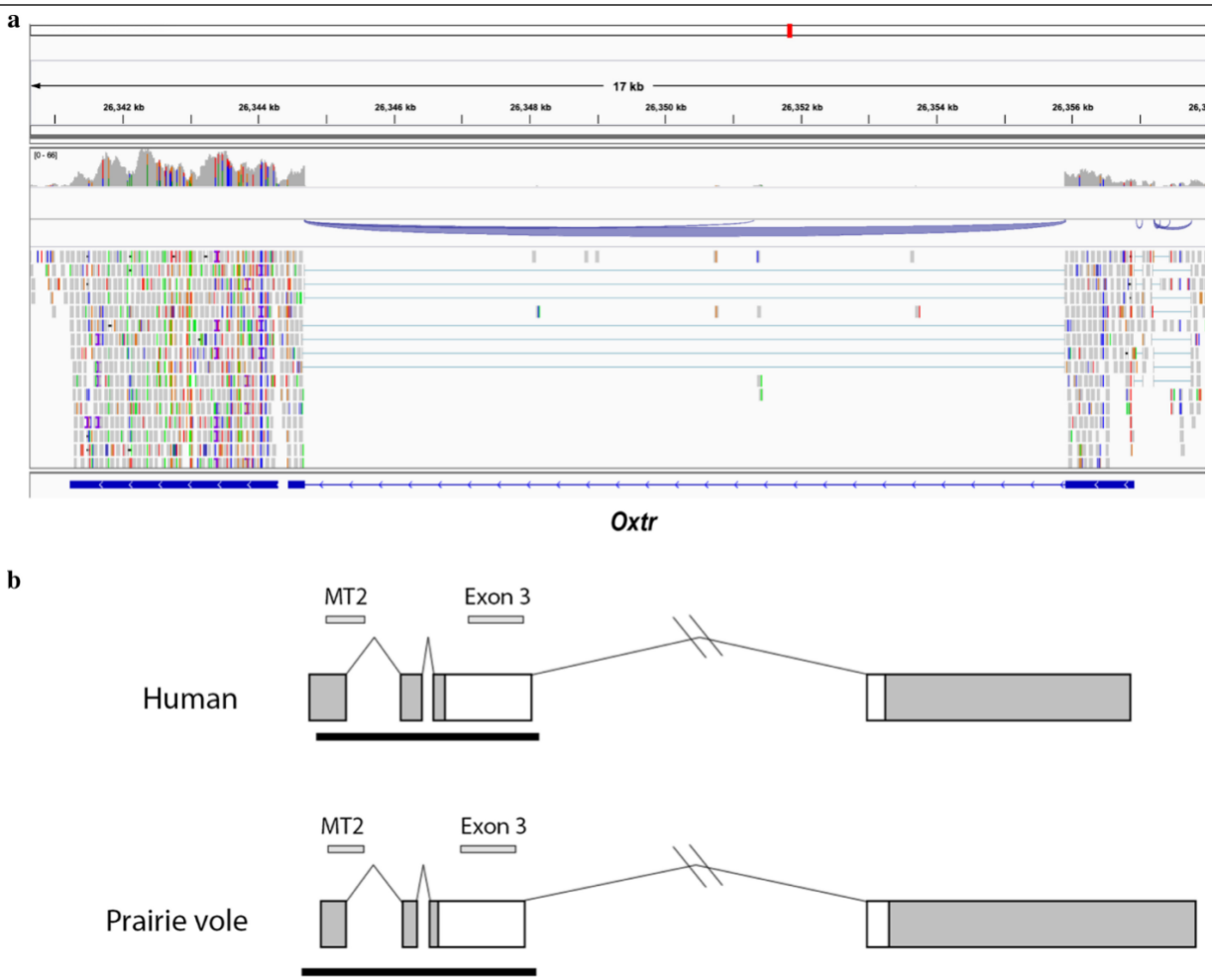

Figure 2.1. *Oxtr* gene structure and homology in prairie voles and humans. A) RNA-seq evidence of *Oxtr* gene structure in prairie voles. The region shown is micOch1.0 scaffold JH996431.1: 26,340,626-26,358,364. B) Gene schematic of *OXTR* in humans and *Oxtr* in prairie voles. Exons are indicated by boxes (coding, white; untranslated, gray). Introns are shown with solid lines. The black boxes below the transcripts delineate a CpG island identified using the CpG island function of the sequence manipulation suite. Gray boxes above the transcripts denote conserved regions of the CpG island labelled as MT2 and exon 3. These conserved regions were assayed for DNA methylation.

We have previously shown that early life experience in the form of nurture prevents *de novo* DNA methylation on 4 sites in MT2 (-934_1, -934_2, -924, and -901) and leads to increased *Oxtr* gene expression as juveniles[37]. We next aimed to characterize how early life experience affects DNA methylation on other sites in MT2. We used a mixed model analysis to account for correlation between DNA methylation values at these sites (Figure S2.2A). Across all sites in MT2, offspring that received less parental care (MAN0) have increased DNA methylation (Figure 2.2A, type II Wald F test $F_{(1,24)}$=8.386, p=0.008). Several of the sites are significantly correlated with expression of *Oxtr* (Figure 2.2B, Table S2.1). In order to determine if this model is instructive for studying humans, we compared *OXTR* DNA methylation to gene expression from human samples collected from Brodmann Area 41/42[14]. In human brain tissue there is also a significant correlation between DNA methylation at CpG sites -934, -924, and -901 and *OXTR* gene expression (Figure 2.2C, Table S2.2, -934: ρ=-0.78, p=0.007; -924: ρ=-0.68, p=0.02; -901: ρ=-0.66, p=0.028).

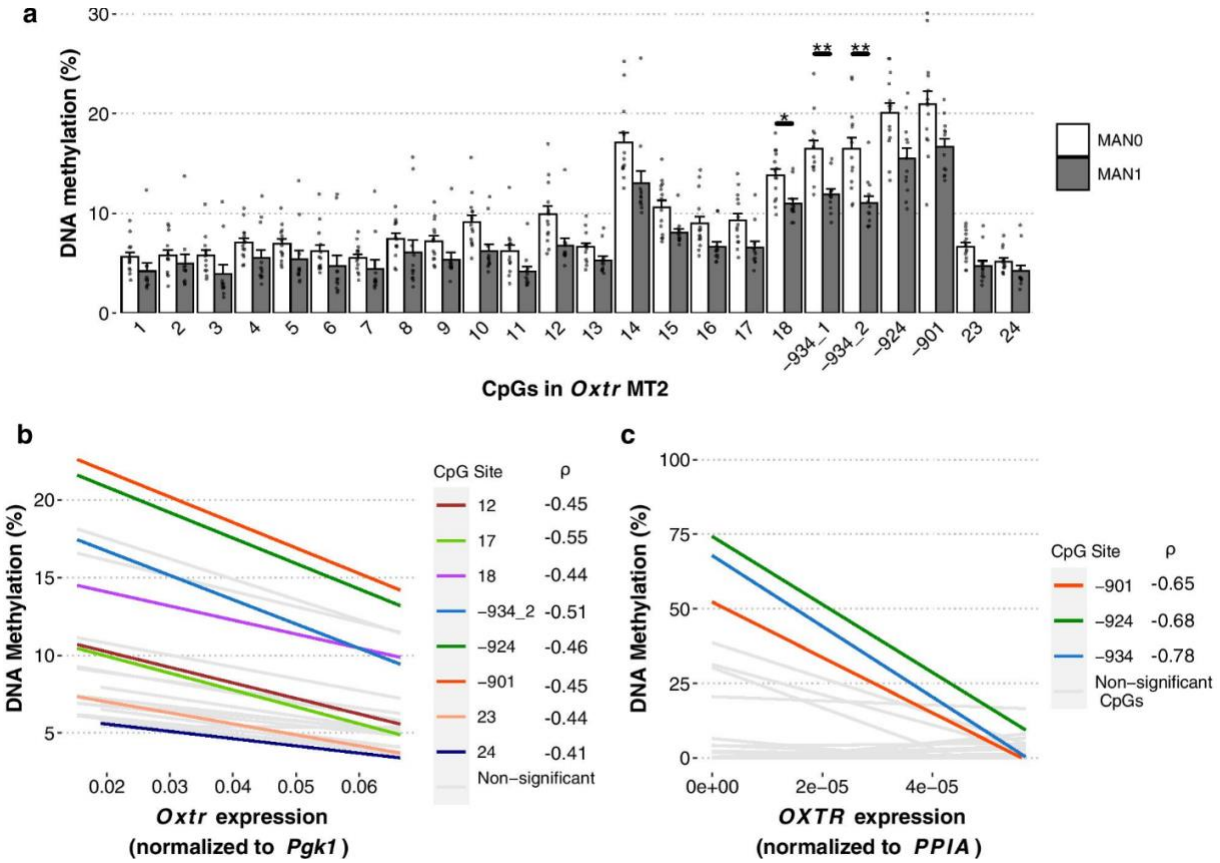

Figure 2.2. DNA methylation in MT2 is impacted by early life experience and associated with *Oxtr* expression. A) Offspring that received less parental care (MAN0) have increased DNA methylation across MT2 in the nucleus accumbens (13 male-female sibling pairs; MAN0: n = 7 males, 7 females; MAN1: n = 6 males, 6 females; mixed effect model with fixed effect of handling condition and random effects of individual and CpG site; Type II Wald F test $F_{(1,24)}$=8.386, p=0.008). Follow up t tests between handling conditions at each site were conducted with Bonferroni correction; * p<0.05, ** p<0.01. B) DNA methylation in MT2 is associated with *Oxtr* expression in prairie vole nucleus accumbens. Spearman's rank correlation was used to determine correlation. Sites with significant correlations (not corrected for multiple comparisons) are shown in color while non-significant sites are in gray. Spearman's rho and p values for each site are in Table S1.1. C) DNA methylation in MT2 is associated with *OXTR* expression in human temporal cortex. Spearman's rank correlation was used to determine correlation. Sites with significant correlations (not corrected for multiple comparisons) are shown in color while non-significant sites are in gray. Spearman's rho and p values for each site are in Table S1.2.

CpG sites -934_1, -934_2, -924, and -901 are most highly associated with Oxtr gene expression

DNA methylation at CpG sites in MT2 are highly correlated with each other (Figure S2.2A). In order to further understand the structure of MT2, we employed Exploratory Graph Analysis (EGA), a dimensionality reduction technique and network structure analysis tool[55,56]. This tool allows us to cluster CpG sites in an unsupervised manner based on the covariance of DNA methylation values into distinct groups which provide non-redundant information. The results from EGA suggest three distinct communities of CpG sites, largely reflecting the physical structure of MT2: community 1 contains 5' sites, community 2 contains sites in the middle, and community 3 contains 3' sites (Figure 2.3A, Fig S2.2B-C). The reliability of the community structure was determined using 1000 bootstrapped replications[57]. The probability of each CpG site remaining in

their community is shown in Figure 2.3B. Probabilities greater than 0.8 are considered stable. Notably, CpG sites -934_1, -934_2, -924, and -901 all remain in their community nearly 100% of the time, and this stability may indicate that these CpG sites are most tightly co-regulated.

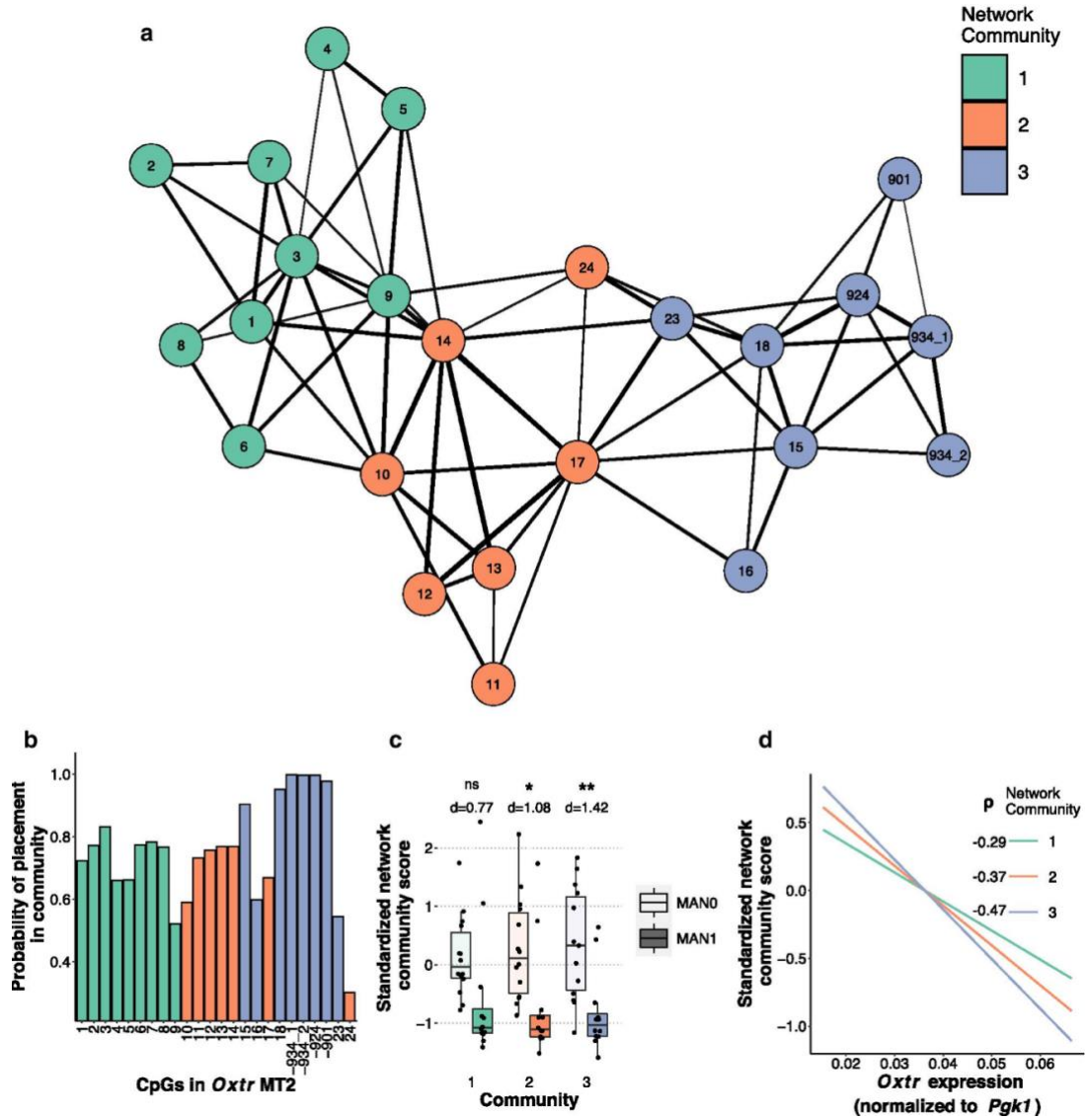

Figure 2.3. Network analysis of MT2 DNA methylation reveals importance of 3' region. A) Community structure network of CpG sites in MT2 containing three communities: community 1 (green) which contains 5' CpGs, community 2 (orange) which contains mostly CpGs in the middle of MT2, and community 3 (blue) which contains mostly 3' CpGs. The weight of edges indicates higher covariance between CpG sites. B) Item stability scores for each CpG site. CpGs with scores greater than 0.8 are considered stable. C) Animals raised by low care parents (MAN0) have higher standardized network community scores, which represent DNA methylation within the community (13 male-female sibling pairs; MAN0: n = 7 males, 7 females; MAN1: n = 6 males, 6 females; 2 way handling condition x community ANOVA, main effect of handling condition, $F_{(1, 72)}$=22.41, p = 1.1e-5; no effect of community, $F_{(2, 72)}$=0.001, p = .99. Follow up t tests between handling conditions at each community were conducted with Bonferroni correction (* p<0.05, ** p<0.01) . Cohen's d is provided to measure effect size.) The effect size of handling condition on standardized network community score is largest in community 3. D) Standardized network community scores for each community are correlated with *Oxtr* gene expression using Spearman's rank-correlation; community 1: ρ=-0.29, p=0.086; community 1: ρ=-0.37, p=0.03; community 3: ρ=-0.47, p=0.003.

In order to determine which community of CpG sites are most sensitive to early nurture, we compared standardized network community scores[58] for each community between the two handling groups. The standardized network community scores are compressed representations of the original DNA methylation data from CpG sites within the community and are analogous to component vectors from principal components analysis. In this way, the network scores represent weighted DNA methylation values from CpG sites within each network community. The standardized network community scores differed by handling condition but not by community (Figure 2.3C, 2-way community x handling condition ANOVA, main effect of handling condition $F_{(1, 72)}$=22.41, p = 1.1e-5, no effect of community $F_{(2, 72)}$=0.001, p = .99). We then performed follow up t tests to determine which community was most affected by early nurture. The largest effect was found in community 3, which contains sites -934_1, -934_2, -924, and -901 (Welch's two sample t test with Bonferroni correction and Cohen's d; community 1: $t_{(17.3)}$=1.88, p=0.229, d=0.77; community 2: $t_{(22.7)}$=2.72, p=0.037, d=1.08; community 3: $t_{(23.4)}$=3.70, p=0.003, d=1.42), indicating DNA methylation at this cluster of sites is particularly sensitive to early nurture.

We then correlated standardized network community score with *Oxtr* expression. Community 3 most correlates with gene expression (Figure 2.3D; community 1: ρ=-0.29, p=0.086; community 1: ρ=-0.37, p=0.03; community 3: ρ=-0.47, p=0.003). Notably, community 3 contains five of the eight sites in MT2 where DNA methylation significantly correlates with *Oxtr* expression (Figure 2.2B). This is also the community where DNA methylation is most sensitive to early life experience, indicating that CpG sites in this community may be functionally responsible for regulation of gene expression.

DNA methylation in exon 3 is sensitive to early life experience but is not associated with gene expression

In human studies, DNA methylation at CpG sites within exon 3 of *Oxtr* have been associated with several neuropsychological outcomes[17,26,31-35]. In prairie voles there is a highly conserved region within exon 3 that contains 42 CpG sites (Figure 2.1B). We analyzed DNA methylation across this region and found that DNA methylation in exon 3 is sensitive to early life experience (Figure 2.4A, fixed main effect of handling condition, type II Wald F test $F_{(1,24)}$=8.386). Follow up t-tests were completed at each site to determine the sites most sensitive to early life experience, but no sites remained significant after Bonferroni correction. DNA methylation in exon 3 was only associated with *Oxtr* gene expression at CpG 36 (Figure 2.4B, Table S2.3). Thus, while early nurture affects DNA methylation in both MT2 and exon 3 of *Oxtr*, DNA methylation levels in MT2 appear to be an important indicator of expression of the gene but the same is not true of exon 3. Studies in humans identifying associations between DNA methylation and neuropsychological outcomes likely find such results because DNA methylation in exon 3 is highly correlated with DNA methylation in the 3' portion of MT2 (Figure 2.5).

Identification of two single nucleotide polymorphisms (SNPs) within exon 3 which are not associated with Oxtr gene expression

Within exon 3 there are two CpG sites with patterns of DNA methylation with a cluster of prairie voles with DNA methylation between 50-75%, a cluster between 25-30%, and a few individuals near 0% methylation. We hypothesized that these two sites are polymorphic with one allele preserving the CpG and the other disrupting the CpG such that the cytosine is not methylated. In the same cohort of MAN0 and MAN1 animals, pyrosequencing analysis revealed that these two sites, KLW1 (CpG 25, JH996431.1:26,356,275, micOch1.0) and KLW2 (CpG 33, JH996431.1:26,356,107, micOch1.0) are indeed single nucleotide polymorphisms (SNPs). KLW1 is an A/G SNP where A is the minor allele in this population (frequency=0.33). KLW2 is also an

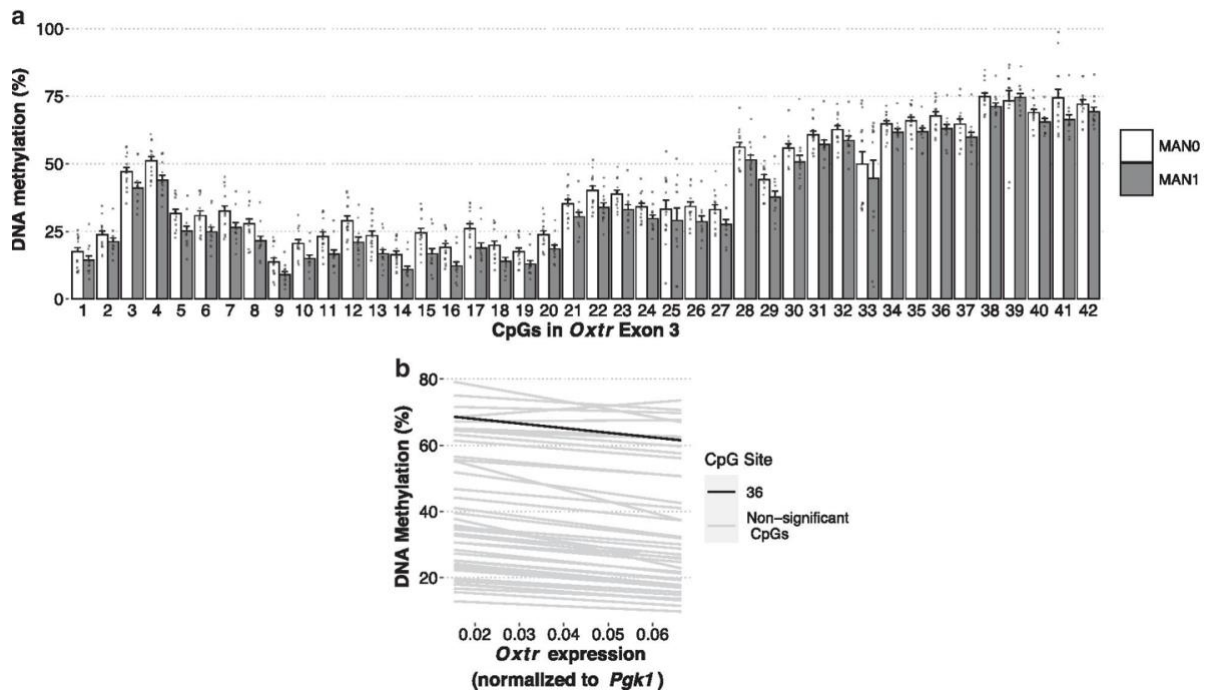

Figure 2.4. Genetic and epigenetic features of exon 3 do not control *Oxtr* expression. A) Offspring receiving less parental care (MAN0) have decreased DNA methylation across exon 3 in the nucleus accumbens (13 male-female sibling pairs; MAN0: n = 7 males, 7 females; MAN1: n = 6 males, 6 females; mixed effect model with fixed effect of handling condition and random effects of individual and CpG site; Type II Wald F test $F_{(1,24)}$=8.386, p=0.018. CpG sites are numbered according to Fig S1.1B. B) DNA methylation in exon 3 is not robustly associated with *Oxtr* expression in prairie vole nucleus accumbens. Spearman's rank correlation was used to determine correlation. CpG 36, the only site that has a significant correlation with *Oxtr* expression (not corrected for multiple comparisons) is shown in black. Sites that do not have a significant correlation with *Oxtr* expression are in gray. Spearman's rho and p values for each site are in Table S1.3.

A/G SNP where A is the minor allele in this population (frequency=0.27). Both SNPs are in Hardy-Weinberg equilibrium in this population (Haldane's exact test[39]; KLW1: D=-0.22, p=0.84; KLW2: D=-0.11, p=0.82). We also tested if these SNPs are in linkage disequilibrium with each other or with another SNP in this gene, NT213739[59]. All three SNPs are in linkage disequilibrium (Table 2.1). However, a larger sample is necessary for more accurate quantitation of linkage disequilibrium. We next examined the effect of genotype at KLW1 and KLW2 on expression of *Oxtr*. Neither KLW1 genotype nor KLW2 genotype impacted *Oxtr* expression (Figure 2.6A,B; KLW1: $t_{(23.9)}$=-0.06, p=0.95; KLW2: $t_{(20.4)}$=-0.89, p=0.38).

An interaction between DNA methylation of *OXTR* and SNP rs53576 genotype has been reported in relation to neuropsychological outcomes in humans[23,31,35]. This led us to hypothesize that there are genetic x epigenetic interactions affecting *Oxtr* expression. In order to study this in the prairie vole sample, we asked if the relationship between the standardized network community score of community 3, which represents DNA methylation at the 3' end of MT2, and *Oxtr* expression differs by genotype at SNPs KLW1, KLW2, or NT213739. There are no significant interactions, likely because of the small sample size,

Table 2.1. Linkage of SNPs KLW1, KLW2, and NT213739.

SNP 1	SNP 2	r^2	χ^2	p value
KLW1	KLW2	0.18	9.29	0.002
KLW1	NT213739	0.10	5.27	0.022
KLW2	NT213739	0.08	4.00	0.046

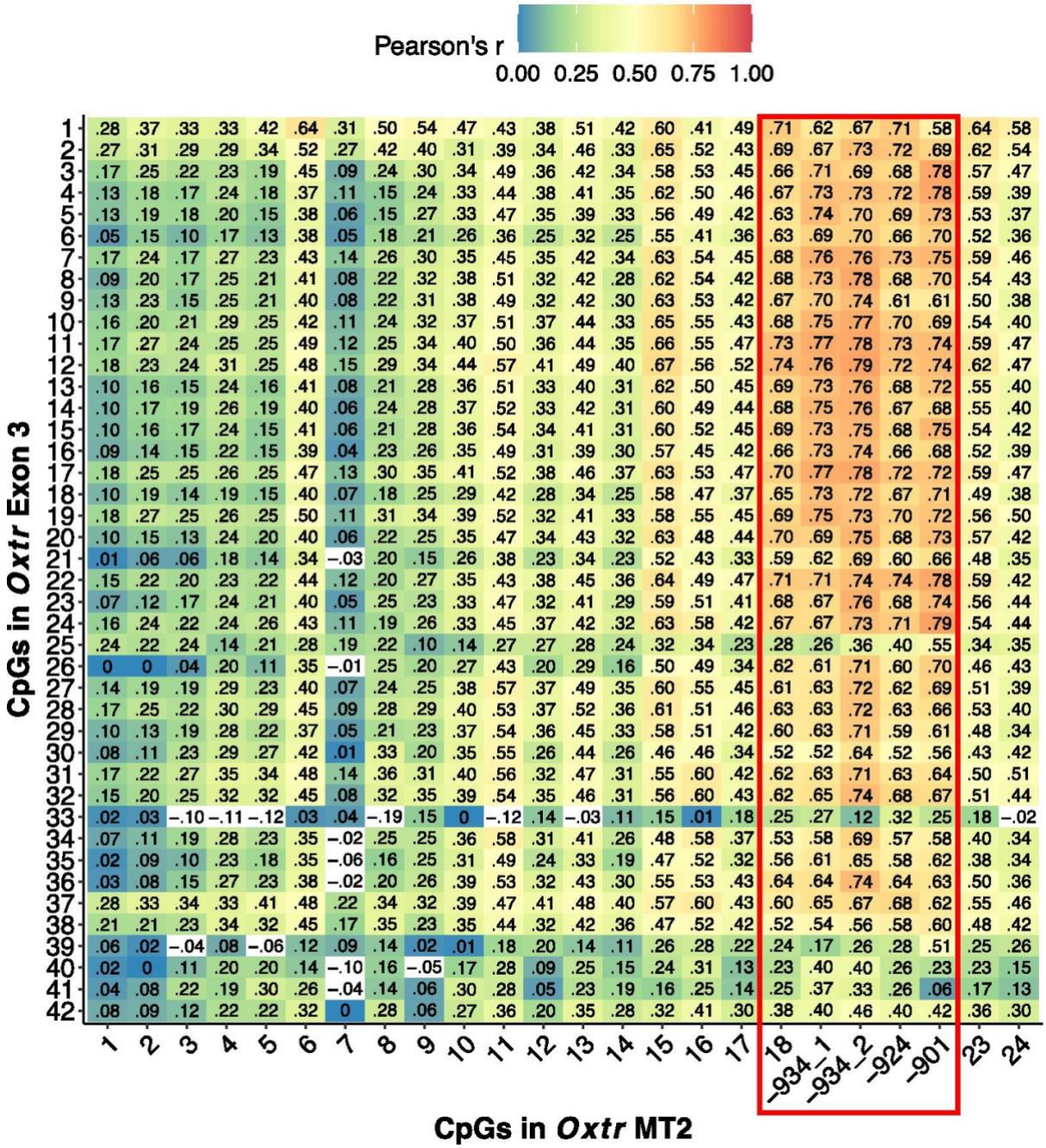

Figure 2.5. Correlation of DNA methylation in MT2 CpG sites and exon 3 CpG sites. Pearson's R correlation of DNA methylation in MT2 and exon 3 CpG sites. The red box around MT2 CpGs 18 through -901 indicates that these CpGs have the highest correlation with exon 3 sites.

but interesting patterns emerge. The correlation between community 3 standardized network score and *Oxtr* expression is very similar in KLW1 A carriers and G/G voles (ρ=-0.56 and -0.48, respectively; Figure 2.6C). 'A' carriers (A/A and A/G) of KLW2 have a stronger correlation between these measures compared to KLW2 G/G voles (ρ=-0.88 and -0.28, respectively; Figure 2.6D). Voles with T/T genotype at NT213739 also have a stronger correlation between these two measures compared to C/T individuals (ρ=-0.67 and -0.20, respectively; Figure 2.6E). These results suggest a genetic by epigenetic interaction may impact *Oxtr* expression, but further studies

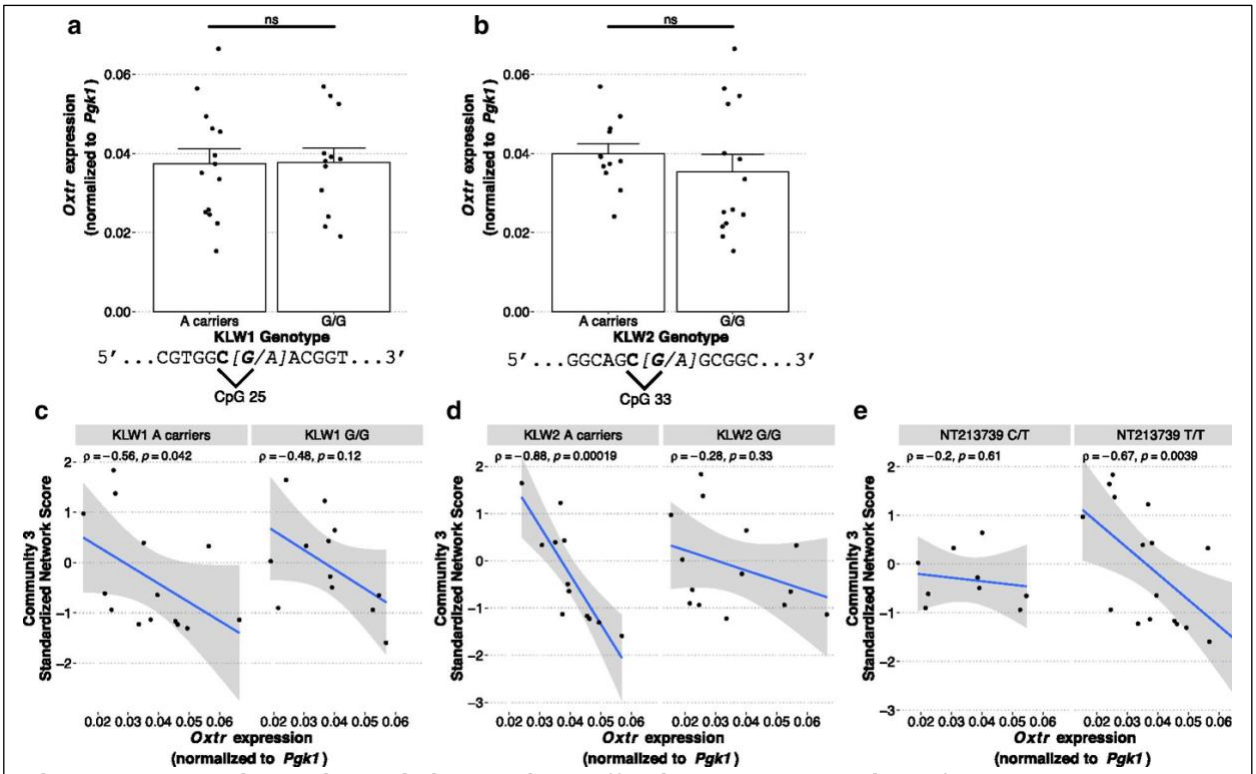

Figure 2.6. Genetic x epigenetic interactions affecting *Oxtr* expression. A) Genotype at KLW1 does not impact *Oxtr* expression (A carriers: n=14; G/G: n=12; Welch two sample t test, $t_{23.9}$=-0.06, p=0.95). Animals are grouped by presence of minor allele (A) because of low abundance of A/A homozygotes. The DNA sequence surrounding KLW1 is shown below the graph. B) Genotype at KLW2 does not impact *Oxtr* expression (A carriers: n=12; G/G: n=14; Welch two sample t test, $t_{20.4}$=-0.89, p=0.38). Animals are grouped by presence of minor allele (A) because of low abundance of A/A homozygotes. The DNA sequence surrounding KLW2 is shown the below the graph. C) The relationship between MT2 DNA methylation (represented by community 3 standardized network score) and *Oxtr* expression does not differ between KLW1 genotypes (A carriers: n=14, R=-0.49, p=0.076; G/G: n=12, R=-0.51, p=0.091), but D) does differ between KLW2 genotypes (A carriers: n=12, R=-0.84, p=0.00065; G/G: n=14, R=-0.35, p=0.22) and E) NT213739 genotypes (C/T: n=9, R=-0.17, p=0.66; T/T: n=17, R=-0.61, p=0.01).

with larger samples from several prairie vole colonies are needed to test this hypothesis.

Identification of an alternative transcript of Oxtr beginning in intron 3 which is associated with KLW2 genotype

In addition to *Oxtr* gene structure, RNA-seq data revealed a possible alternative transcript in *Oxtr* consisting of a small exon in the third intron of the main transcript and the fourth exon of the main transcript (Figure 2.7A, reads highlighted in yellow). We then measured this transcript in samples from the early nurture experiment using RT-PCR. The transcript is present in all samples, and there are no differences in expression based on nurture (Figure 2.7B, W=82, p=0.85) or sex (Figure 2.7C, W=63, p=0.44). Expression of the alternative transcript is associated with the KLW2 A allele (Figure 2.7D, W=156, p=3.85e-7). Alternative transcript expression is not associated with either KLW1 genotype (Figure S2.3A, W=77, p=0.98) or NT213739 genotype (Figure S2.3B, W= 42, p=0.10).

We next asked if the main transcript and this alternative transcript are co-regulated, meaning that animals with high expression of the main transcript could also have high levels of

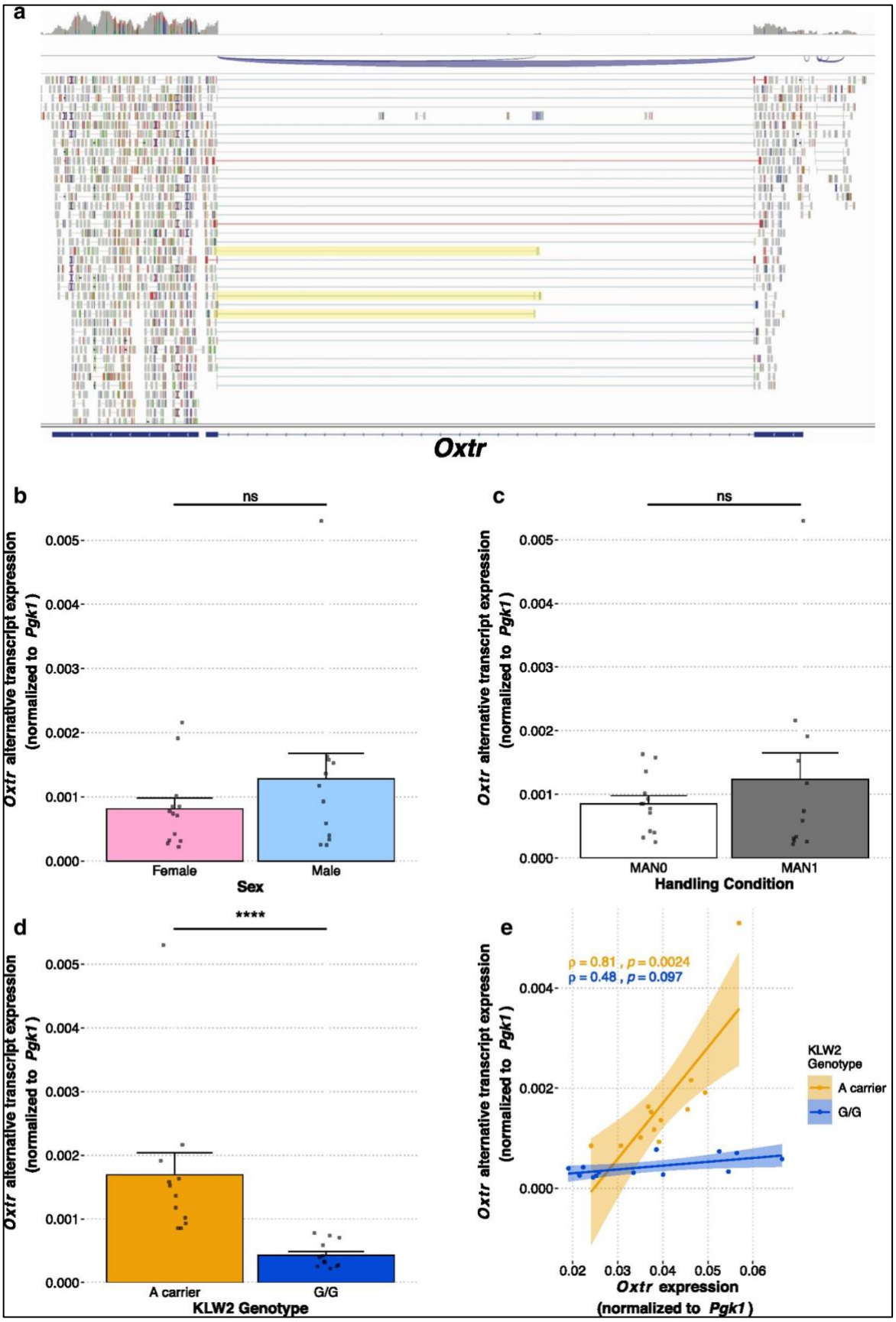
a
Oxtr
b
ns
Oxtr alternative transcript expression (normalized to Pgk1)
0.005
0.004
0.003
0.002
0.001
0.000
Female
Male
Sex
c
ns
Oxtr alternative transcript expression (normalized to Pgk1)
MAN0
MAN1
Handling Condition
d
****
Oxtr alternative transcript expression (normalized to Pgk1)
A carrier
G/G
KLW2 Genotype
e
ρ = 0.81 , p = 0.0024
ρ = 0.48 , p = 0.097
Oxtr alternative transcript expression (normalized to Pgk1)
0.02
0.03
0.04
0.05
0.06
Oxtr expression (normalized to Pgk1)
KLW2 Genotype
A carrier
G/G

Figure 2.7. Identification of an alternative transcript of *Oxtr* that is associated with KLW2 genotype. A) RNA-seq evidence of a novel alternative transcript of *Oxtr* originating in the third intron. Reads providing evidence of this transcript are highlighted in yellow. B) Expression of the alternative transcript is not impacted by sex (males: n=13, females: n=13; Wilcoxon rank-sum test, W=63, p=0.44). C) Expression of the alternative transcript is not impacted by handling condition (MAN0: n=14, MAN1: n=12; Wilcoxon rank-sum test, W=82, p=0.85). D) Expression of the alternative transcript is associated with the A allele of KLW2 (A carrier: n=12, G/G: n=14; Wilcoxon rank sum test, W=156, p=3.85e-7). E) Expression of the alternative transcript is positively correlated with expression of the main *Oxtr* transcript in animals carrying the A allele of KLW2 (2 way KLW2 genotype x *Oxtr* main transcript expression ANOVA, interaction effect $F_{(1,21)}$=23.723, p=8.14e-5, adjusted R^2=0.734; A carriers: Spearman's ρ=0.81, p=0.0024; G/G: Spearman's ρ=0.48, p=0.097).

alternative transcript expression. A 2-way ANOVA was conducted to determine the influence of main transcript expression while accounting for KLW2 genotype. There was a significant interaction between the expression of the main *Oxtr* transcript and KLW2 genotype (Figure 2.7E, $F_{(1,21)}$=23.723, p=8.14e-5) such that *Oxtr* main transcript expression is positively correlated with alternative transcript expression in KLW2 A carriers (ρ=0.81, p=0.0024) but there is no correlation in animals with KLW2 G/G genotype (ρ=0.48, p=0.097). Thus, it appears that the main transcript of *Oxtr* is co-regulated with the alternative transcript via a mechanism that is associated with the A allele of KLW2.

Discussion

The results from these studies clarify the contributions of genetic, epigenetic, and environmental factors in determining *Oxtr* expression in the prairie vole brain. We show that the structure of *Oxtr* in prairie voles resembles human *OXTR*. Within the CpG island spanning the first 3 exons of *OXTR*, two regions have been associated with human neuropsychological outcomes: MT2 and exon 3, both of which are highly conserved in the prairie vole. Using the prairie vole model, we show that *Oxtr* expression in the nucleus accumbens is significantly associated with DNA methylation in MT2 but not DNA methylation in exon 3. Furthermore, network analysis implemented in EGA indicates that DNA methylation in the 3' end of MT2, which contains CpG sites -901, -924, -934_1, and -934_2 that we have previously reported on[37,38], is most strongly associated with *Oxtr* expression. Notably, we previously showed that DNA methylation of these CpG sites in whole blood samples are correlated with gene expression in the brain in prairie voles[37]. Additionally, we show that CpG sites -901, -924, and -934 are strongly associated with *OXTR* expression in human temporal cortex while other sites within MT2 are not. Previous studies finding associations between DNA methylation in exon 3 and neuropsychological outcomes in humans likely find this because DNA methylation in exon 3 reports on DNA methylation at CpG sites in the 3' portion of MT2. Collectively, these results indicate that human studies measuring *OXTR* DNA methylation should focus measurements on MT2, where DNA methylation in both central and peripheral tissues serve as a biomarker for gene expression in the brain.

Our findings expand upon our previous studies examining the relationship between early life experience and *Oxtr* DNA methylation. Here, we show that increased parental care results in hypomethylation across MT2 and exon 3 in the prairie vole brain. These results mirror human studies which find that DNA methylation of *OXTR* is impacted by early life experience in both MT2[60,61] and exon 3[62]. Additionally, childhood abuse in humans interacts with *OXTR* DNA methylation in both MT2 and exon 3 to predict anxiety and depression[26]. Our results further establish prairie voles as an excellent rodent model for studying how early life experience impacts regulation of the oxytocin system and social behavior.

We identified two novel SNPs in prairie vole *Oxtr* within exon 3. Both are A/G SNPs where A is the minor allele and disrupts a CpG site. These SNPs, in addition to the previously identified

SNP NT213739[59] offer an opportunity to model the common association of *OXTR* SNPs with behavioral and psychiatric outcomes in humans[63]. Our results show that neither KLW1 nor KLW2 genotype is associated with *Oxtr* expression in the nucleus accumbens. It was previously reported that the C allele of NT213739 was associated with increased *Oxtr* expression in the prairie vole nucleus accumbens[59], although our group found no association[37]. However, we found that there is a stronger negative association between *Oxtr* DNA methylation and gene expression in animals with A/A and A/G genotypes at KLW2 compared to those with G/G genotypes. Similarly, we found that animals with T/T genotype at NT213739 show a strong negative association between *Oxtr* DNA methylation and gene expression while there was no association in animals with the C/T genotype. Although this analysis is underpowered, these results suggest that the KLW2 G allele and NT213739 C allele lead to epigenetic dysregulation of *Oxtr*, perhaps by impeding the binding of factors that regulate the gene. Further studies with appropriate sample size will be necessary to study this phenomenon. These studies may shed light on mechanisms underlying the common finding in human studies that *OXTR* DNA methylation interacts with genotype at *OXTR* SNP rs53576 in certain psychopathologies[23,31,35].

RNA-sequencing results led to the identification of a novel transcript of *Oxtr*. This transcript, which is homologous to mouse *Oxtr* isoform H (GenBank KU686801.1)[64], originates in the third intron of *Oxtr*. Expression of this transcript is associated with the A allele of KLW2, though further work is necessary to determine if this SNP is functionally related to transcription of this alternative transcript. In animals with a KLW2 A allele, expression of the main transcript and the alternative transcript of *Oxtr* are positively correlated. The function of the novel transcript is unknown. One possibility is that the alternative transcript regulates expression of the main transcript. For example, it has been reported that non-coding RNAs bind DNMT1 to prevent DNA methylation in a gene-specific manner, which in turn increases expression of that gene[65]. If the novel transcript is translated, it would result in a peptide containing most of the seventh transmembrane helix and the C-terminus of OXTR. This peptide could alter the activity of the OXTR protein. Oxtr has been shown to dimerize with type 2 dopamine receptors, though the precise dimerization sites are unknown[66,67]. It is possible that this OXTR fragment could dimerize with D2Rs, affecting the function of oxytocin-dopamine interactions in the nucleus accumbens. This novel OXTR fragment could also disrupt desensitization of OXTR after oxytocin stimulation, which is dependent on β-arrestin binding to serine triplets in the C-terminus of OXTR[68], by sequestering available β-arrestin. Further studies are necessary to determine the function of this alternative transcript. While this transcript is present in mouse brain, we could not find any evidence of this transcript in human nucleus accumbens using publicly available RNA-seq data from the GTEx project[69]. Further characterization of this transcript in humans will require appropriate, high quality human brain samples.

Taken together, the results from these experiments offer insight into mechanisms of regulation of *Oxtr* expression in the brain. These results will inform future studies of *OXTR* involvement in human psychopathologies. Further work should focus on the 3' region of MT2, where DNA methylation is most sensitive to early life experience and most strongly correlates with *OXTR* expression in both prairie vole and human brain. Additional studies in prairie voles focused on the SNPs KLW2 and NT213739 can elucidate genetic by epigenetic interactions in *OXTR* which mediate behavioral outcomes. The identification of a novel transcript of *OXTR*, if also present in humans, has implications for *OXTR* gene regulation, protein function, and behavioral outcomes.

Conclusions

These results provide strong evidence that DNA methylation in MT2, particularly the 3' portion, is a better indicator of *OXTR* gene expression than DNA methylation in exon 3 in prairie

voles. We also provide evidence that in human temporal cortex, DNA methylation in the 3' portion of MT2 is associated with *OXTR* gene expression while DNA methylation in other MT2 CpG sites is not. Though associations exist between DNA methylation in *OXTR* exon 3 and neuropsychological outcomes in humans, such results may reflect that DNA methylation in exon 3 is correlated with DNA methylation in MT2. Our findings suggest that future studies of *OXTR* DNA methylation in humans should focus on MT2, particularly CpG sites -934, -924, and -901, as these sites are most related to gene expression in both prairie vole and human brains.

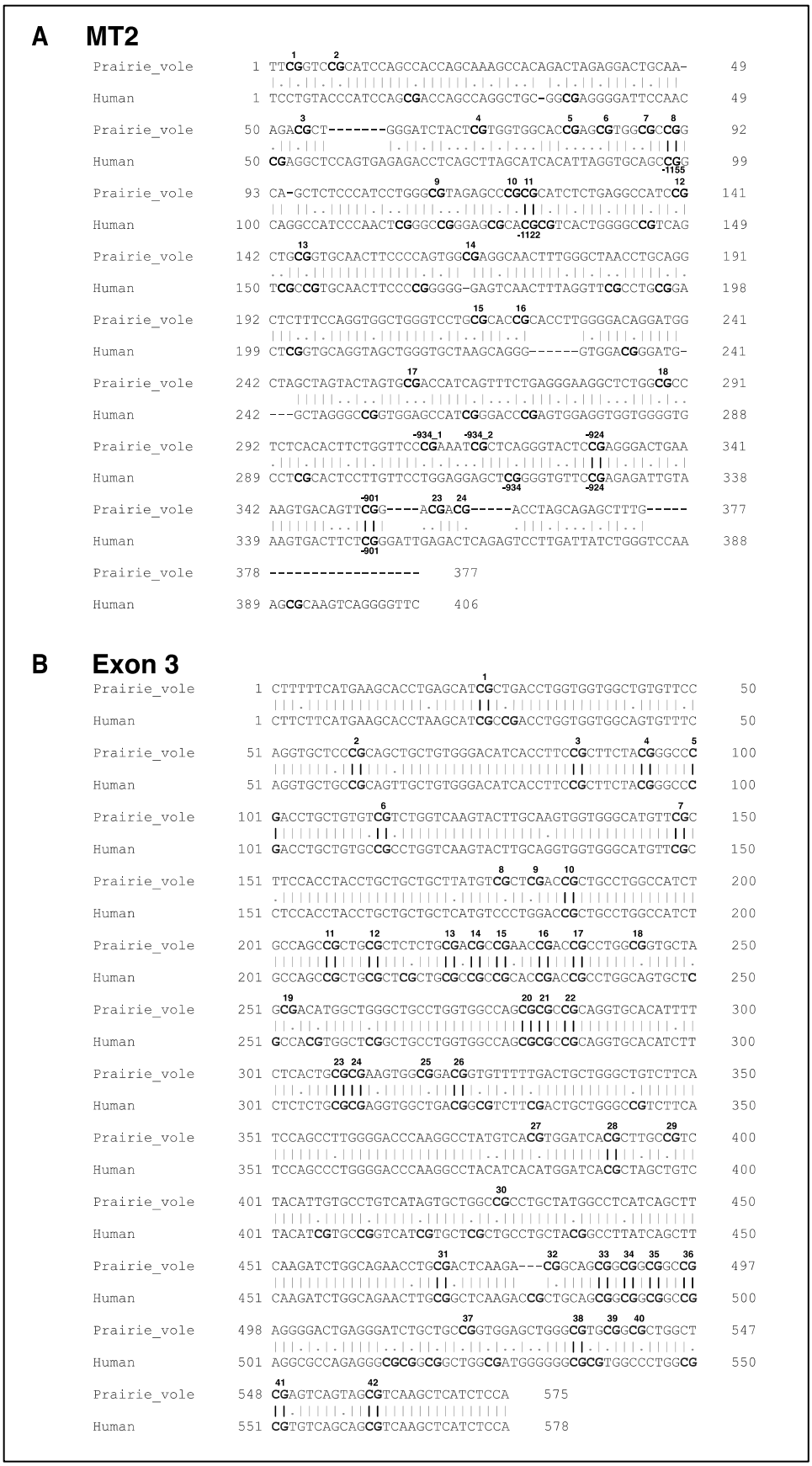
A MT2
Prairie_vole 1 TTCGGTCCGCATCCAGCCACCAGCAAAGCCACAGACTAGAGGACTGCAA- 49
Human 1 TCCTGTACCCATCCAGCGACCAGCCAGGCTGC-GGCGAGGGGATTCCAAC 49
Prairie_vole 50 AGACGCT-------GGGATCTACTCGTGGTGGCACCGAGCGTGGCGCCGG 92
Human 50 CGAGGCTCCAGTGAGAGACCTCAGCTTAGCATCACATTAGGTGCAGCCGG 99
Prairie_vole 93 CA-GCTCTCCCATCCTGGGCGTAGAGCCCGCGCATCTCTGAGGCCATCCG 141
Human 100 CAGGCCATCCCAACTCGGGCCGGGAGCGCACGCGTCACTGGGGCCGTCAG 149
Prairie_vole 142 CTGCGGTGCAACTTCCCCAGTGGCGAGGCAACTTTGGGCTAACCTGCAGG 191
Human 150 TCGCCGTGCAACTTCCCCGGGGG-GAGTCAACTTTAGGTTCGCCTGCGGA 198
Prairie_vole 192 CTCTTTCCAGGTGGCTGGGTCCTGCGCACCGCACCTTGGGGACAGGATGG 241
Human 199 CTCGGTGCAGGTAGCTGGGTGCTAAGCAGGG------GTGGACGGGATG- 241
Prairie_vole 242 CTAGCTAGTACTAGTGCGACCATCAGTTTCTGAGGGAAGGCTCTGGCGCC 291
Human 242 ---GCTAGGGCCGGTGGAGCCATCGGGACCCGAGTGGAGGTGGTGGGGTG 288
Prairie_vole 292 TCTCACACTTCTGGTTCCCGAAATCGCTCAGGGTACTCCGAGGGACTGAA 341
Human 289 CCTCGCACTCCTTGTTCCTGGAGGAGCTCGGGGTGTTCCGAGAGATTGTA 338
Prairie_vole 342 AAGTGACAGTTCGG----ACGACG-----ACCTAGCAGAGCTTTG----- 377
Human 339 AAGTGACTTCTCGGGATTGAGACTCAGAGTCCTTGATTATCTGGGTCCAA 388
Prairie_vole 378 ---------- 377
Human 389 AGCGCAAGTCAGGGGTTC 406
B Exon 3
Prairie_vole 1 CTTTTTCATGAAGCACCTGAGCATCGCTGACCTGGTGGTGGCTGTGTTCC 50
Human 1 CTTCTTCATGAAGCACCTAAGCATCGCCGACCTGGTGGTGGCAGTGTTTC 50
Prairie_vole 51 AGGTGCTCCCGCAGCTGCTGTGGGACATCACCTTCCGCTTCTACGGGCCC 100
Human 51 AGGTGCTGCCGCAGTTGCTGTGGGACATCACCTTCCGCTTCTACGGGCCC 100
Prairie_vole 101 GACCTGCTGTGTCGTCTGGTCAAGTACTTGCAAGTGGTGGGCATGTTCGC 150
Human 101 GACCTGCTGTGCCGCCTGGTCAAGTACTTGCAGGTGGTGGGCATGTTCGC 150
Prairie_vole 151 TTCCACCTACCTGCTGCTGCTTATGTCGCTCGACCGCTGCCTGGCCATCT 200
Human 151 CTCCACCTACCTGCTGCTGCTCATGTCCCTGGACCGCTGCCTGGCCATCT 200
Prairie_vole 201 GCCAGCCGCTGCGCTCTCTGCGACGCCGAACCGACCGCCTGGCGGTGCTA 250
Human 201 GCCAGCCGCTGCGCTCGCTGCGCCGCCGCACCGACCGCCTGGCAGTGCTC 250
Prairie_vole 251 GCGACATGGCTGGGCTGCCTGGTGGCCAGCGCGCCGCAGGTGCACATTTT 300
Human 251 GCCACGTGGCTCGGCTGCCTGGTGGCCAGCGCGCCGCAGGTGCACATCTT 300
Prairie_vole 301 CTCACTGCGCGAAGTGGCGGACGGTGTTTTTGACTGCTGGGCTGTCTTCA 350
Human 301 CTCTCTGCGCGAGGTGGCTGACGGCGTCTTCGACTGCTGGGCCGTCTTCA 350
Prairie_vole 351 TCCAGCCTTGGGGACCCAAGGCCTATGTCACGTGGATCACGCTTGCCGTC 400
Human 351 TCCAGCCCTGGGGACCCAAGGCCTACATCACATGGATCACGCTAGCTGTC 400
Prairie_vole 401 TACATTGTGCCTGTCATAGTGCTGGCCGCCTGCTATGGCCTCATCAGCTT 450
Human 401 TACATCGTGCCGGTCATCGTGCTCGCTGCCTGCTACGGCCTTATCAGCTT 450
Prairie_vole 451 CAAGATCTGGCAGAACCTGCGACTCAAGA---CGGCAGCGGCGGCGGCCG 497
Human 451 CAAGATCTGGCAGAACTTGCGGCTCAAGACCGCTGCAGCGGCGGCGGCCG 500
Prairie_vole 498 AGGGGACTGAGGGATCTGCTGCCGGTGGAGCTGGGCGTGCGGCGCTGGCT 547
Human 501 AGGCGCCAGAGGGCGCGGCGGCTGGCGATGGGGGGCGCGTGGCCCTGGCG 550
Prairie_vole 548 CGAGTCAGTAGCGTCAAGCTCATCTCCA 575
Human 551 CGTGTCAGCAGCGTCAAGCTCATCTCCA 578

Figure S2.1. Alignment of conserved MT2 ad exon 3 regions in prairie voles and humans. A) Alignment of MT2 region in prairie voles (micOch1.0 JH996431.1:26,357,582-26,357,959) and humans (GRCh38, chr3: 8,769,034-8,769,438). In both prairie voles and humans, the minus (coding) strand is shown. Prairie vole CpGs are in bold and numbered 1 through 24, with the exception of previously studied CpG sites -934_1, -934_2, -924, and -901, which are named according to homology with human CpG sites. Human CpGs are also in bold; select sites which have been previously studied or are directly conserved in prairie voles are named according to distance from the translation start site [70]. B) Alignment of exon 3 region in prairie voles (micOch1.0 JH996431.1:26,356,019-26,356,593) and humans (GRCh38 chr3: 8,767,386-8,767,963). In both prairie voles and humans, the minus (coding) strand is shown. CpGs in both humans and prairie voles are in bold; prairie vole CpGs are numbered 1 through 42.

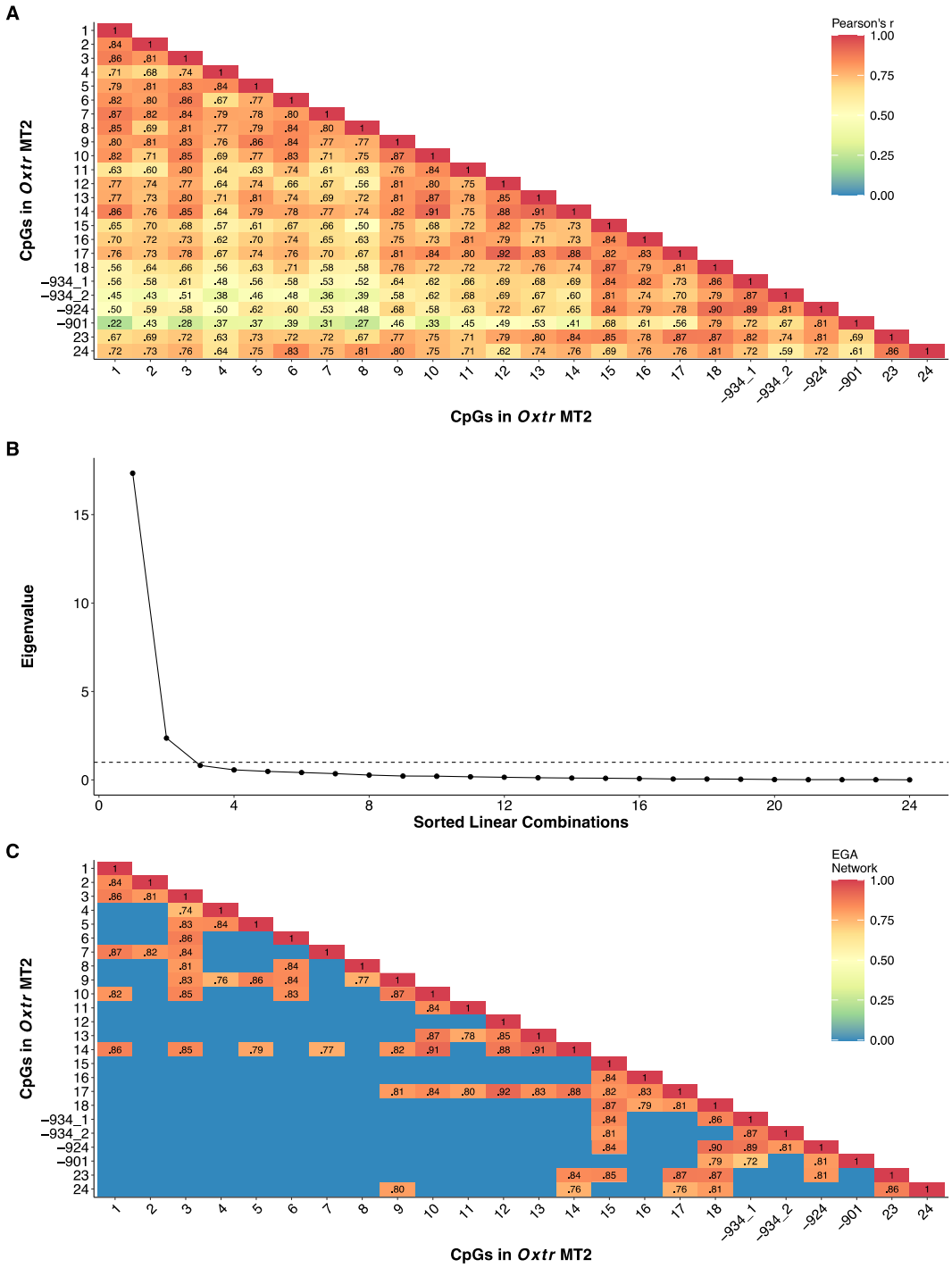

Figure S2.2. Dimensionality reduction of MT2 using Exploratory Graph Analysis. A) Correlation matrix for DNA methylation in MT2 in prairie vole nucleus accumbens. B) Scree plot indicating that DNA methylation in MT2 can be represented using 3 linear combinations. C) Adjacency matrix indicating remaining correlations after dimension reduction displaying correlations of DNA methylation at CpG sites with connections in the EGA network.

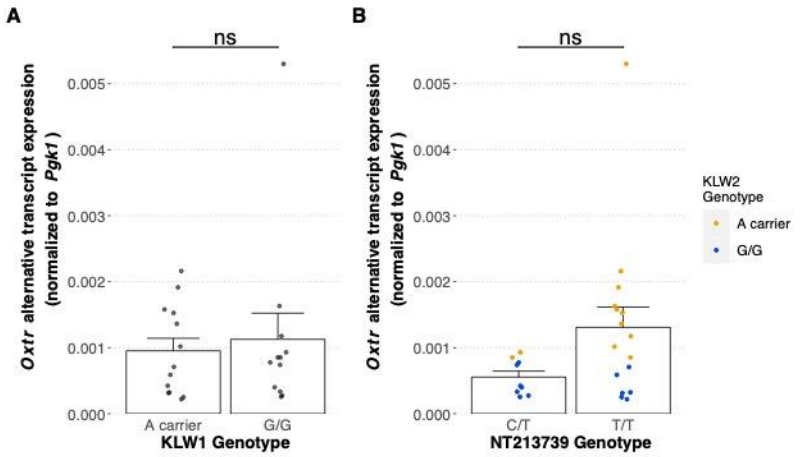

Figure S2.3. Expression of the *Oxtr* alternative transcript is not impacted by KLW1 or NT213739 genotype. A) There is no significant difference in *Oxtr* alternative transcript expression levels between KLW1 genotypes (A carrier: n=14, G/G: n=12; Wilcoxon rank sum test, W=77, p=0.98). B) There is so significant difference in *Oxtr* alternative transcript expression levels between NT213739 genotypes (C/T: n=9, T/T: n=17; Wilcoxon rank sum test, W=42, p=0.1). The data points are colored according to KLW2 genotype to show that the observed increased present in NT213739 T/T animals is because of increased numbers of KLW2 A carriers.

Table S2.1. Correlation of MT2 CpG Sites with *Oxtr* gene expression in prairie vole brain.

MT2 CpG Site	Genomic Coordinate (bp) (michOch1.0)	ρ	p value
1	JH996431.1: 26,357,956	-0.282608696	0.180369104
2	JH996431.1: 26,357,952	0.165217391	0.438653492
3	JH996431.1: 26,357,905	-0.145248971	0.498285055
4	JH996431.1: 26,357,892	-0.273162393	0.176435702
5	JH996431.1: 26,357,881	-0.228120797	0.272750625
6	JH996431.1: 26,357,877	-0.210434783	0.322103767
7	JH996431.1: 26,357,872	-0.297749573	0.148302135
8	JH996431.1: 26,357,869	-0.235429895	0.257256834
9	JH996431.1: 26,357,848	-0.376923077	0.064109728
10	JH996431.1: 26,357,839	-0.355897436	0.075012607
11	JH996431.1: 26,357,837	-0.272307692	0.187272965
12	JH996431.1: 26,357,819	**-0.455726496**	**0.020292825**
13	JH996431.1: 26,357,814	-0.273162393	0.176435702
14	JH996431.1: 26,357,794	-0.347692308	0.082347948
15	JH996431.1: 26,357,743	-0.316923077	0.114856522
16	JH996431.1: 26,357,738	-0.238974359	0.238642685
17	JH996431.1: 26,357,701	**-0.547350427**	**0.004354648**
18	JH996431.1: 26,357,671	**-0.435897436**	**0.027038443**
-934_1	JH996431.1: 26,357,648	-0.293675214	0.145172394
-934_2	JH996431.1: 26,357,642	**-0.508376068**	**0.00877823**
-924	JH996431.1: 26,357,628	**-0.458461538**	**0.019482501**
-901	JH996431.1: 26,357,607	**-0.454358974**	**0.020708305**
23	JH996431.1: 26,357,603	**-0.44957265**	**0.022218149**
24	JH996431.1: 26,357,600	**-0.413076923**	**0.041186079**

Correlation between DNA methylation in MT2 and gene expression was measured using Spearman's rho. Bolded sites indicate significant correlation of DNA methylation and *Oxtr* expression. p-values are not adjusted for multiple comparisons. CpG sites in MT2 are named according to Figure 1C. Genomic coordinates are provided using genome build michOch1.0 (**GCA_000317375.1**).

Table S2.2. Correlation of MT2 CpG Sites with *OXTR* gene expression in human brain (BA41/42).

MT2 CpG Site	Genomic coordinate (bp) (GRCh38.p12 /hg38)	ρ	p value
-1155	Chr3: 8,769,343	NA	NA
-1137	Chr3: 8,769,325	NA	NA
-1132	Chr3: 8,769,320	0.5	0.1173068
-1126	Chr3: 8,769,314	-0.3	0.37008312
-1122	Chr3: 8,769,310	0.5	0.1173068
-1120	Chr3: 8,769,308	NA	NA
-1109	Chr3: 8,769,297	-0.5597585	0.07334733
-1101	Chr3: 8,769,289	0.3	0.37008312
-1098	Chr3: 8,769,286	-0.094388	0.78251392
-1085	Chr3: 8,769,273	0.07515581	0.82616973
-1063	Chr3: 8,769,251	0.57981188	0.06152632
-1057	Chr3: 8,769,245	-0.175292	0.60618047
-1051	Chr3: 8,769,239	0.31013194	0.35332506
-1017	Chr3: 8,769,205	0.1	0.769875
-1002	Chr3: 8,769,190	0.5	0.1173068
-990	Chr3: 8,769,178	-0.4	0.22286835
-983	Chr3: 8,769,171	-0.363756	0.27146808
-959	Chr3: 8,769,147	-0.1284458	0.70663663
-934	Chr3: 8,769,122	**-0.7818182**	**0.00701211**
-924	Chr3: 8,769,112	**-0.6833731**	**0.02043986**
-901	Chr3: 8,769,089	**-0.6560381**	**0.02837692**
-860	Chr3: 8,769,048	-0.2186794	0.518272

Correlation between DNA methylation in MT2 and gene expression was measured using Spearman's rho. Bolded sites indicate significant correlation of DNA methylation and *Oxtr* expression. p-values are not adjusted for multiple comparisons. CpG sites in MT2 are named according to distance from translation start site, as was done in Gregory, Connelly et al [70]. Genomic coordinates are provided using Genome Reference Consortium Human GRCh38.p12 (GCA_000001405.27). At some CpG sites, there was no variation in DNA methylation, as all subjects had 0% methylation. For these sites, Spearman's rho could not be calculated.

Table S2.3. Correlation of Exon 3 CpG Sites with *Oxtr* gene expression.

Site	Genomic Coordinates (bp) (michOch1.0)	ρ	p value
1	JH996431.1: 26,356,568	-0.21983	0.279245
2	JH996431.1: 26,356,533	-0.27521	0.173111
3	JH996431.1: 26,356,507	-0.24444	0.227812
4	JH996431.1: 26,356,499	-0.31897	0.112429
5	JH996431.1: 26,356,493	-0.19863	0.329126
6	JH996431.1: 26,356,480	-0.2294	0.258417
7	JH996431.1: 26,356,445	-0.22667	0.26426
8	JH996431.1: 26,356,416	-0.18496	0.364051
9	JH996431.1: 26,356,412	-0.09265	0.6515
10	JH996431.1: 26,356,408	-0.08581	0.675853
11	JH996431.1: 26,356,386	-0.18222	0.371291
12	JH996431.1: 26,356,381	-0.19179	0.346322
13	JH996431.1: 26,356,372	-0.18974	0.351584
14	JH996431.1: 26,356,369	-0.15077	0.460516
15	JH996431.1: 26,356,366	-0.19658	0.334229
16	JH996431.1: 26,356,361	-0.15832	0.439846
17	JH996431.1: 26,356,357	-0.1665	0.414551
18	JH996431.1: 26,356,350	-0.12479	0.542051
19	JH996431.1: 26,356,341	-0.11521	0.573724
20	JH996431.1: 26,356,313	-0.24103	0.234541
21	JH996431.1: 26,356,311	-0.17197	0.399192
22	JH996431.1: 26,356,308	-0.32923	0.100864
23	JH996431.1: 26,356,285	-0.32513	0.105377
24	JH996431.1: 26,356,283	-0.25949	0.199765
25	JH996431.1: 26,356,275	-0.20342	0.31741
26	JH996431.1: 26,356,271	-0.31522	0.142866
27	JH996431.1: 26,356,212	-0.20957	0.302733
28	JH996431.1: 26,356,203	-0.20615	0.310833
29	JH996431.1: 26,356,196	-0.16991	0.404913
30	JH996431.1: 26,356,166	-0.15419	0.450299
31	JH996431.1: 26,356,123	-0.21162	0.297938
32	JH996431.1: 26,356,113	-0.27726	0.16983
33	JH996431.1: 26,356,107	-0.2588	0.200985
34	JH996431.1: 26,356,104	-0.12068	0.555523
35	JH996431.1: 26,356,101	-0.1159	0.571434
36	**JH996431.1: 26,356,097**	**-0.39077**	**0.049325**
37	JH996431.1: 26,356,073	-0.1453	0.477117
38	JH996431.1: 26,356,060	-0.13641	0.504746
39	JH996431.1: 26,356,056	-0.21641	0.286939
40	JH996431.1: 26,356,053	0.063932	0.755875
41	JH996431.1: 26,356,045	0.026325	0.898975
42	JH996431.1: 26,356,034	-0.05299	0.796906

Correlation between DNA methylation in exon 3 and gene expression was measured using Spearman's rho. Bolded sites indicate significant correlation of DNA methylation and *Oxtr* expression. p-values are not adjusted for multiple comparisons. CpG sites in exon 3 are named according to Figure 1D. Genomic coordinates are provided using genome build michOch1.0 (**Assembly accession ID: GCA_000317375.1**).

Table S2.4: PCR Primers and conditions for DNA methylation and SNP analysis

Region of interest	Primer Names	PCR primers	PCR conditions	Pyrosequencing primer
MT2	KLW201_F	5'-GTAGTTTTGTATTGTGGGAAAGT-3'	Step 1: 95°C/15 min, 1 cycle Step 2: 94°C/30s, 58.6°C/30s, 72°C/30s, 45 cycles Step 3: 72°C/10 min, 1 cycle Step 4: 4°C hold	KLW201_S1: 5'-TTGGTTATAGTTTTTTTTTGTTTT-3'
	TSL201_R	5'-[biotin]CCAACAACCTCAAAACTCTACT-3'		KLW201_S2: 5'-GTTATAGATTAGAGGATTGTAAAGA-3'
				KLW201_S3: 5'-TGGAGTAGGTAGTTTTTTTATTTTG-3'
				KLW201_S4: 5'-AGAGTTAGAGTATTTTTGAGGTTA-3'
				KLW201_S5: 5'-AGGTTTTTTTTAGGTGG-3'
				KLW201_S6: 5'-GATGGTTAGTTAGTATTAGTG-3'
				TSL201_S1: 5'-GAGGGAAGGTTTTGGAGTTTTTTATAT-3'
				TSL201_S2: 5'-AGGGATTGAAAAGTGA-3'
Exon 3 Section 1	KLW301_F	5'-GAGGTGGAGGTGTTGTGTTTTATTTTGT-3'	Step 1: 95°C/15 min, 1 cycle Step 2: 94°C/30s, 58°C/30s, 72°C/30s, 45 cycles Step 3: 72°C/10 min, 1 cycle Step 4: 4°C hold	KLW301_S1: 5'-TTTTTTTTTATGAAGTATTTGAGTA-3'
	KLW301_R	5'-[biotin]ACCAAACAACCCAACCATATC-3'		
Exon 3 Section 2-4	KLW302_F	5'-AGGTGTTTTAGTAGTTGTTGTGGGATATT-3'	Step 1: 95°C/15 min, 1 cycle Step 2: 94°C/30s, 63°C/30s, 72°C/30s, 45 cycles Step 3: 72°C/10 min, 1 cycle Step 4: 4°C hold	KLW302_S2: 5'-GTTGTTGTGGGATATTATTTT -3'
	KLW302_R	5'-[biotin]CATAAACCTTAAATCCCCAAAACTAAA-3'		KLW302_S3: 5'-TTTGTAGGTGGTGGG-3'
				KLW302_S4: 5'-GTTGTTTGGTTATTTGTTAGT-3'
Exon 3	KLW305_F	5'-TATGGTTGGGTTGTTTGGTGGTTA-3'	Step 1: 95°C/15 min, 1 cycle	KLW305_S5: 5'-GTTGTTTGGTGGTTAG-3'

Section 5	KLW305_R	5'-[biotin]CATAAACCTTAAATCCCCAAAACTAAA-3'	Step 2: 94°C/30s, 57°C/30s, 72°C/30s, 45 cycles Step 3: 72°C/10 min, 1 cycle Step 4: 4°C hold	
Exon 3 Sections 6-8	KLW306_F	5'-ATTTAGTTTTGGGGATTTAAGGTTTA-3'	Step 1: 95°C/15 min, 1 cycle Step 2: 94°C/30s, 57°C/30s, 72°C/30s, 45 cycles Step 3: 72°C/10 min, 1 cycle Step 4: 4°C hold	KLW306_S6: 5'-GGGGATTTAAGGTTTATG-3'
	KLW306_R	5'-[biotin]ACCAATACAATAATAAAAATCATCTTCACT-3'		KLW306_S7: 5'-AGTTTTAAGATTTGGTAGAAT-3'
				KLW306_S8: 5'-GAGGGGATTGAGGGA-3'
KLW1	KLW325_F	5'- TGTTCGCTTCCACCTACCTG-3'	Step 1: 95°C/15 min, 1 cycle Step 2: 94°C/30s, 63°C/30s, 72°C/30s, 45 cycles Step 3: 72°C/10 min, 1 cycle Step 4: 4°C hold	KLW325_S1: 5'-TTTCTCACTGCGCGA-3'
	KLW325_R	5'- [biotin]ATGAGCTTGACGCTACTGACTC-3'		
KLW2	KLW333_F	5'- GGACCCAAGGCCTATGTCA-3'	Step 1: 95°C/15 min, 1 cycle Step 2: 94°C/30s, 58°C/30s, 72°C/30s, 45 cycles Step 3: 72°C/10 min, 1 cycle Step 4: 4°C hold	KLW333_S1: 5'-TCAAGATCTGGCAGAAC-3'
	KLW333_R	5'- [biotin]ATGAGCTTGACGCTACTGACTCG-3'		

Table S2.5: RT-PCR primers and conditions

Gene	Primers	PCR conditions	Efficiency
Oxtr main transcript	F (TSL401_F): 5′-GCCTTTCTTCTTCGTGCAGATG-3′ R (TSL401_R): 5′-ATGTAGATCCAGGGGTTGCAG-3′	Step 1: 95°C/10 min, 1 cycle Step 2: 95°C/15s, 63.4°C/60s, 35 cycles	E: 99.7% R^2: 0.993
Oxtr alternative transcript	F (JSD_201_F): 5'-TTTTTGCTTTCCCAATGTGC-3' R (JSD_201_R): 5'-CCGTGAACAGCATGTAGATCCA-3'	Step 1: 95°C/10 min, 1 cycle Step 2: 95°C/15s, 59.5°C/60s, 35 cycles	E: 100.3% R^2: 0.971
Pgk1	F (TSL402_F): 5′-TTGCCCGTTGACTTTGTCAC-3′ R (TSL402_R): 5′-GCCACAGCCTCAGCATATTTC-3′	Step 1: 95°C/10 min, 1 cycle Step 2: 95°C/15s, 65.3°C/60s, 35 cycles	E: 93.5% R^2: 0.998

References

1. Lozupone, M. *et al.* The Role of Biomarkers in Psychiatry. in *Advances in Experimental Medicine and Biology* vol. 1118 135–162 (Springer New York LLC, 2019).
2. Rutigliano, G. *et al.* Peripheral oxytocin and vasopressin: Biomarkers of psychiatric disorders? A comprehensive systematic review and preliminary meta-analysis. *Psychiatry Research* **241**, 207–220 (2016).
3. Romano, A., Tempesta, B., Di Bonaventura, M. V. M. & Gaetani, S. From autism to eating disorders and more: The role of oxytocin in neuropsychiatric disorders. *Frontiers in Neuroscience* **9**, 497 (2016).
4. Carter, C. S. *et al.* Is Oxytocin "Nature's Medicine"? *Pharmacological Reviews* **72**, 829–861 (2020).
5. Zik, J. B. & Roberts, D. L. The many faces of oxytocin: Implications for psychiatry. *Psychiatry Research* **226**, 31–37 (2015).
6. Jones, C., Barrera, I., Brothers, S., Ring, R. & Wahlestedt, C. Oxytocin and social functioning. *Dialogues in Clinical Neuroscience* **19**, 193–201 (2017).
7. Andari, E., Hurlemann, R. & Young, L. J. A precision medicine approach to oxytocin trials. in *Current Topics in Behavioral Neurosciences* vol. 35 559–590 (Springer Verlag, 2018).
8. MacLean, E. L. *et al.* Challenges for measuring oxytocin: The blind men and the elephant? *Psychoneuroendocrinology* **107**, 225–231 (2019).
9. Berdasco, M. & Esteller, M. Clinical epigenetics: seizing opportunities for translation. *Nature Reviews Genetics* **20**, 109–127 (2019).
10. Bird, A. The dinucleotide CG as a genomic signalling module. *Journal of Molecular Biology* **409**, 47–53 (2011).
11. Inoue, T. *et al.* Structural organization of the human oxytocin receptor gene. *The Journal of biological chemistry* **269**, 32451–6 (1994).
12. Kusui, C. *et al.* DNA methylation of the human oxytocin receptor gene promoter regulates tissue-specific gene suppression. *Biochemical and Biophysical Research Communications* **289**, 681–686 (2001).
13. Quintana, D. S. *et al.* Oxytocin pathway gene networks in the human brain. *Nature Communications* **10**, (2019).
14. Gregory, S. G. *et al.* Genomic and epigenetic evidence for oxytocin receptor deficiency in autism. *BMC Medicine* **7**, (2009).
15. Uhrig, S. *et al.* Reduced oxytocin receptor gene expression and binding sites in different brain regions in schizophrenia: A post-mortem study. *Schizophrenia Research* **177**, 59–66 (2016).
16. Lee, M. R. *et al.* Oxytocin receptor mRNA expression in dorsolateral prefrontal cortex in major psychiatric disorders: A human post-mortem study. *Psychoneuroendocrinology* **96**, 143–147 (2018).
17. Cecil, C. *et al.* Environmental risk, Oxytocin Receptor Gene (OXTR) methylation and youth callous-unemotional traits: a 13-year longitudinal study. *Molecular Psychiatry* **19**, 1071–1077 (2014).
18. Dadds, M. R. *et al.* Methylation of the oxytocin receptor gene and oxytocin blood levels in the development of psychopathy. *Development and Psychopathology* **26**, 33–40 (2014).
19. Kim, Y. R., Kim, J. H., Kim, M. J. & Treasure, J. Differential methylation of the oxytocin receptor gene in patients with anorexia nervosa: A pilot study. *PLoS ONE* **9**, (2014).
20. Thaler, L. *et al.* Methylation of the *OXTR* gene in women with anorexia nervosa: Relationship to social behavior. *European Eating Disorders Review* **28**, 79–86 (2020).
21. Rubin, L. H. *et al.* Sex and Diagnosis-Specific Associations between DNA Methylation of the Oxytocin Receptor Gene with Emotion Processing and Temporal-Limbic and Prefrontal

Brain Volumes in Psychotic Disorders. *Biological Psychiatry: Cognitive Neuroscience and Neuroimaging* **1**, 141–151 (2016).
22. Bang, M. *et al.* Reduced DNA Methylation of the Oxytocin Receptor Gene Is Associated with Anhedonia-Asociality in Women with Recent-Onset Schizophrenia and Ultra-high Risk for Psychosis. *Schizophrenia Bulletin* **45**, 1279–1290 (2019).
23. Bell, A. F. *et al.* Interaction between oxytocin receptor DNA methylation and genotype is associated with risk of postpartum depression in women without depression in pregnancy. *Frontiers in Genetics* **6**, 243 (2015).
24. Ebner, N. C. *et al.* Associations between oxytocin receptor gene (OXTR) methylation, plasma oxytocin, and attachment across adulthood. *International Journal of Psychophysiology* **136**, 22–32 (2019).
25. Park, C. I., Kim, H. W., Jeon, S., Kang, J. I. & Kim, S. J. Reduced DNA methylation of the oxytocin receptor gene is associated with obsessive-compulsive disorder. *Clinical Epigenetics* **12**, 101 (2020).
26. Smearman, E. L. *et al.* Oxytocin Receptor Genetic and Epigenetic Variations: Association With Child Abuse and Adult Psychiatric Symptoms. *Child Development* **87**, 122–134 (2016).
27. Jack, A., Connelly, J. J. & Morris, J. P. DNA methylation of the oxytocin receptor gene predicts neural response to ambiguous social stimuli. *Frontiers in Human Neuroscience* **6**, 280 (2012).
28. Puglia, M. H., Lillard, T. S., Morris, J. P. & Connelly, J. J. Epigenetic modification of the oxytocin receptor gene influences the perception of anger and fear in the human brain. *Proceedings of the National Academy of Sciences* **112**, 3308–3313 (2015).
29. Krol, K. M., Puglia, M. H., Morris, J. P., Connelly, J. J. & Grossmann, T. Epigenetic modification of the oxytocin receptor gene is associated with emotion processing in the infant brain. *Developmental Cognitive Neuroscience* **37**, 100648 (2019).
30. Puglia, M. H., Connelly, J. J. & Morris, J. P. Epigenetic regulation of the oxytocin receptor is associated with neural response during selective social attention. *Translational Psychiatry* **8**, 116 (2018).
31. Chagnon, Y. C., Potvin, O., Hudon, C. & Préville, M. DNA methylation and single nucleotide variants in the brain-derived neurotrophic factor (BDNF) and oxytocin receptor (OXTR) genes are associated with anxiety/depression in older women. *Frontiers in Genetics* **6**, 230 (2015).
32. Ziegler, C. *et al.* Oxytocin Receptor Gene Methylation: Converging Multilevel Evidence for a Role in Social Anxiety. *Neuropsychopharmacology* **40**, 1528–1538 (2015).
33. Cappi, C. *et al.* Epigenetic evidence for involvement of the oxytocin receptor gene in obsessive-compulsive disorder. *BMC Neurosci* **17**, 79 (2016).
34. Nawijn, L. *et al.* Oxytocin receptor gene methylation in male and female PTSD patients and trauma-exposed controls. *European Neuropsychopharmacology* **29**, 147–155 (2019).
35. Rijlaarsdam, J. *et al.* Prenatal stress exposure, oxytocin receptor gene (*OXTR*) methylation, and child autistic traits: The moderating role of *OXTR* rs53576 genotype. *Autism Research* **10**, 430–438 (2017).
36. Tabbaa, M., Paedae, B., Liu, Y. & Wang, Z. Neuropeptide regulation of social attachment: The prairie vole model. *Comprehensive Physiology* **7**, 81–104 (2017).
37. Perkeybile, A. M. *et al.* Early nurture epigenetically tunes the oxytocin receptor. *Psychoneuroendocrinology* **99**, 128–136 (2019).
38. Kenkel, W. M. *et al.* Behavioral and epigenetic consequences of oxytocin treatment at birth. *Science Advances* **5**, eaav2244 (2019).
39. Graffelman, J. Exploring diallelic genetic markers: The HardyWeinberg package. *Journal of Statistical Software* **64**, (2015).
40. Warnes, G. genetics: Population Genetics. (2019).

41. Boda, E., Pini, A., Hoxha, E., Parolisi, R. & Tempia, F. Selection of reference genes for quantitative real-time RT-PCR studies in mouse brain. *Journal of Molecular Neuroscience* **37**, 238–253 (2009).
42. Martin, M. Cutadapt removes adapter sequences from high-throughput sequencing reads. *EMBnet.journal* (2011) doi:10.14806/ej.17.1.200.
43. Ewels, P., Magnusson, M., Lundin, S. & Käller, M. MultiQC: Summarize analysis results for multiple tools and samples in a single report. *Bioinformatics* **32**, 3047–3048 (2016).
44. Pertea, M., Kim, D., Pertea, G. M., Leek, J. T. & Salzberg, S. L. Transcript-level expression analysis of RNA-seq experiments with HISAT, StringTie and Ballgown. *Nature Protocols* **11**, 1650–1667 (2016).
45. Dobin, A. *et al.* STAR: Ultrafast universal RNA-seq aligner. *Bioinformatics* **29**, 15–21 (2013).
46. Pertea, M. *et al.* StringTie enables improved reconstruction of a transcriptome from RNA-seq reads. *Nature Biotechnology* **33**, 290–295 (2015).
47. Thorvaldsdóttir, H., Robinson, J. T. & Mesirov, J. P. Integrative Genomics Viewer (IGV): High-performance genomics data visualization and exploration. *Briefings in Bioinformatics* **14**, 178–192 (2013).
48. Team, R. C. R: A Language and Environment for Statistical Computing. (2018).
49. Wickham, H. ggplot2: Elegant Graphics for Data Analysis. (2016).
50. Kassambara, A. ggpubr: 'ggplot2' Based Publication Ready Plots. R package version 0.1.7. *https://CRAN.R-project.org/package=ggpubr* (2018) doi:R package version 0.1.8.
51. Bates, D., Mächler, M., Bolker, B. M. & Walker, S. C. Fitting linear mixed-effects models using lme4. *Journal of Statistical Software* **67**, (2015).
52. Fox, J. & Weisberg, S. An {R} Companion to Applied Regression, (top). *Thousand Oaks CA: Sage.* (2019).
53. Golino, H. & Christensen, A. EGAnet: Exploratory Graph Analysis -- A framework for estimating the number of dimensions in multivariate data using network psychometrics. (2020).
54. Massara, G. P., Di Matteo, T. & Aste, T. Network filtering for big data: Triangulated maximally filtered graph. *Journal of Complex Networks* **5**, 161–178 (2016).
55. Golino, H. F. & Epskamp, S. Exploratory graph analysis: A new approach for estimating the number of dimensions in psychological research. *PLoS ONE* **12**, e0174035 (2017).
56. Golino, H. *et al.* Investigating the Performance of Exploratory Graph Analysis and Traditional Techniques to Identify the Number of Latent Factors: A Simulation and Tutorial. *Psychological Methods* **25**, 292 (2020).
57. Christensen, A. & Golino, H. Estimating the stability of the number of factors via Bootstrap Exploratory Graph Analysis: A tutorial. (2019) doi:10.31234/osf.io/9deay.
58. Christensen, A. P., Golino, H. & Silvia, P. J. A Psychometric Network Perspective on the Validity and Validation of Personality Trait Questionnaires. *European Journal of Personality* per.2265 (2020) doi:10.1002/per.2265.
59. King, L. B., Walum, H., Inoue, K., Eyrich, N. W. & Young, L. J. Variation in the Oxytocin Receptor Gene Predicts Brain Region–Specific Expression and Social Attachment. *Biological Psychiatry* **80**, 160–169 (2016).
60. Gouin, J. P. *et al.* Associations among oxytocin receptor gene (OXTR) DNA methylation in adulthood, exposure to early life adversity, and childhood trajectories of anxiousness. *Scientific Reports* **7**, 1–14 (2017).
61. Krol, K. M., Moulder, R. G., Lillard, T. S., Grossmann, T. & Connelly, J. J. Epigenetic dynamics in infancy and the impact of maternal engagement. *Science Advances* **5**, (2019).
62. Unternaehrer, E. *et al.* Childhood maternal care is associated with DNA methylation of the genes for brain-derived neurotrophic factor (BDNF) and oxytocin receptor (OXTR) in peripheral blood cells in adult men and women. *Stress* **18**, 451–461 (2015).

63. Feldman, R., Monakhov, M., Pratt, M. & Ebstein, R. P. Oxytocin Pathway Genes: Evolutionary Ancient System Impacting on Human Affiliation, Sociality, and Psychopathology. *Biological Psychiatry* **79**, 174–184 (2016).
64. Towers, A. J. *et al.* Epigenetic dysregulation of Oxtr in Tet1-deficient mice has implications for neuropsychiatric disorders. *JCI Insight* **6**, e120592 (2018).
65. Di Ruscio, A. *et al.* DNMT1-interacting RNAs block gene-specific DNA methylation. *Nature* **503**, 371–376 (2013).
66. de la Mora, M. P. *et al.* Signaling in dopamine D2 receptor-oxytocin receptor heterocomplexes and its relevance for the anxiolytic effects of dopamine and oxytocin interactions in the amygdala of the rat. *Biochimica et Biophysica Acta - Molecular Basis of Disease* **1862**, 2075–2085 (2016).
67. Romero-Fernandez, W., Borroto-Escuela, D. O., Agnati, L. F. & Fuxe, K. Evidence for the existence of dopamine d2-oxytocin receptor heteromers in the ventral and dorsal striatum with facilitatory receptor-receptor interactions. *Molecular Psychiatry* **18**, 849–850 (2013).
68. Oakley, R. H., Laporte, S. A., Holt, J. A., Barak, L. S. & Caron, M. G. Molecular Determinants Underlying the Formation of Stable Intracellular G Protein-coupled Receptor-β-Arrestin Complexes after Receptor Endocytosis. *Journal of Biological Chemistry* **276**, 19452–19460 (2001).
69. Lonsdale, J. *et al.* The Genotype-Tissue Expression (GTEx) project. *Nature Genetics* **45**, 580–585 (2013).
70. Gregory, S. G. *et al.* Genomic and epigenetic evidence for oxytocin receptor deficiency in autism. *BMC Medicine* **7**, (2009).

Chapter 3: Explore transcriptomic, neurodevelopmental, and behavioral consequences of early nurture.

Manuscript in preparation for submission to a peer reviewed journal.

Joshua S. Danoff[1,2], Erin N. Ramos[1,2], Allison M. Perkeybile[1,2], Taylor D. Hinton[1,2], Andrew J. Graves[1,2], Graham C. Quinn[1], Aaron R. Lightbody-Cimer[1], Juozas Gordevičius[3], Robert T. Brooke[3], Xiaorong Liu[1,2], C. Sue Carter[1], Karen L. Bales[4], Alev Erisir[1,2]*, Jessica J. Connelly[1,2]*

[1]Department of Psychology, University of Virginia, Charlottesville, VA
[2]Program in Fundamental Neuroscience, University of Virginia, Charlottesville, VA
[3]Epigenetic Clock Development Foundation, Torrance, CA
[4]Department of Psychology, University of California, Davis, Davis, CA

*These authors contributed equally.

Abstract

Parental care during the critical period of early life influences developmental trajectories with consequences throughout the life span. In prairie voles, a socially monogamous and biparental species, early life parental care leads to increased sociality later in life. Though these effects are partially due to changes in the endogenous oxytocin system, how early life parental care may alter larger neurodevelopmental processes is not well understood. First, we examine how epigenetic age is impacted by early nurture and find that prairie voles raised by higher care parents have lower epigenetic age than those raised by low care parents, suggesting that early nurture prevents epigenetic age acceleration. Next, using RNA-sequencing, we show that early life parental care has a large, sex-specific impact on transcription in the nucleus accumbens: males raised by high care parents have 321 differentially expressed genes at genome-wide significance compared to males raised by low-care parents while females only have three. In males, differentially expressed genes that are sensitive to early life care in the brain included autism risk genes and genes involved in neurodevelopment and synaptic transmission. Using a quantitative electron microscopy approach, we then show that the density of synapses in male offspring is highly correlated with parental care composition, such that males raised with more care by their fathers have more excitatory synapses with small synaptic zones. The same measures are not impacted by parental care composition in female offspring. Finally, we show parental care composition has sex-specific effects on pup retrieval behavior in juveniles such that males raised with high paternal care display more pup retrievals while females raised by high paternal care display fewer pup retrievals, indicting sex-specific impacts of parental care composition on social behavior development. These results suggest that the developing male brain is uniquely sensitive to paternal care which impacts sociality throughout the lifespan.

Introduction

Early life experiences, particularly nurture by parents, are critical determinants of the developmental trajectory of neuropsychological outcomes. In humans, early life stress is associated with many adverse neuropsychological outcomes, including disruptions in emotion regulation[1] as well as changes to the structure and connectivity of limbic regions. More subtle variations in parental behavior also have long lasting effects on neuropsychological outcomes in children. For example, maternal and paternal warmth is correlated with increased prosocial behavior[2], and maternal warmth early in childhood is associated with decreased activation in the

medial prefrontal cortex and striatum during reward anticipation in early adulthood[3]. While the effects of early life experience in the form of parenting are well documented, the neurobiological mechanisms mediating the effects are not well defined.

One mechanism by which early life experience impacts behaviors later in life is by changing the pace of development. In humans, early life stress, particularly via lower parental care, accelerates biological aging, with implications for stress response and emotion regulation throughout the lifespan[4,5]. One biological indicator of aging is epigenetic age, which uses DNA methylation measurements to predict age[6]. If one's predicted epigenetic age is higher than their chronological age, they would be age-accelerated – that is, they have aged faster than their chronological age suggests. We and others have shown that early life social experiences impact epigenetic aging. Early life experiences that increase epigenetic age include exposure to violence, trauma, low socioeconomic status, and poor peer relationships[7–11].

In rodent models, it is well established that variation in maternal care leads to individual differences in development and behavior[12–14]. One relevant model for studying development of social behaviors is the prairie vole (*Microtus ochrogaster*), a species which displays human-like social behaviors including monogamous pair bonding and both maternal and paternal care of offspring[15,16]. Prairie voles display a naturally wide range of parental behaviors which are linked to offspring's variability in pair bond formation and alloparenting (parenting a pup that is not one's own) later in life[17–20]. Early nurture can be increased in the laboratory by a single episode of handling on the first day of life, leading to increased parental care behavior by the parents and increased pair bond formation and parental care in the offspring[21,22].

In mice and rats, it has been shown that early life nurture alters genome-wide gene expression throughout the lifespan in many brain regions[23–28]. We have previously shown differences in early nurture lead to changes in the epigenetic state and expression of the oxytocin receptor gene, *Oxtr*, in the nucleus accumbens, the central brain region for reward pathways and a node of the social decision making network critical for species-typical parental behaviors[21,29,30]. Further, early nurture has consequences for neurodevelopmental outcomes including synapse development and neuroimmune activity. For example, paternal deprivation in the biparental rodent degu (*Octodon degus*) results in decreased spine density in cortical areas in juvenile offspring[31,32]. In addition to oxytocin, early nurture and other early life stressors impact the development of many neurotransmitter systems in the nucleus accumbens, including glutamatergic signaling[27], catecholamines[33], and opioids[34], indicating numerous experience-dependent changes in the circuitry in this region. Early nurture can also alter neuroimmune outcomes including the number and morphology of microglia[35,36], the expression of cytokines[37,38] and other immune regulators[39]. In prairie voles, microglia proliferation is sensitive to social experience[40,41]. Altogether, these studies suggest that early life experience profoundly impacts the development and circuitry of the brain, including nucleus accumbens.

Many studies of early life experience use models that are not naturalistic, including maternal separation and paternal deprivation, which may not recapitulate the typical childhood experience[42]. Additionally, even more naturalistic early life stress models such as the limited bedding and nesting model, which induces chronic stress to the mother, results in atypical parental behavior[43]. Here, we examine the impact of parental care on neurodevelopment using two types of parental care paradigms. The first is a handling model, where the parents of one group are directly handled (MAN1) and the control group is indirectly handled (MAN0). We have previously shown that this subtle manipulation increases parental care during the first week of life[21] and promotes adult species typical behavior in offspring[22]. The second paradigm is a natural parenting observation where the breeding pairs are unmanipulated and instead the parental behaviors are directly quantified. Using these paradigms, we provide epigenetic and neuroanatomical evidence that early nurture leads to slowed development. We also identify transcriptional programs that are sensitive to early nurture in males only. Further, we found that paternal care is associated with changes in excitatory synapses in nucleus accumbens of male

offspring only. We also identify a sex-specific impact of paternal care on pup retrieval behavior in juvenile prairie voles. These findings provide evidence that male prairie voles are uniquely sensitive to early life paternal care with consequences for neurodevelopment and behavior and provide a foundation for investigation of human male-biased neurodevelopmental disorders.

Material and Methods

Animal Model

Subjects were laboratory-bred prairie voles (*Microtus ochrogaster*) descended from a wild-caught stock captured near Champaign, Illinois, previously used in our study of *Oxtr* DNA methylation and expression[21]. The procedures for the MAN paradigm, tissue collection, and DNA and RNA isolation are repeated below. Breeding pairs were housed in polycarbonate hamster cages (44cm x 22cm x 16cm). Same sex sibling pairs were housed in polycarbonate mouse cages (27cm x 16cm x 16cm) after weaning on postnatal day 20 (PND20). Animals were given food (high-fiber Purina rabbit chow) and water *ad libitum*, cotton nestlets for nesting material, and were maintained on a 14:10 light:dark cycle. All procedures were approved by the IACUC at the University of California, Davis (subjects for RNA-sequencing), the IACUC at Indiana University (subjects for neuroanatomy), or the IACUC at the University of Virginia (subjects for behavior and microglia time course). 13 male-female sibling pairs were used for RNA sequencing and DNA methylation analysis. 11 male-female sibling pairs were used for immunohistochemistry and a subset of 6 sibling pairs were used for electron microscopy. An additional 23 animals were used for a developmental time course of microglia cell density. 27 male-female sibling pairs were used for alloparenting testing. The total number of animals used in these studies is 125.

The MAN handling paradigm

Within 24 hours of giving birth, breeding pairs experienced a single handling manipulation, either MAN0 (indirect) or MAN1 (direct), a paradigm used to increase parental care in prairie voles[21,22,44]. MAN0, the indirect handling manipulation, consists of picking up the animals in a clear plastic cup for 30 seconds. If animals were sitting, they were scooped into the cup. If animals were walking around the cage, the cup was positioned so that the animals would walk into it. In MAN1, the direct handling manipulation, the mother and father were picked up by the scruff of the neck by a gloved hand for 30 seconds. In both manipulations, both the mother and father were handled in the same way and pups were not handled by the experimenter. MAN1 breeders display higher levels of parenting after the manipulation, which disappears before PND8[21]. There were seven MAN0 litters and six MAN1 litters in this study. A total of 26 pups (one male and one female from each litter) were used for the RNA-sequencing and DNA methylation experiments.

Tissue collection and nucleic acid isolation

Seven male-female sibling pairs from MAN0 litters and six male-female sibling pairs from MAN1 litters were used for RNA-sequencing. Within three days of weaning (PND21-24), brain and blood tissues were collected, immediately frozen on dry ice, and stored at -80˚C until nucleic acid isolation. Brains were equilibrated to -20˚C for two hours prior to dissection. Brains were dissected by 1) a coronal cut to remove the olfactory bulbs, 2) a coronal cut at the optic nerve chiasma just rostral to the hypothalamus and bregma, and 3) bilateral punches (1mm in diameter and 2 mm in depth) to isolate the tissue including nucleus accumbens and cell-devoid regions of anterior commissure. Following dissection,the nucleus accumbens tissue was placed in a DNAse/RNAse free microcentrifuge tube and flash frozen with liquid nitrogen. DNA and RNA were extracted from the nucleus accumbens punches with the Qiagen AllPrep DNA/RNA Mini Kit (Qiagen, Valencia, CA) following manufacturer instructions, and stored at -20˚C (DNA) or -80˚C (RNA) until further analysis.

RNA-seq and transcript alignment

RNA quality was assessed using Agilent Tape Station. All samples had RIN score greater than 7. Libraries were generated from 500 ng RNA using the NEBNext Ultra Directional RNA Library Prep Kit (New England Biolabs, Ipswich, MA) with mRNA magnetic isolation. Multiplexed libraries were sequenced at 2 X 75 basepair paired-end reads on the Illumina NextSeq 500 platform at Genome Analysis and Technology Core, University of Virginia, with 25 million reads per sample. The raw sequencing data was subjected to pre-processing steps of adapter removal and quality-based trimming using TrimGalore with removal of auto-detected Illumina adapters and trimming of low-quality ends up to a threshold of Q20[45]. Reads that became shorter than 35 bp due to either adapter removal or quality trimming were discarded. Quality control was completed with MultiQC[46]. Transcript abundances in the dataset were quantified using pseudoalignment approach of Kallisto[47], against the annotated transcriptome of Prairie vole (*Microtus ochrogaster, MicOch v1.0,* Ensembl release version 96, which includes 19,648 annotated genes. One sample (MAN1 male) was excluded from further analysis because of poor sequencing quality.

Pan-mammalian DNA Methylation Array and Clock Scores

DNA concentration was measured using the Qubit 1X dsDNA BR assay (Invitrogen, Eugene OR). 250 ng DNA was bisulfite converted using the EZ DNA methylation kit (Zymo, Irvine, CA) and DNA methylation was assayed using the custom Illumina chip "HorvathMammalMethylChip40", which provides coverage of CpG site high conserved in mammals[48]. Array data was preprocessed and beta values were defined using SeSaMe normalization[49,50]. Epigenetic age estimates were calculated for the universal mammalian clock[51].

RT-PCR validation of RNA-seq results

RNA was processed for cDNA synthesis following the protocol provided in the iScript cDNA Synthesis kit (Bio-Rad, Hercules, CA). Real-time PCR was conducted using the CFX96 System (Bio-Rad) using *Power* SYBR Green (Applied Biosystems). Real-time PCR for *Pgk1* was completed on both Real-time PCR systems. See Supplementary Table 2.1 for all RT-PCR primers and cycling conditions. All reactions were run in triplicate (replicate standard deviation was <0.05) and their specificity verified by melting curve analysis and separation on a 2% agarose gel. Primer performance was evaluated using standard serial dilution and all primer sets performed within acceptable range for efficiency (See Appendix A, Table A.1). Relative gene expression is presented using the comparative Ct method, $2^{-\Delta Ct}$, comparing target expression to *Pgk1* expression measured on the same Real-time PCR system.

Statistical analysis of RNA-seq, qPCR, and Epigenetic Age Data

Principal components analysis on the 500 most variably expressed genes was completed using the pcaExplorer package[52] in R version 3.5.2[53]. Differential expression analysis was completed using the DESeq2 package, which identifies significance at the genome-wide level[54]. Only genes with greater than 1 transcript per million on average across samples (13,751 genes) were included in the DESeq2 analysis. Samples were subset by sex before DESeq2 analysis, such that MAN0 males were compared to MAN1 males and MAN0 females were compared to MAN1 females.

Gene ontology (GO) analysis and Kyoto Encyclopedia of Genes and Genomes (KEGG) enrichment analysis was completed using the clusterProfiler package[55]. Input genes were converted to mouse entrez IDs using biomaRt[56]. To test for enriched GO terms, input genes were restricted to genes with unadjusted p-values less than 0.05 and absolute fold change greater than

1.25 compared to the background list of 13,751 genes with average expression greater than 1 transcript per million in our dataset. Upregulated and downregulated genes were examined separately. For KEGG analysis, all genes with average expression greater than 1 transcript per million were ranked by fold change and analyzed using gene set enrichment analysis.

Epigenetic age data was analyzed using a mixed linear model as implemented in the *afex* R package. The age estimate from UniversalClock2 was regressed onto chronological age to retrieve an epigenetic age acceleration score, which was the outcome in the model. The model included fixed effects of handling condition, sex, and a handling by sex interaction, as well as a random effect of litter ID to account for litter effects.

Natural parenting behavior scoring

Unmanipulated parenting behavior was observed for litters used for neuroanatomy and behavior experiments. Scoring of natural parenting behavior was completed according to previously published methods[18]. Briefly, animals were observed in their home cage for 20 minutes and the following behaviors were scored for duration in both mothers and fathers: huddling, non-huddling contact, licking and grooming, nest building, and autogrooming. Pup retrievals and removals were scored for frequency. Additionally, active nursing, lateral nursing, and neutral nursing were scored for duration in mothers only. Behavioral scoring was performed once on day of birth (PND0) and once on PND1. Behavioral scores were generated for each parent by taking the average of pup-directed behaviors from both observations.

Tissue preparation for neuroanatomy

Ten male-female sibling pairs were used for immunohistochemistry and a subset of six sibling pairs were used for electron microscopy. Animals were deeply anesthetized using isoflurane gas and transcardially perfused with Tyrode's solution (137mM NaCl, 5.5mM dextrose, 1.2mM $MgCl_2$, 2mM KCl, 0.4mM NaH_2PO_4, 0.9mM $CaCl_2$, 11.9mM $NaHCO_3$) until fluids ran clear followed by a fixative solution containing 4% paraformaldehyde and 0.5% glutaraldehyde in 0.1M phosphate buffer for 4-5 minutes. Brains were post-fixed in the skull overnight in a 4% paraformaldehyde solution at 4˚C. Brains were then removed, blocked and sectioned coronally at 60 µm using a vibratome (Leica VT1000S) and collected in four series. One of the series was mounted on subbed slides for myelin staining. All other sections were rinsed in 1% sodium borohydride and stored in 0.05% azide in 0.01M PBS at 4˚C until immunohistochemistry and electron microscopy. An additional cohort of animals was used for a time course of microglia cell density. Male-female sibling pairs were collected from our breeding colony at postnatal day 14, 20, and 30. They were deeply anaesthetized with an overdose of Euthasol and transcardially perfused with Tyrode's solution until fluids ran clear followed by 4% paraformaldehyde in 0.1M phosphate buffer for 4-5 minutes and further treated as described above.

Myelin staining and light microscopy

Sections mounted on subbed slides were rehydrated in 0.02M PBS for 2 min and incubated in 0.2% $HAuCl_4$ for 12-15 min at 60˚C[57]. Once fine myelinated fibers were differentiated, the slides were transferred to an intensification solution of 0.2% $KAuCl_4$ for 2 min. Finally, sections were incubated in 1% sodium thiosulfate for 3 min and rinsed three times in 0.02M PBS. Slides were treated through a series of ethanol solutions for dehydration and through xylenes for clearing the lipids from the tissue. All slides were cover slipped using the DPX mounting media (Sigma Aldrich, St. Louis, MO). Sections were photographed using a Leica microscope (model LMDC 888011) and Leica MC170 digital camera.

Images of myelin stains were examined and sections included nucleus accumbens were opened in Image Pro Plus, version 5.1 (Media Cybernetics). The area of the nucleus accumbens was calculated by tracing the nucleus accumbens. Each area was multiplied by 240 to calculate

a volume (each section represents 4 60 μm sections) and these volumes were summed to calculate total volume of nucleus accumbens.

Immunohistochemistry and confocal microscopy

One series of sections from light microscopy brains (n=22) were stained for microglia markers. Free-floating tissue sections were rinsed in 0.01M PBS then blocked in 10% normal donkey serum (Jackson ImmunoResearch) in 0.01M PBS for two hours. Sections were then incubated in anti-Iba1 (Wako #019-19741, 1:1000) diluted 0.01M PBS containing 0.2% Triton-X and 5% normal donkey serum at room temperature for three days. Following three three-minute rinses in 0.01M PBS, the sections were incubated in anti-rabbit AF488 (Jackson ImmunoResearch #711-545-152) for two hours in the dark. Sections were then rinsed in 0.01M PBS (five three-minute rinses), mounted on slides and cover slipped using anti-fade mounting medium containing DAPI (Vector Laboratories #H-1200-10). From each brain, the coronal section containing nucleus accumbens was chosen based on the following criteria: corpus callosum is present at the midline; lateral ventricles extend ventrally into nucleus accumbens; and hippocampal formation is not present. Chosen sections were then imaged using a Carl Zeiss LSM 800 microscope using a 40X objective in 3D Z stack mode (0.825 μm steps). For each section, three images were taken from nucleus accumbens core from each hemisphere, totaling 6 images per section.

Analysis of microglial morphology

Z stacks were imported into Fiji software (National Institutes of Health)[58]. Labeled cells were manually counted by a researcher blinded to parental care and divided by area to calculate cell density. Two images, one from each hemisphere, were randomly selected for Sholl analysis to examine microglial morphology. Sholl analysis was completed using the Sholl analysis plugin in Fiji[59]. Sholl analysis was performed by a researcher blinded to parental care on each cell in each chosen image. First, surrounding processes not belonging to the cell of interest were removed. Then, the line segment tool was used to draw a line from the center of each soma to their longest process. The first shell was set at 4 μm and subsequent shells were set in increments of 2 μm. The intersections at each shell were counted by the plugin.

Electron microscopy

One series of sections were resin-embedded for electron microscopy from 12 brains. Following two three-minute rinses in 0.1M PB, the sections were treated with 1% osmium tetroxide for one hour and subsequently rinsed in 0.1M PB three times for three minutes. Sections were then dehydrated in 50% ethanol for three minutes and counterstained in 4% uranyl acetate in 70% alcohol overnight. The sections were then fully dehydrated in a series of ethanol rinses and rinsed twice in acetone (three minutes each). Sections were infiltrated with resin (Embed 812, EMS, Hatfield, PA), flat embedded between two Aclar sheets, and cured in a 60˚C oven for 1-2 days. A region containing nucleus accumbens (coronal section was selected following the same criterial above) was excised and placed in BEEM capsules (EMS, Hatfield, PA). Capsules were filled with resin and cured for another 2-3 days until polymerized. The area of interest was documented with a camera lucida and trimmed to a 1mm by 2 mm trapezoid. Ultrathin sections of 70 nm thickness were collected on 200 mesh copper grids (Ted Pella, Redding, CA) using a Leica Ultracut UCT7 ultramicrotome.

Ultrathin sections were examined on a JEOL1010 electron micrograph equipped with a 16-megapixel CCD camera (SIA). Images were taken from three regions of interest in nucleus accumbens core, just medial to the anterior commissure which was easily identified via the bundle of myelinated axons. From each region of interest, 12-15 non-overlapping EM images were

captured as 12,000X magnification. One male had poor ultrastructure and was not used for further analysis.

Electron microscopy image analysis and quantification

Each EM micrograph was examined using Image-Pro Plus software, version 5.1 (Media Cybernetics) by a researcher blinded to sex and parental care. In each micrograph, the number of synapses were counted and the terminal profile areas, synapse lengths, and effective sampling area were calculated. Profiles were identified as synaptic terminals if they met the following criteria: 1) a vesicle docking at the membrane, 2) at least 3 vesicles within the same profile, and 3) parallel alignment of the postsynaptic plasma membrane with that of the terminal. The length of the synapse was measured along the length of the parallel-aligned plasma membranes. If the synapse was perforated, the synapse length included the perforation. Synapses were identified as either asymmetric if a postsynaptic density was present or symmetric if a postsynaptic density was absent. If a single terminal contacted two different postsynaptic profiles, each contact was considered its own synapse. The postsynaptic profile was classified as a spine, dendritic shaft, terminal, or cell body. A dendritic shaft was identified by the presence of microtubules organized in parallel and/or the presence of mitochondria. Cell bodies were identified by the presence of organelles such as endoplasmic reticulum, Golgi apparatus, or nucleus. Terminals were identified by the presence of vesicles. Spines were identified by the absence of mitochondria and microtubules. Additionally, the presence of a spine apparatus was used for classifying postsynaptic profiles as spines, but was not necessary. The effective sampling area was calculated as the total area of the individual micrograph minus the area of cell bodies, blood vessels, and myelinated axons, as these elements are not expected to receive synaptic contact.

Volumetric synapse density was calculated as previously described ($N_V=N_A/d$ where N_A is the number of synapses per square micrometer and d is the average synapse length in micrometers)[60,61]. This calculation was performed for each region of interest, resulting in three measurements of synapse density per animal.

Alloparenting behavior

On PND 24, one male and one female from the litter (n=27 litters) were observed in an alloparenting test to examine social behavior towards an infant pup. In a small polycarbonate cage, a novel unrelated infant pup (1-3 days) was placed in a corner. The test animal was placed in the opposite corner and was observed for 20 minutes while being videotaped from above. Videos were scored for frequency of pup retrievals and duration of the following pup-directed behaviors: sniffing, licking/grooming, huddling, non-huddling contact. Autogrooming was also scored for duration. Latency to approach and latency to attack (if the animal attacked) were also scored. Attacks were rare, but when they did occur, the test was ended and the infant was immediately removed and checked for injury. The infant was treated and returned to its home cage if the injury was minor or euthanized if necessary. Infants were used for a maximum to two tests before being returned to their home cage.

Genotyping of Oxtr SNPs

Animals were genotyped for previously described SNPs NT213739[62] and KLW2[29], which have been associated with oxytocin receptor expression and social behavior in prairie voles. DNA was isolated from ear punches collected from animals used for behavior using the DNeasy Blood and Tissue Kit (Qiagen, Valencia, CA) according to manufacturer instruction. 2 uL of DNA was used as template for PCR using a Pyromark PCR kit (Qiagen, Valencia, CA) which were then pyrosequenced using a Pyromark Q24 with Pyromark Gold Q24 reagents (Qiagen, Valencia, CA). For NT213739, 0.2uM of primers TSL202F 5’ CAGGGACGTTCACGTTACATG-3′ and TSL202R 5′- GACAGAGTCTCCAGCCAAGAAG-3′ were used to amplify the *Oxtr* target fragment including

SNP NT213739 with the following cycling conditions: [Step 1: (95 °C/15 min)/1 cycle, Step 2: (94 °C/30 s, 56 °C/30 s, 72 °C/30 s)/45 cycles, Step 3: (72 °C/10 min)/1 cycle, Step 4: 4 °C hold]. The sequencing primer TSL202S 5′- GAATCATCCCACCGT-3′ was used for pyrosequencing. For KLW2, 0.2 uM of primers KLW333_F 5'- GGACCCAAGGCCTATGTCA-3' and KLW33_R 5'-ATGAGCTTGACGCTACTGACTCG-3' were used to amplify the *Oxtr* target fragment including SNP KLW2 with the following cycling conditions: [Step 1: (95 °C/15 min)/1 cycle, Step 2: (94 °C/30 s, 58 °C/30 s, 72 °C/30 s)/45 cycles, Step 3: (72 °C/10 min)/1 cycle, Step 4: 4 °C hold]. The sequencing primer KLW333_S1 5'-TCAAGATCTGGCAGAAC-3' was used for pyrosequencing.

Statistical analysis

For comparisons of synapse density across conditions, a linear mixed model was used with fixed effects of total parental care, percent of total care comprised of paternal care, sex, and nucleus accumbens volume. Random effects of litter ID and subject ID were used to account for within-subject repeated measurements and litter effects. P-values for linear mixed models were calculated using the Sattherwaithe method as implemented in the *afex* R package. Both terminal profile areas and synapse length were non-normally distributed as they likely arise from multiple populations of inputs each with their own normal distribution. As such, they were analyzed using a generalized mixed model against a Gamma distribution with fixed effects of total parental care, percent of total care comprised of paternal care, sex, and nucleus accumbens volume and random effects of litter ID and subject ID with p-values for generalized linear mixed models were calculated using the likelihood ratio test method as implemented in *afex*.

Statistical analysis of microglia cell density was conducted using a generalized linear mixed model against a Gamma distribution with fixed effects of total parental care, percent of total care comprised of paternal care, sex, and random effects of litter ID and subject ID. Sholl analysis data was analyzed using a linear mixed model against a poisson distribution with fixed effects of total parental care, percent of total care comprised of paternal care, sex, and nucleus accumbens volume and random effects of shell radius, litter ID, and subject ID.

Alloparenting behavior was analyzed for three features: attack, total duration of pup directed behavior, and frequency of pup retrievals during the test. Attack behavior was analyzed using a mixed effects logistic regression model. Pup directed behavior and pup retrieval behavior were only analyzed in animals which did not attack the stimulus pup. Pup directed behavior was analyzed using a mixed linear model. Pup retrieval behavior was analyzed using a mixed effects generalized linear model against a Poisson distribution. In all cases, a random effect of litter ID was included to account for genetic relatedness. For each behavior, we tested for a sex by total parental care interaction and a sex by parental care composition interaction within the same model. Separately, we also tested for an effect of genotype at SNPs NT213739 and KLW2, which has previously been associated with oxytocin receptor expression and social behavior in this species[62]. All plots were created with the ggplot2 package[63].

Results

Early nurture prevents epigenetic age acceleration

Previous research indicates that high parental care delays development in prairie voles: animals raised with high care open their eyes, eat solid food, and leave the nest later than those raised with higher care[18]. DNA methylation estimators of age can be used to determine if an individual is aging at a faster or slower pace than predicted by their chronological age[6]. Recently, a pan-mammalian methylation array and clock was developed to extend this tool to non-human species[48,51]. To examine if epigenetic age is lower in high care offspring, we used a commonly used handling paradigm to manipulate parental care, then raised offspring to juveniles and

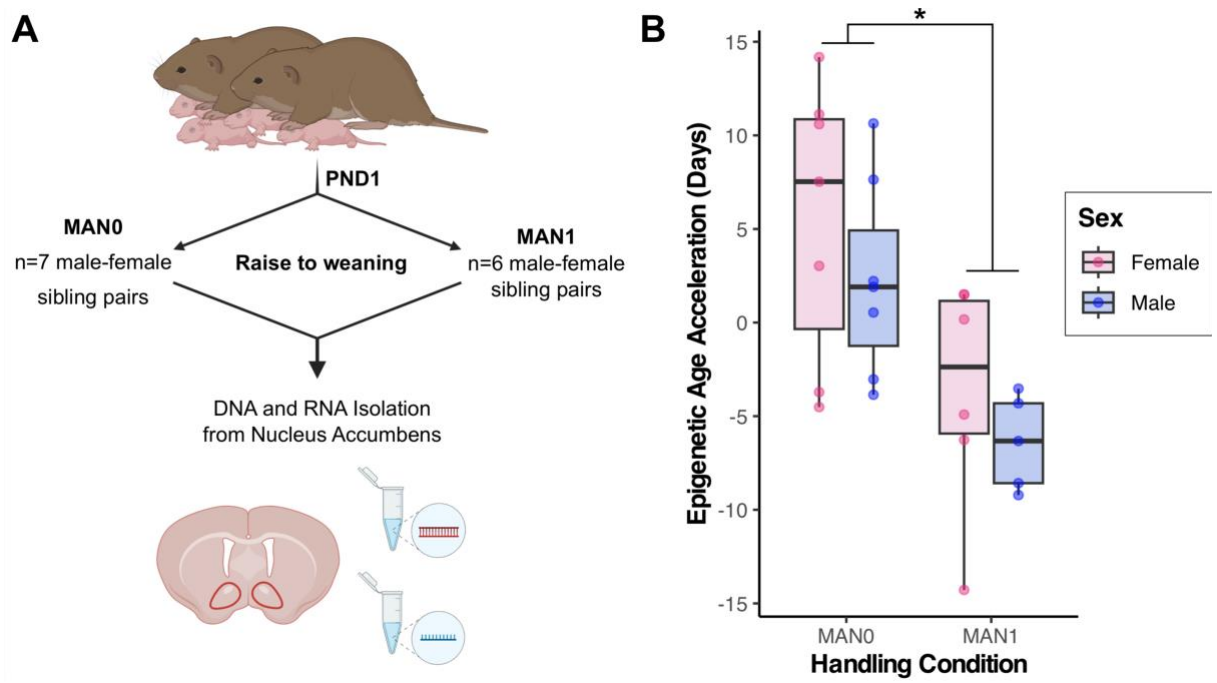

Figure 3.1. High parental care leads to slowed maturation. A) Schematic showing experimental design. Litters were placed in either the indirect (MAN0) or direct (MAN1) handling condition and raised until weaning. DNA and RNA were then isolated from nucleus accumbens. B) Prairie voles raised in the MAN1 condition have lower epigenetic age acceleration ($F_{(1,11)}$=9.45, p=0.011).

isolated DNA from the nucleus accumbens, a brain region involved in reward and social behavior (Figure 3.1A). We find that animals raised in the MAN0 condition, which receive lower total parental care, have accelerated epigenetic aging ($F_{(1,11)}$=9.45, p=0.011, Figure 3.1B). Notably, the difference in the epigenetic ages of the two groups is over a week: the mean epigenetic age acceleration of the MAN0 (low care) group is +3.869 days while the mean epigenetic age acceleration of the MAN1 (high care) group is -4.928 days (in the case of MAN1, this is actually age deceleration). There was no effect of sex ($F_{(1,10.48)}$=2.44, p=0.148) nor an interaction between sex and handling condition ($F_{1,10.48)}$=0.08, p=0.777). These results provide evidence that early nurture leads to slowed development and prevent physiological aging.

Early nurture impacts expression of genes related to synaptic activity, neuroimmune processes, and metabolism in male offspring only

In order to investigate how early nurture impacts gene expression, we performed RNA-sequencing on PND24 nucleus accumbens samples exposed to a handling manipulation where the MAN0 group receives less parental care during the first week of life than the MAN1 group[21]. Differential expression analysis was performed separately for males and females because previous literature indicated sex-specific transcriptomic responses to early life stress in other rodent species[26–28] and sex-specific behavioral responses to the handling manipulation in prairie voles[22]. In females, only three genes were differentially expressed at genome-wide significance (FDR < 0.1): ENSMOCG00000004642, *Ak8*, and ENSMOCG00000000123 (Figure 3.2A, Appendix A, Table A.2). In contrast, there were 321 differentially expressed genes in male offspring, indicating higher sensitivity to early nurture in males (Figure 3.2A, Figure 3.3, Appendix A, Table A.2). We used gene ontology analysis to investigate the biological processes that differentially expressed genes are involved in. Gene ontology analysis was performed separately for upregulated and downregulated genes. Upregulated genes (genes with higher expression in

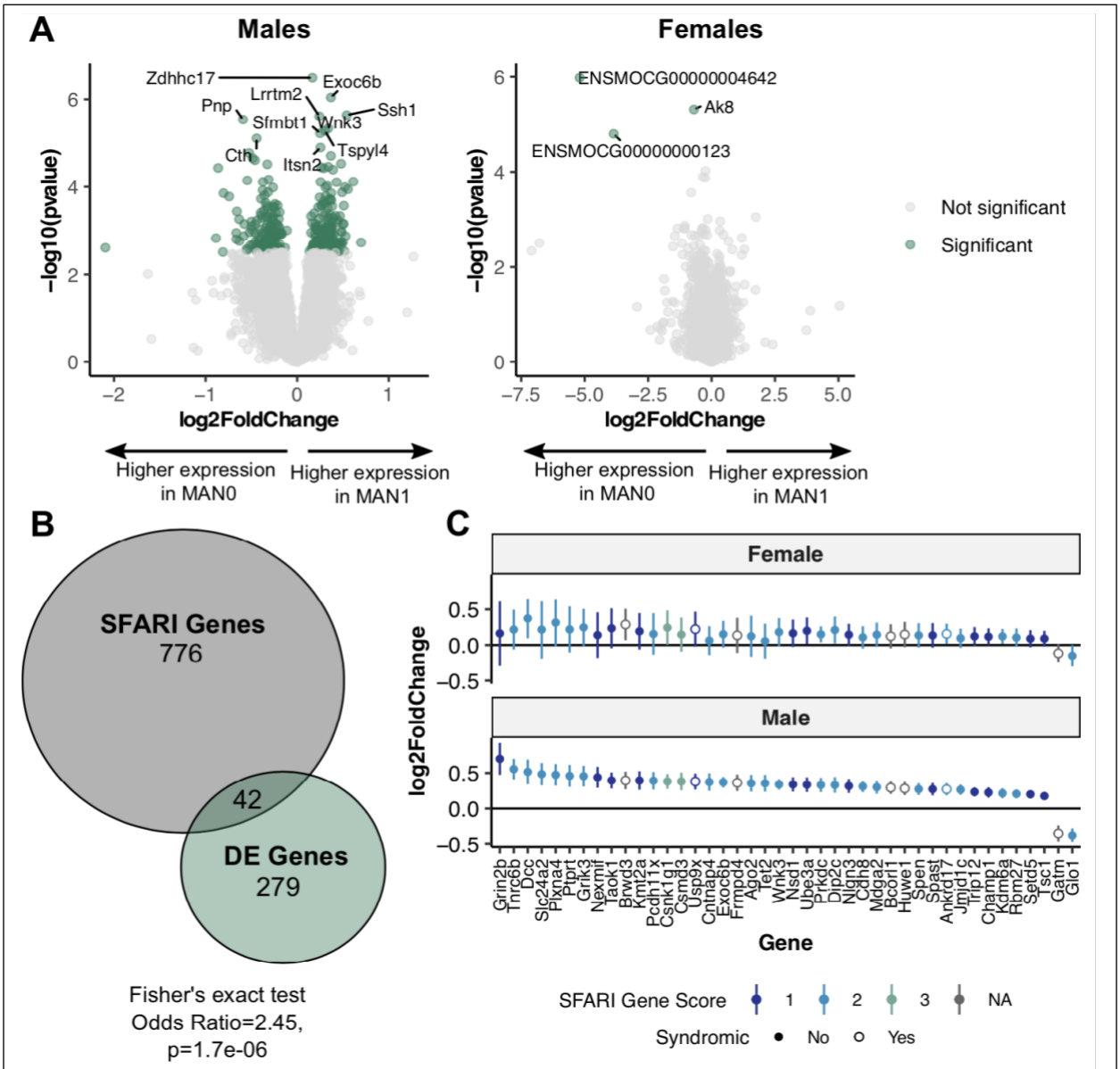

Figure 3.2. Early nurture impacts transcription of autism risk genes in male offspring only. A) RNA-sequencing reveals 321 differentially expressed genes in males raised by high care parents vs low care parents, but only 3 differentially expressed genes in females. B) Enrichment (n=42) of SFARI autism risk genes in differentially expressed (DE) gene set in males. C) Graph showing log2(Fold Change) of SFARI autism risk genes in both males and females. Points indicate log2(Fold Change) and bars indicate the standard error of the estimate. Points are colored by SFARI risk category (1=high confidence for autism risk, 2= strong candidate for autism risk, 3=suggestive evidence for autism risk). Open points indicate genes responsible for syndromic forms of autism.

MAN1/high parental care males) are involved in neuronal processes including neural development, synapse organization, and synaptic signaling (Appendix A, Table A.3). Further, upregulated genes are localized to synaptic structures and are functionally involved in ion channel activity and cell-cell adhesion (Appendix A, Table A.3). Downregulated genes (genes with lower expression in MAN1/high parental care males) are involved in metabolic processes and immune processes (Appendix A, Table A.4). A separate KEGG pathways analysis further supports this finding, with enriched KEGG pathways including neuroactive ligand- receptor interactions, axon

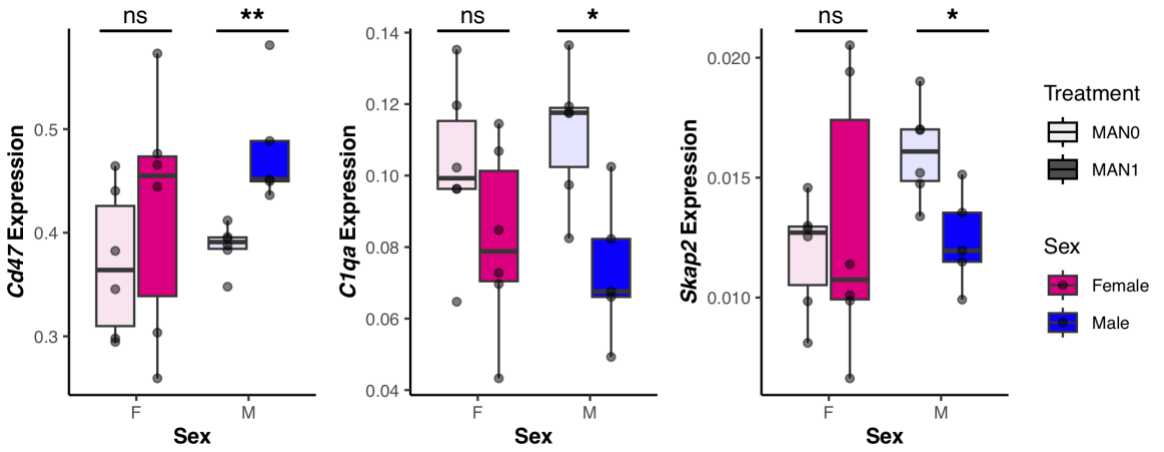

Figure 3.3. RT-qPCR validation of RNA-seq. Three differentially expressed genes in males were chosen for RT-qPCR validation. All genes are normalized to housekeeping gene *Pgk1*. Within-sex comparisons are tested using Wilcoxon rank sum test. For each gene, there is no effect of treatment on expression in females, but there is a significant effect of handling condition on expression in male offspring. * $p<0.05$, ** $p<0.01$, ns $p>0.05$.

guidance, and several synaptic pathways (Appendix A, Table A.5). Given the male-specific effects of early nurture on gene expression and social behavior, we tested if the differentially expressed genes in males were enriched for autism risk genes. We found a significant enrichment of genes in the SFARI gene set (Figure 3.2B&C) indicating that genes which are disrupted in autism are also sensitive to early life experience and are related to more subtle variability in social behaviors.

Parental care composition is associated with excitatory synapse density in male offspring only

The results from the RNA-sequencing experiment indicate a male-specific impact of early nurture on expression of genes related to neurodevelopment and synaptic activity. This led us to hypothesize that male offspring raised by high care parents have more synapses in the nucleus accumbens. We used electron microscopy to quantify the volumetric synapse density in the nucleus accumbens core (Figure 3.4A). In 11 animals (6 female, 5 male), we characterized 2,335 synapses (median 204 synapses per animal) from 433 electron micrographs (median 36 images per animal). Synapses were identified by the presence of a vesicle-filled profile abutting a membrane and were classified as asymmetric or symmetric by comparing the presynaptic and postsynaptic densities (Figure 3.4B&C). The most common type of synapse observed was asymmetric onto spines (64.5%), followed by asymmetric onto dendrites (19.9%). Symmetric synapses were less common and occurred more frequently onto dendrites (10.9%) than spines (3.4%). Synapses onto cell bodies or axons were rare (<1%).

We first examined the effect of total parental care on synapse density using a linear mixed model with fixed effects of the three way interaction of sex, total parental care, and synapse type and random effect of sample (to account for repeated measurement) and litter ID (to account for litter effects). Contrary to our hypothesis, there was no significant three-way interaction between sex, total parental care, and synapse type ($F_{(1,51)}=0.496$, $p=0.49$), but there was significant interaction of total parental care and synapse symmetry ($F_{(1,51)}=13.3$, $p<0.001$) such that increased total parental care was moderately associated with an increase specifically in asymmetric synapse density in both sexes (Figure 3.4D). While there was no significant interaction of total parental care and sex on volumetric synapse density, we next asked if other

aspects of parental care might be associated with synapse density in a sex-specific manner. Recent studies indicate that in prairie voles there is a specific effect of paternal care on the development of social behaviors and neuropeptide systems in male offspring only[64,65]. We next tested if parental care composition (calculated as the paternal care duration divided by total parental care duration), rather than total parental care, impacted synapse density. Though

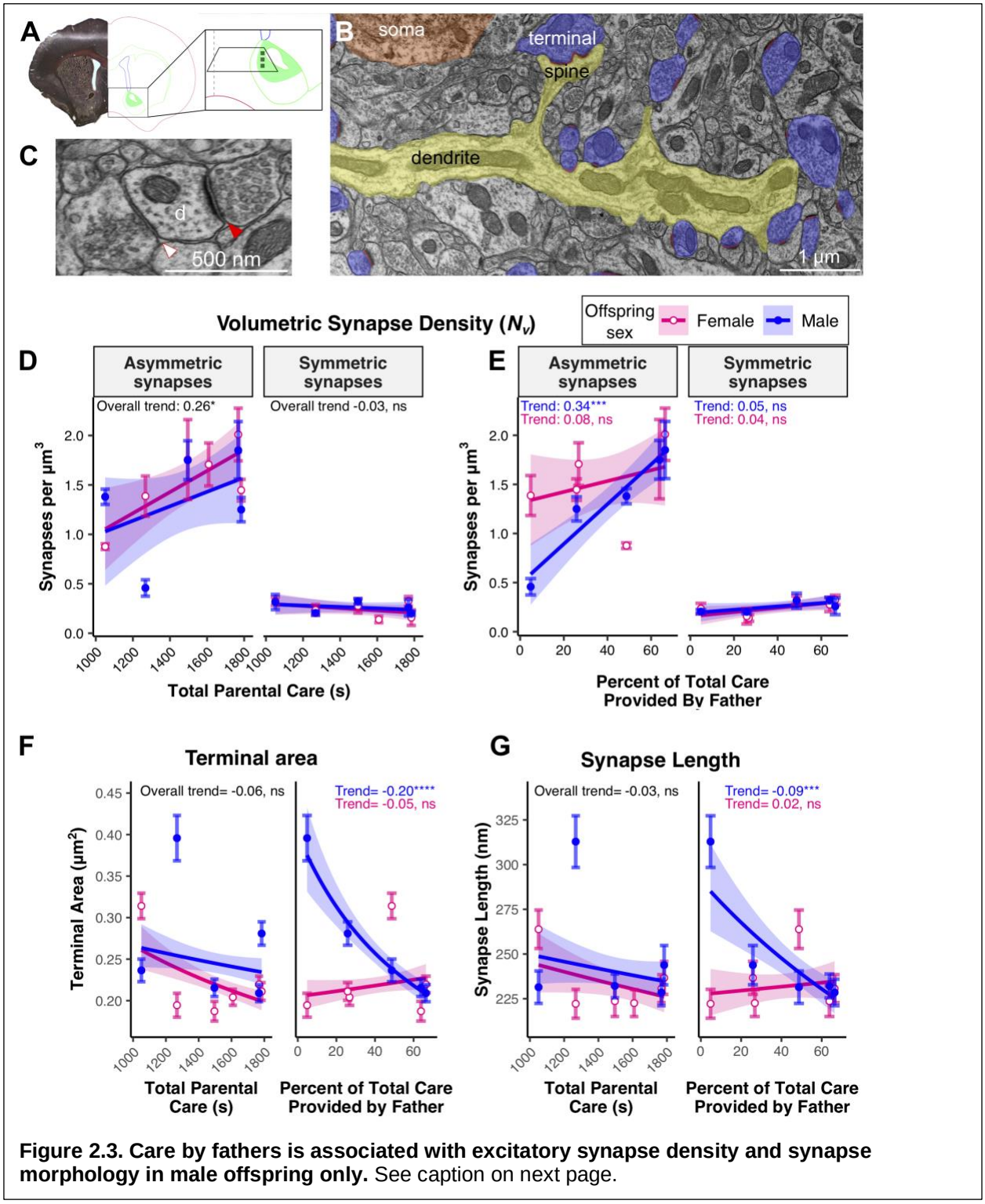

Figure 2.3. Care by fathers is associated with excitatory synapse density and synapse morphology in male offspring only. See caption on next page.

Figure 2.3. Care by fathers is associated with excitatory synapse density and synapse morphology in male offspring only. A) Example myelin stain and atlas of brain section containing nucleus accumbens (with the core filled in green). The zoomed inset contains the trapezoid sectioned for electron microscopy, and the shaded black boxes show where pictures were taken from. B) Example electron micrograph at 12,000X magnification. A dendrite is pseudocolored in yellow. Terminals are blue and synapses are red. A cell soma is pseudocolored orange. C) A cross section of a dendrite receiving two synapses, indicated by red arrowheads. The filled arrowhead shows an asymmetric synapse, where the postsynaptic density is dark and thick. The blank arrowhead shows a symmetric synapse, where the postsynaptic density is not darker or thicker than the presynaptic density. D) There is a moderate effect of total parental care on asymmetric synapse density, but no effect on symmetric synapse density (total parental care x synapse symmetry interaction, $F_{1,51}$=13.3, p<0.001). E) There is a significant three-way sex x parental care composition x synapse symmetry interaction ($F_{1,50}$=6.222, p=0.016) such that male offspring raised with more paternal care are higher in excitatory synapse density. Data points represent the average synapse density of three regions of interest in an animal and bars represent the standard error. F) Male offspring raised with more paternal care have more small-area synapses while female offspring show no relationship (sex x parental care composition interaction, $\chi^2_{(1)}$=9.83, p=0.002). G) Male offspring raised with more paternal care have shorter synaptic zones (sex x parental care composition interaction, $\chi^2_{(1)}$=6.27, p=0.012).

maternal and paternal care are inversely related, there is no correlation between total parental care and the composition of that care (Supplementary Figure 3.5A-C), indicating that these are independent features of parental care. Using a linear mixed model, we found a significant interaction between sex, parental care composition, and synapse symmetry while accounting for total parental care ($F_{(1,50)}$=6.222, p=0.016) such that higher levels of paternal care are associated with increased asymmetric synapse density in male offspring only (Figure 3.4E). These results suggest that increased paternal care specifically alters the development of glutamatergic synapses in the nucleus accumbens in male offspring only. Notably, males raised with low paternal involvement have much lower synapse density than their sisters while no such sex difference exists in siblings raised with more paternal involvement, suggesting that care by fathers feminizes the nucleus accumbens.

The increased synapse density resulting from paternal care may occur for three reasons: 1) decreased nucleus accumbens volume 2) increased synaptogenesis, and/or 3) decreased synapse pruning. Nucleus accumbens volume was measured using serial myelin sections. There was no correlation between nucleus accumbens volume and total parental care (ρ(11)=-0.03, p=0.93) nor was there a correlation between nucleus accumbens volume and parental care composition (ρ(11)=-0.22, p=0.51). These results indicate that nucleus accumbens volume does not change with parental care, nor do changes in synapse density result from changes in nucleus accumbens volume.

Parental care composition impacts synapse morphology in male offspring only

We next tested if aspects of parental care were associated with cross-sectional terminal areas. Terminal areas were non-normally distributed, so we used a generalized linear mixed model with a gamma distribution. There was no significant effect of total parental care ($\chi^2_{(1)}$=2.56, p=0.109) nor an interaction of total parental care and sex on terminal areas (Figure 3.4E, $\chi^2_{(1)}$=1.40, p=0.238). There was, however, a significant interaction of sex and parental care composition (Figure 3.4F, $\chi^2_{(1)}$=9.83, p=0.002) such that more care by fathers was associated with on average smaller terminals in male offspring only. Similarly, there was no effect of total parental care on synapse length ($\chi^2_{(1)}$=1.22, p=0.270), nor an interaction of total parental care and sex (Figure 3.4F, $\chi^2_{(1)}$=0.24, p=0.623). There was a significant interaction of parental care composition and sex ($\chi^2_{(1)}$=6.27, p=0.012, Figure 3.4G) such that more care by fathers was associated with on average shorter synapses in males only. Much like volumetric synapse density,

there is a sex difference in both terminal area and synapse length in litters raised with less care from fathers which is not present in the litters raised with more care from fathers.

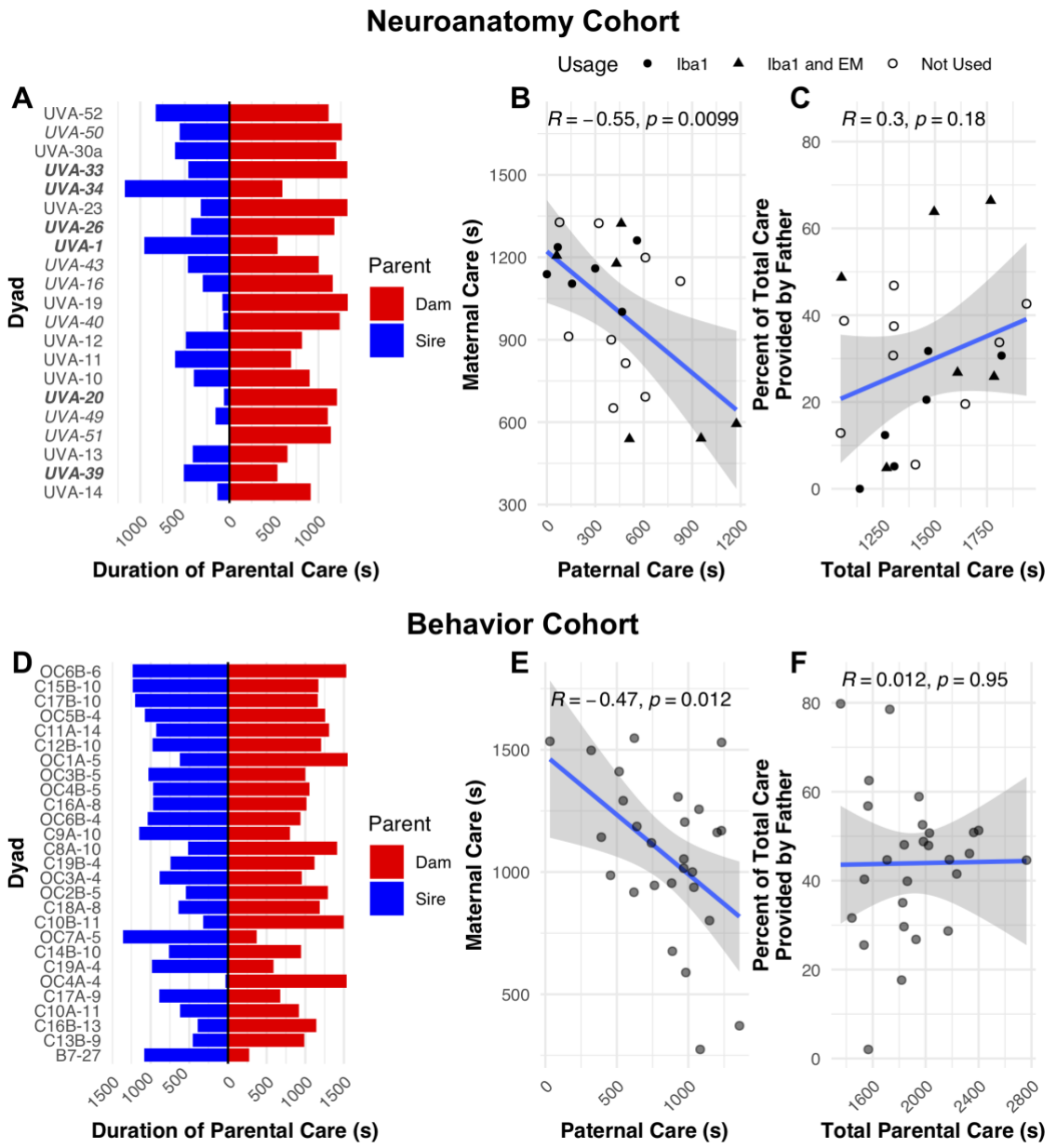

Figure 3.5. Analysis of natural parental care. Descriptive analysis of natural parenting cohort used for neuroanatomy (A-C) and alloparenting behavior (D-F). A) Bar graph showing total duration of parental care provided by dams (red) and sires (blue). Not all observed litters were used in the study because of single-sex litters or poor perfusions. Litters used for Iba1 staining are italicized and litters used for Iba1 staining and electron microscopy are bold italicized. B) Maternal and paternal care are inversely related. Litters used for Iba1 staining are shown as filled circles. Litters used for Iba1 staining and electron microscopy are shown as filled triangles. Unused litters are shown as open circles. C) Total parental care and composition of parental care are not correlated. Litters used for Iba1 staining are shown as filled circles. Litters used for Iba1 staining and electron microscopy are shown as filled triangles. Unused litters are shown as open circles. D) Bar graph showing total duration of parental care provided by dams (red) and sires (blue). E) Maternal and paternal care are inversely related. F) Total parental care and composition of parental care are not correlated.

Microglia density is impacted by total parental care in both sexes, but microglia morphology is not impacted by parental care

Results from the RNA-sequencing experiment indicate that male offspring of lower care parents have higher expression of genes related to immune processes. Microglia, the resident immune cells in the brain, are involved in the pruning of synapses during development[66]. In the nucleus accumbens, microglial elimination of dopaminergic synapses during adolescence contributes to the development of social behaviors in rats in a sex-specific manner[67]. In order to investigate possible changes to microglial activity resulting from different early life parental care, we examined the number and morphology of microglia cells using Iba1 immunostaining. First, we examined the density of microglia. Using a mixed model with a Gamma distribution, we found a moderate effect of total parental care on microglia density ($\chi^2_{(1)}$=4.43, p=0.035) where more care led to increased density, but no interaction with sex ($\chi^2_{(1)}$=0.94, p=0.333, Figure 3.6A&B). There

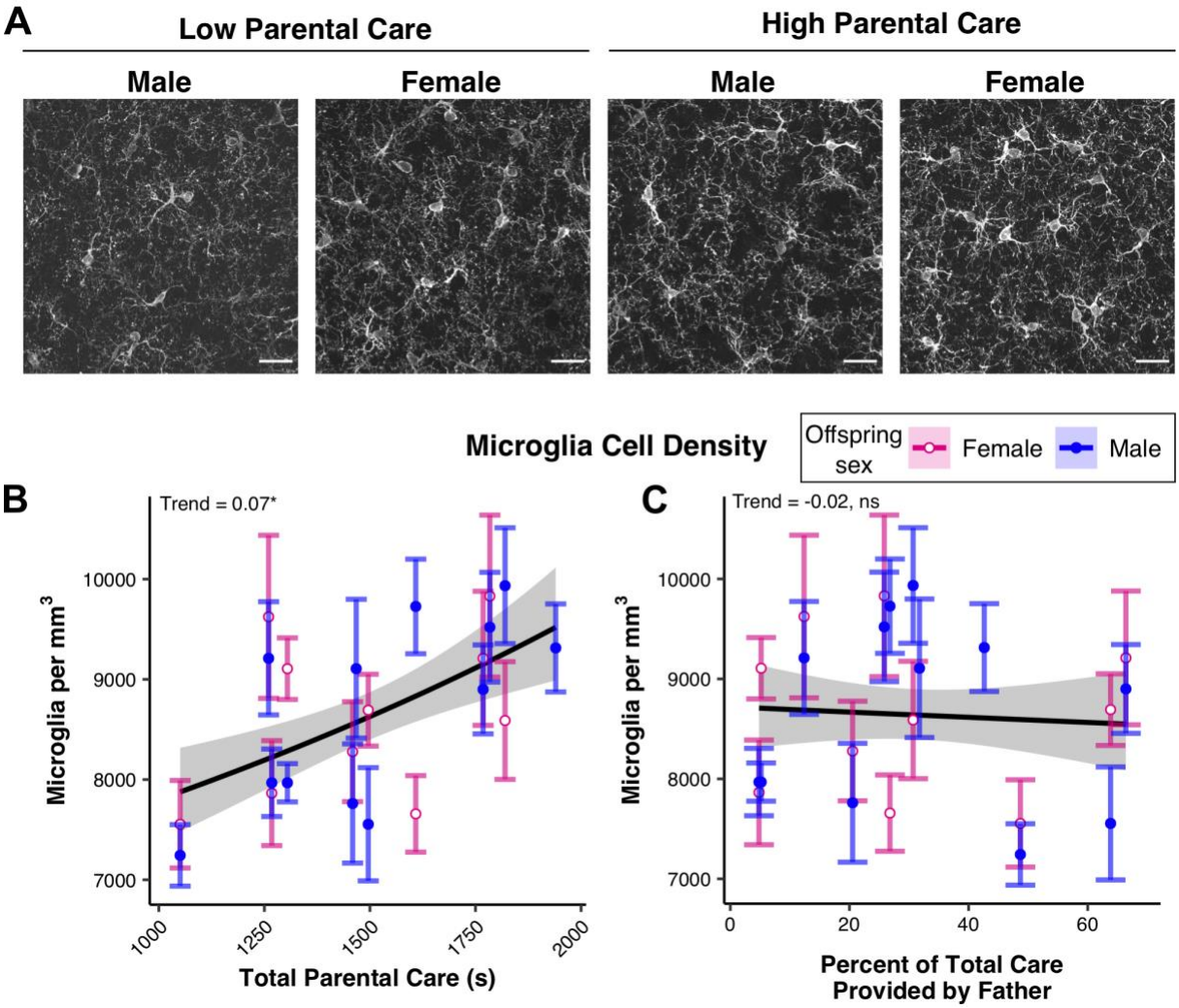

Figure 3.6. Total parental care is associated with microglia cell density in both sexes. A) Example confocal microscopy images of Iba1+ cells in male and female offspring raised by low and high care parents. Scale bars = 20 µm. B) Total parental care is associated with higher microglia cell density ($\chi^2_{(1)}$=4.43, p=0.035). Data points represent the average microglia cell density of six regions of interest images in nucleus accumbens core and bars represent the standard error. C) No effect of parental care composition on microglia cell density ($\chi^2_{(1)}$=1.14, p=0.286).

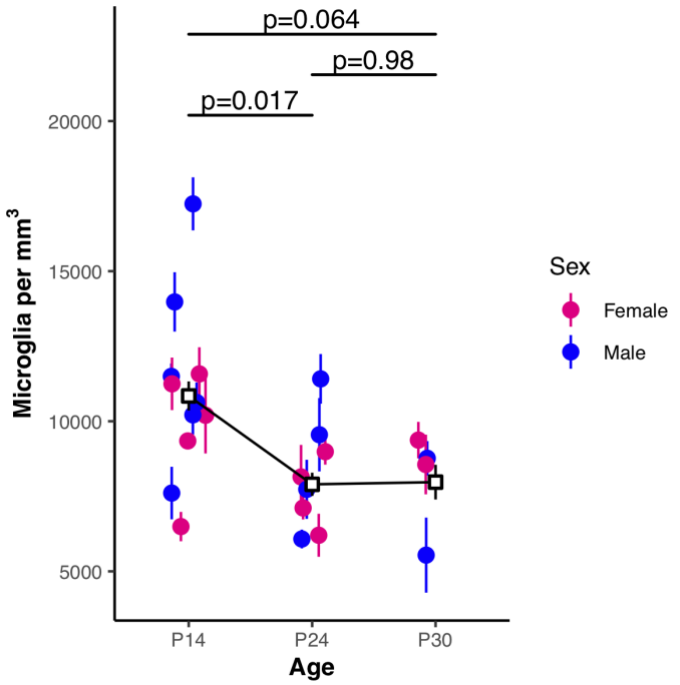

Figure 3.7. Microglia cell density decreases between postnatal days 14 and 30. Group averages for each age are shown with black squares with bars representing standard error. Average cell density of each subject (from multiple images) is shown with circles with bars representing standard error and color representing sex. Data was analyzed using a mixed model against a Gamma distribution with random effects of subject and breeder pair. There was a main effect of age ($\chi^2_{(2)}$=6.26, p=0.044) but no effect of sex ($\chi^2_{(1)}$=0.0001, p=0.991) nor an interaction between age and sex ($\chi^2_{(2)}$=2.27, p=0.321). Post-hoc group comparisons indicate that P14 animals have significantly higher microglia cell density than P24 animals (p=0.017) and are trending towards higher microglia cell density in P30 animals (p=0.064). Microglia cell density does not differ between P24 and P30 animals (p=0.98).

was no effect of parental care composition ($\chi^2_{(1)}$=1.14, p=0.286), nor an interaction of parental care composition and sex ($\chi^2_{(1)}$=0.37, p=0.541, Figure 3.6C). We next used Sholl analysis to examine the morphology of the microglia. We found no significant effects of sex, total parental care, or parental care composition on microglial morphology (all p values > 0.1). These results indicate that in both sexes, parental care is positively associated with microglia cell density. This may be a result of a change in the pace of development: it has previously been shown that offspring of low care parents hit developmental markers earlier than those of high care parents[18]. Our results are consistent with this finding, as microglia cell density decreases rapidly between postnatal days 14 and 30 (Figure 3.7).

Parental care composition has sex-specific effects on pup retrieval behavior

We next tested if aspects of parental care, including total parental care and parental care composition (see Figure 3.5D-F), were related to social behavior during an alloparenting task (Figure 3.8A). Alloparenting behavior, or parental care towards offspring that is not one's own, is a commonly studied social behavior in prairie voles and is sensitive to early life nurture[18,22,68]. In both sexes, total parental care was associated with less likelihood for a test animal to attack the stimulus pup ($\chi^2_{(1)}$=5.31, p=0.021, Figure 3.9A) and in non-attackers, a trend towards higher duration of pup-directed care ($F_{(1,18.73)}$=4.08, p=0.058, Figure 3.9C). There was no association of parental care composition with either of these behaviors (attack: $\chi^2_{(1)}$=0.01, p=0.924; pup directed care: $F_{(1,17.17)}$=0.13, p=0.727, Figure 3.9B&D). Previous work in the monogamous California mouse indicates father-to-son transmission of pup retrieval behavior[69,70]. We examined the sex-specific impacts of total parental care and parental care composition on pup retrieval behavior in an alloparenting task. There was no effect of total parental care ($\chi^2_{(1)}$=0.03, p=0.857) nor an interaction of total parental care and sex ($\chi^2_{(1)}$=0.25, p=0.618) on total pup retrievals (Figure 3.8B). There was, however, a significant interaction of parental care composition and sex ($\chi^2_{(1)}$=18.44, p<0.001) such that males raised with more care by fathers show increased pup retrieval behavior while females do not (Figure 3.8B). Pup retrieval and other alloparenting behavior was not

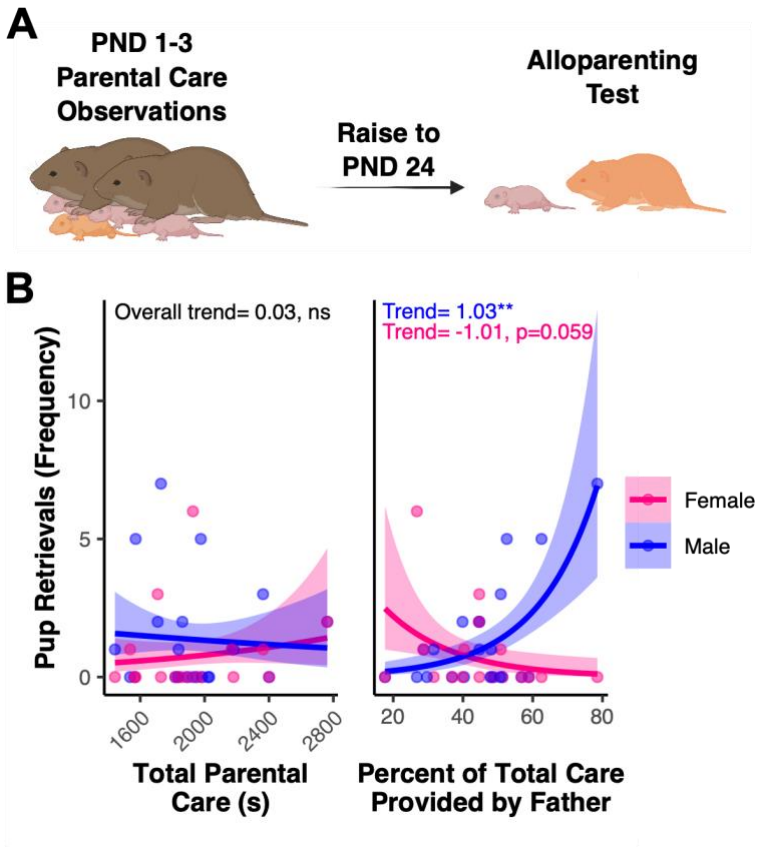

Figure 3.8. Care by fathers increases pup retrievals in male offspring but decreases pup retrievals in female offspring. A) Schematic showing experimental design. B) There is no association of total parental care received and pup retrieval behavior during an alloparenting test ($\chi^2_{(1)}$=0.03, p=0.857). There is a significant interaction of parental care composition and sex ($\chi^2_{(1)}$=18.44, p<0.001) such that males raised with more paternal care display more pup retrievals as juveniles. Females raised with higher paternal care display fewer pup retrievals as juveniles.

associated with genotype at SNP NT213739 which has been associated with social behaviors in adulthood and is a moderator of the impact of early life experience on affiliative behavior in adulthood, nor were they associated with SNP KLW2, which we have previously shown impacts expression of an oxytocin receptor alternative isoform[29,62,71] (Figure 3.10).

Discussion

The experiments in this study indicate that while both male and female prairie voles are sensitive to total parental care, male prairie voles are uniquely sensitive to the composition of that care. Specifically, we find that increased total parental care is associated with decelerated aging, evidenced by decreased epigenetic age of brain tissue, and higher microglia cell density consistent with younger brains. In male offspring only, we find that early nurture exerts large effects on gene expression in the nucleus accumbens, especially of genes related to neurodevelopment and excitatory synaptic transmission. Using quantitative electron microscopy, we find that paternal care specifically is associated with increased excitatory synapse density in the nucleus accumbens in male offspring only. These effects appear to be independent of microglia, as the density and morphology of microglia are not significantly related to early nurture in a sex-specific manner. Finally, we show that paternal involvement has opposing effects on pup retrieval behavior in male and female offspring. Males raised with high paternal care are more likely to perform more pup retrievals than those raised with lower paternal care while their sisters raised with more paternal care are less likely to display pup retrieval behavior. These findings provide evidence that early life experience fundamentally alters the development of male and female brains and social behavior in a sex-specific manner, which has widespread implications for studying how early life experience relates to future mental health disorder, the underlying etiology of which may need to be understood to be different for men and women.

The RNA-sequencing results suggest that early nurture sets up a male-specific transcriptional program that supports increased synaptic activity in nucleus accumbens. Genes that are upregulated by parental care in males are involved in neurodevelopmental and synaptic processes, with particular enrichment for genes which make proteins that act at asymmetric

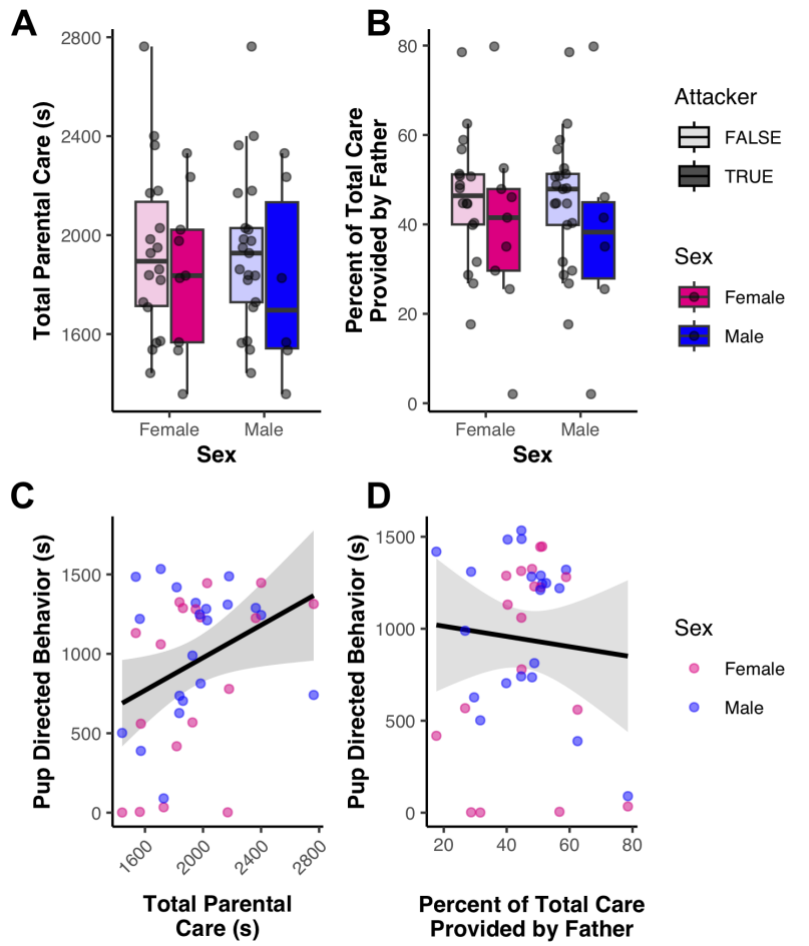

Figure 3.9. Total parental behavior, but not parental care composition, impacts alloparenting behavior in both sexes. A) Attack behavior is significantly predicted by sex ($\chi^2_{(1)}$=11, p<0.001, higher in females) and total parental care ($\chi^2_{(1)}$=5.31, p=0.021), B) but not parental care composition ($\chi^2_{(1)}$=0.01, p=0.924). Data were analyzed with a mixed logistic regression but are presented with parental care features on y axis and sex and attackers on the x axis for data visualization purposes. C) In non-attackers, duration of pup directed behavior is trending towards relationship with total parental care ($F_{(1, 18.73)}$=4.08, p=0.058), D) but not parental care composition ($F_{(1, 17.17)}$=0.13, p=0.727) or sex ($F_{(1, 19.52)}$=1.99, p=0.174).

synapses. Further, there is an enrichment of autism risk genes in the differentially expressed genes in males, with higher expression of genes disrupted in autism in the MAN1 (high care) offspring (Figure 3.2B&C). While variation in parental care does not alter expression of these genes to levels that might cause autism phenotypes (i.e. all voles in this study display species-typical social behaviors), it remains interesting that expression of these genes are highly variable and malleable by changes in parental care in males offspring only. Further studies of mechanisms by which autism risk genes are programmed by the environment may lead to insights into the male bias for autism and other neurodevelopmental disorders.

Using quantitative electron microscopy to examine the impact of early life parental care on synapse density and morphology, we identify that while putative excitatory synapse density is sensitive to total parental care in both sexes, the composition of that parental care is strongly associated with synapse density in male offspring only. These results are in line with work in other monogamous rodents that indicate male sensitivity to paternal care. For example, paternal deprivation leads to synaptic changes throughout the brain in degus, including changes to both dopamine innervation and the number of parvalbumin positive interneurons in the nucleus accumbens[33,72,73]. We observe increased density of asymmetric synapses in males raised with more paternal care, and an increase in small-area terminals and shorter synaptic zones. These results may indicate upregulation of a specific excitatory input characterized by small terminals and short synapses or a generalized increase in synaptogenesis which would result in small, immature synapses. While paternal care increases excitatory synapse

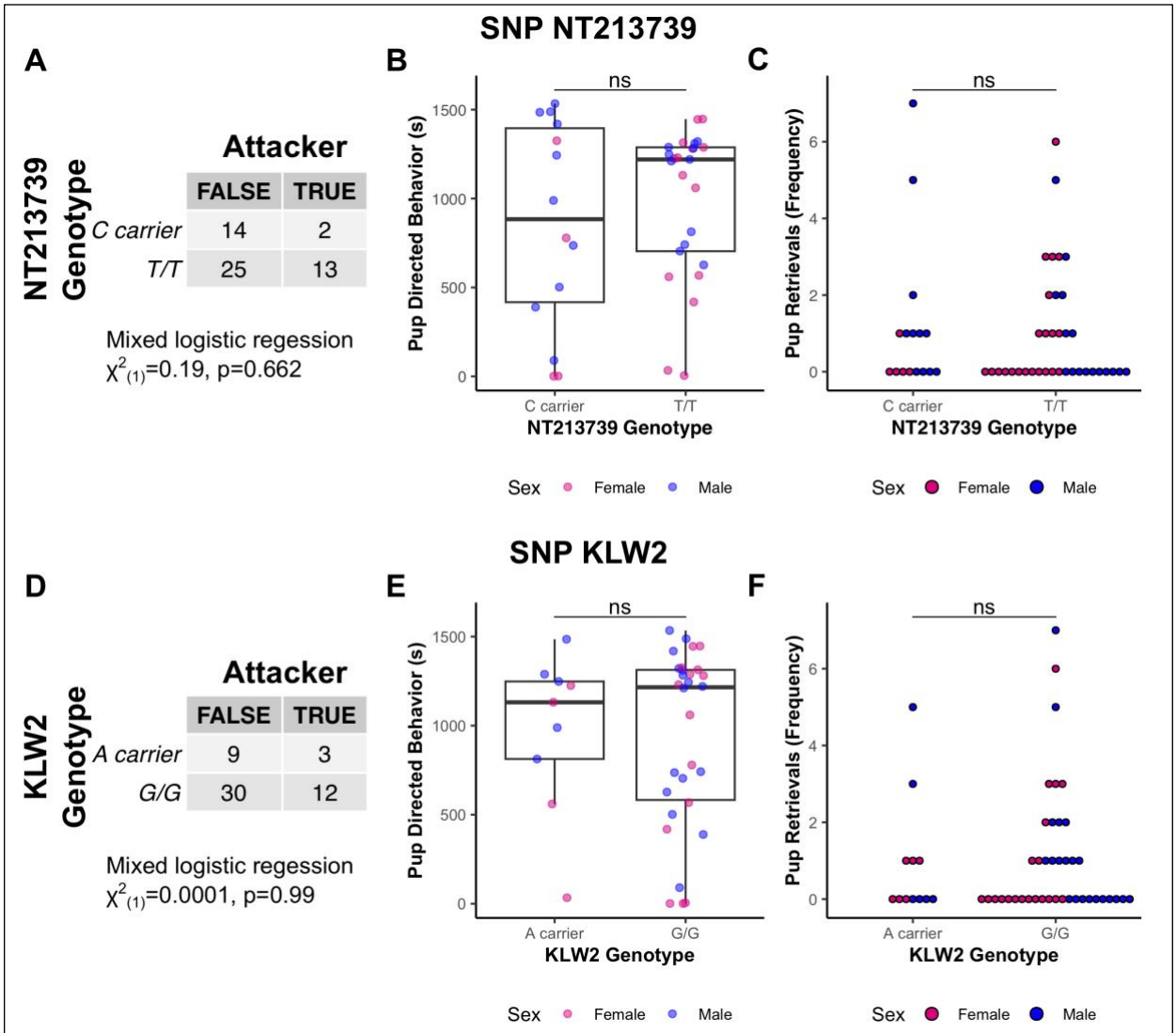

Figure 3.10. No effect of SNPs NT213739 and KLW2 on alloparental behavior. A) Attack behavior is not predicted by genotype at NT213739 ($\chi^2_{(1)}$=0.19, *p*=0.662). B) In non-attackers, duration of pup directed behavior does not differ by NT213739 genotype ($F_{(1, 36.81)}$=0.35, *p*=0.557). C) Frequency of pup retrievals does not differ by genotype at NT213739 ($\chi^2_{(1)}$=0.83, *p*=0.362). D) Attack behavior is not predicted by genotype at KLW2 ($\chi^2_{(1)}$=0.0001, *p*=0.99). E) In non-attackers, duration of pup directed behavior does not differ by KLW2 genotype ($F_{(1, 36.99)}$=0.07, *p*=0.798). F) Frequency of pup retrievals does not differ by genotype at KLW2 ($\chi^2_{(1)}$=0.05, *p*=0.818).

density in male offspring, there is no association between parental care composition and microglia cell density or morphology. It may be that the synapse density results are independent of microglial sculpting of accumbens circuitry or that differences in microglia cell density or morphology might be observed earlier in development.

Finally, we show a sex-specific behavioral phenotype associated with care by fathers in prairie voles. Previous work in prairie voles indicates that males are uniquely sensitive to care by fathers which relates to social behavior as juveniles and adults and changes in neuropeptide receptor density[64,65,74]. Here, we show that paternal involvement is related to pup retrieval behavior such that males raised with more care by fathers display more pup retrievals during an

alloparenting task while female offspring display fewer pup retrievals when raised with more care by fathers. These results are consistent with studies in California mouse which suggest that paternal pup retrievals are associated with pup retrievals by male offspring later in life[70]. However, California mouse female offspring also display higher pup retrieval behavior when raised by fathers who display high pup retrieval[75]. Our study is different from the previous work in three critical ways (other than species): first, the studies in California mouse manipulate paternal pup retrieval behavior while we do not. Second, the age of the offspring differs: we use juveniles while the previous studies use adults. Third, and perhaps most importantly, our study uses an alloparenting test where the test subject is exposed to a pup that is not theirs, while the studies in California mouse expose the test subject to their biological offspring. This may account for the different behaviors in females, as female prairie voles are generally less alloparental than males as juveniles[76]. Altogether, our results suggest that male prairie voles are uniquely sensitive to paternal care in terms of neurodevelopmental and social behavior processes. Further work should focus on specific circuitries that are sensitive to paternal care and are related to alloparental behavior.

One possible explanation for our results is that early paternal care alters the developmental trajectory of male offspring such that there is increased synapse density, which ultimately increases social behavior throughout the lifespan. A second explanation is that high paternal care alters the pace of development such that at the juvenile timepoint there are differences in gene expression, nucleus accumbens ultrastructure, and social behavior which converge by adulthood. Further, these explanations are not necessarily mutually exclusive: differences in pace of development may lead to dramatic differences during development and more subtle differences in adulthood. While direct examination of these features in adulthood is necessary to determine which explanation may be more likely, there is good evidence from this study and others supporting either explanation. First, effects of early nurture and paternal care impact social behavior in prairie voles throughout the lifespan, suggesting that behaviors among voles raised with different parental care experiences do not converge by adulthood. There is a strong impact of early life experience on partner preference behavior in adulthood[64,77]. However, developmental timing is also impacted by early nurture, with prairie voles raised by high care parents having lower epigenetic age (Figure 3.1B) and reaching developmental markers such as eye opening, eating solid food, and leaving the nest later than those raised by high care parents[18]. Our microglia cell density results also support this explanation, as voles raised by high care parents show increased microglia cell density which is indicative of a less mature brain (Figure 2.4B).

Our results indicate that parental care, and in particular the composition of that care, are associated with gene expression programs and synapse density and morphology in male offspring only. While it is possible that females are not as sensitive to early life experience, a more likely explanation is that effects of early nurture in females may be found in other brain regions or developmental timepoints. For example, the handling manipulation used in this study has sexually dimorphic impacts on behavior: in males, MAN1 (high care parents) increases alloparenting behaviors as juveniles while in females, MAN1 increases pair bond formation as adults[22]. Additionally, we do provide evidence that total parental care impacts aging and neurodevelopmental processes in females, but we may have examined a timepoint where differences in gene expression and neuroanatomical outcomes are larger in male offspring. Future studies should aim to examine the timing of developmental changes associated with early life experience in female prairie voles.

One limitation of these experiments is that gene expression, neuroanatomy, and behavior were not measured in the same animal cohorts. These experiments are interested in baseline potential for social behavior, not response to social stimuli, so we did not perform gene expression or anatomy experiments on animals after an alloparenting test. Further work should be done to connect excitatory synapse density to social behavior directly. A second limitation of these

experiments is that the natural parenting experiments presented cannot differentiate between effects of early experience and genetic effects. However, a previous cross-fostering experiment indicates that alloparental behaviors are largely driven by rearing parents, not genetic parents[78]. A cross-fostering study to determine how development of synapse density in nucleus accumbens is impacted by both genetic and environmental effects would build upon our results.

Overall, results from these experiments indicate that male prairie voles are uniquely sensitive to their early rearing environment, with paternal care being very important for neurodevelopment and the development of social behaviors. Our results are relevant to understanding male-specific neurodevelopmental processes which may be associated with male bias for neurodevelopmental disorders including autism. Prairie voles are an excellent model for these studies given their enriched rearing environment resulting from biparental care. Further, our results indicate that while many features of offspring development are related to total parental care in both sexes, including aggression towards a pup, excitatory synapse density, and gene expression, males are additionally sensitive to variation in the composition of this parental care, which impacts specific neurodevelopmental and behavioral phenotypes.

Acknowledgements and Funding

We thank the Animal Care Staff at University of California, Davis, Indiana University, and University of Virginia. RNA-sequencing was completed by University of Virginia Genome Analysis and Technology Core (RRID:SCR_018883). We thank Dr. Hardik Parikh for assistance with alignment of RNA-seq data. We thank the following people for assistance with tissue processing for electron microscopy: Kathryn Mahach, Zoe Anderson, Francesca Sciaccotta, and Anila Tynan. We also thank Dr. Forrest Rogers and Dr. Adele Seelke for collecting tissue used for related pilot studies. Funding for this project was provided by: This research was supported by Autism Speaks grant #7110 to J.J.C. and C.S.C., NIH grant HD075750 to C.S.C. and J.J.C., NIH grant HD098117 to J.J.C and C.S.C., National Alliance for Autism Research grant to C.S.C., NIH grant MH073022 to C.S.C. and K.L.B., NIH grant HD060117 to K.L.B., NSF grant 0437523 to K.L.B, and University of Virginia School of Arts and Sciences funds to A.E.

References

1. Smith, K. E. & Pollak, S. D. Early life stress and development: potential mechanisms for adverse outcomes. *Journal of Neurodevelopmental Disorders* **12**, 34 (2020).
2. Daniel, E., Madigan, S. & Jenkins, J. Paternal and maternal warmth and the development of prosociality among preschoolers. *Journal of Family Psychology* **30**, 114–124 (2016).
3. Morgan, J. K., Shaw, D. S. & Forbes, E. E. Maternal depression and warmth during childhood predict age 20 neural response to reward. *Journal of the American Academy of Child and Adolescent Psychiatry* **53**, 108-117.e1 (2014).
4. McEwen, B. S. Stress, Adaptation, and Disease: Allostasis and Allostatic Load. *Annals of the New York Academy of Sciences* **840**, 33–44 (1998).
5. Roubinov, D., Meaney, M. J. & Boyce, W. T. Change of pace: How developmental tempo varies to accommodate failed provision of early needs. *Neuroscience & Biobehavioral Reviews* **131**, 120–134 (2021).
6. Horvath, S. & Raj, K. DNA methylation-based biomarkers and the epigenetic clock theory of ageing. *Nat Rev Genet* **19**, 371–384 (2018).
7. Jovanovic, T. *et al.* Exposure to Violence Accelerates Epigenetic Aging in Children. *Sci Rep* **7**, 8962 (2017).
8. Hamlat, E. J., Prather, A. A., Horvath, S., Belsky, J. & Epel, E. S. Early life adversity, pubertal timing, and epigenetic age acceleration in adulthood. *Developmental Psychobiology* **63**, 890–902 (2021).

9. McCrory, C. *et al.* Early life adversity and age acceleration at mid-life and older ages indexed using the next-generation GrimAge and Pace of Aging epigenetic clocks. *Psychoneuroendocrinology* **137**, 105643 (2022).
10. Austin, M. K. *et al.* Early-life socioeconomic disadvantage, not current, predicts accelerated epigenetic aging of monocytes. *Psychoneuroendocrinology* **97**, 131–134 (2018).
11. Allen, J. P. *et al.* Adolescent peer struggles predict accelerated epigenetic aging in midlife. *Development and Psychopathology* 1–14 (2022) doi:10.1017/S0954579422000153.
12. DENENBERG, V. H., OTTINGER, D. R. & STEPHENS, M. W. Effects of maternal factors upon growth and behavior of the rat. *Child development* **33**, 65–71 (1962).
13. Levine, S., Haltmeyer, G. C., Karas, G. G. & Denenberg, V. H. Physiological and behavioral effects of infantile stimulation. **2**, 55–59 (1967).
14. Francis, D., Diorio, J., Liu, D. & Meaney, M. J. Nongenomic transmission across generations of maternal behavior and stress responses in the rat. *Science* **286**, 1155–1158 (1999).
15. Getz, L. L., Carter, C. S. & Gavish, L. The mating system of the prairie vole, Microtus ochrogaster: Field and laboratory evidence for pair-bonding. *Behavioral Ecology and Sociobiology* **8**, 189–194 (1981).
16. Gavish, L., Carter, C. S. & Getz, L. L. Further evidences for monogamy in the prairie vole. *Animal Behaviour* **29**, 955–957 (1981).
17. Finton, C. J. & Ophir, A. G. Prairie vole offspring only prefer mothers over fathers when mothers are a unique resource, yet fathers are the primary source of variation in parental care. *Behav Processes* **171**, 104022 (2020).
18. Perkeybile, A. M., Griffin, L. L. & Bales, K. L. Natural variation in early parental care correlates with social behaviors in adolescent prairie voles (Microtus ochrogaster). *Frontiers in Behavioral Neuroscience* (2013) doi:10.3389/fnbeh.2013.00021.
19. Perkeybile, A. M. & Bales, K. L. Early rearing experience is related to altered aggression and vasopressin production following chronic social isolation in the prairie vole. *Behav Brain Res* **283**, 37–46 (2015).
20. del Razo, R. A. & Bales, K. L. Exploration in a dispersal task: effects of early experience and correlation with other behaviors in prairie voles (Microtus ochrogaster). *Behav Processes* **132**, 66–75 (2016).
21. Perkeybile, A. M. *et al.* Early nurture epigenetically tunes the oxytocin receptor. *Psychoneuroendocrinology* (2019) doi:10.1016/j.psyneuen.2018.08.037.
22. Bales, K. L., Lewis-Reese, A. D., Pfeifer, L. A., Kramer, K. M. & Sue Carter, C. Early experience affects the traits of monogamy in a sexually dimorphic manner. *Developmental Psychobiology* **49**, 335–342 (2007).
23. Weaver, I. C. G., Meaney, M. J. & Szyf, M. Maternal care effects on the hippocampal transcriptome and anxiety-mediated behaviors in the offspring that are reversible in adulthood. *Proceedings of the National Academy of Sciences* (2006) doi:10.1073/pnas.0507526103.
24. Vogel Ciernia, A. *et al.* Experience-dependent neuroplasticity of the developing hypothalamus: integrative epigenomic approaches. *Epigenetics* **13**, 318–330 (2018).
25. Peña, C. J. *et al.* Early life stress confers lifelong stress susceptibility in mice via ventral tegmental area OTX2. *Science* (2017) doi:10.1126/science.aan4491.
26. Peña, C. J. *et al.* Early life stress alters transcriptomic patterning across reward circuitry in male and female mice. *Nature Communications* **10**, (2019).
27. Ordoñes Sanchez, E. *et al.* Early life adversity promotes resilience to opioid addiction-related phenotypes in male rats and sex-specific transcriptional changes. *Proceedings of the National Academy of Sciences* **118**, e2020173118 (2021).
28. Eck, S. R. *et al.* Effects of early life adversity on male reproductive behavior and the medial preoptic area transcriptome. *Neuropsychopharmacol.* **47**, 1231–1239 (2022).

29. Danoff, J. S. *et al.* Genetic, epigenetic, and environmental factors controlling oxytocin receptor gene expression. *Clin Epigenetics* **13**, 23 (2021).
30. O'Connell, L. A. & Hofmann, H. A. The Vertebrate mesolimbic reward system and social behavior network: A comparative synthesis. *Journal of Comparative Neurology* **519**, 3599–3639 (2011).
31. Helmeke, C. *et al.* Paternal deprivation during infancy results in dendrite- and time-specific changes of dendritic development and spine formation in the orbitofrontal cortex of the biparental rodent Octodon degus. *Neuroscience* **163**, 790–798 (2009).
32. Pinkernelle, J., Abraham, A., Seidel, K. & Braun, K. Paternal deprivation induces dendritic and synaptic changes and hemispheric asymmetry of pyramidal neurons in the somatosensory cortex. *Developmental Neurobiology* **69**, 663–673 (2009).
33. Braun, K., Seidel, K., Holetschka, R., Groeger, N. & Poeggel, G. Paternal deprivation alters the development of catecholaminergic innervation in the prefrontal cortex and related limbic brain regions. *Brain Struct Funct* **218**, 859–872 (2013).
34. Chang, L. *et al.* Early life stress alters opioid receptor mRNA levels within the nucleus accumbens in a sex-dependent manner. *Brain Res* **1710**, 102–108 (2019).
35. Roque, A., Ochoa-Zarzosa, A. & Torner, L. Maternal separation activates microglial cells and induces an inflammatory response in the hippocampus of male rat pups, independently of hypothalamic and peripheral cytokine levels. *Brain, Behavior, and Immunity* **55**, 39–48 (2016).
36. Delpech, J.-C. *et al.* Early life stress perturbs the maturation of microglia in the developing hippocampus. *Brain Behav Immun* **57**, 79–93 (2016).
37. Schwarz, J. M., Hutchinson, M. R. & Bilbo, S. D. Early-Life Experience Decreases Drug-Induced Reinstatement of Morphine CPP in Adulthood via Microglial-Specific Epigenetic Programming of Anti-Inflammatory IL-10 Expression. *J Neurosci* **31**, 17835–17847 (2011).
38. Lumertz, F. S. *et al.* Effects of Early Life Stress on Brain Cytokines: A Systematic Review and Meta-Analysis of Rodent Studies. *Neuroscience & Biobehavioral Reviews* 104746 (2022) doi:10.1016/j.neubiorev.2022.104746.
39. Wei, L., Simen, A., Mane, S. & Kaffman, A. Early Life Stress Inhibits Expression of a Novel Innate Immune Pathway in the Developing Hippocampus. *Neuropsychopharmacology* **37**, 567–580 (2012).
40. Pohl, T. T., Jung, O., Di Benedetto, B., Young, L. J. & Bosch, O. J. Microglia react to partner loss in a sex- and brain site-specific manner in prairie voles. *Brain, Behavior, and Immunity* **96**, 168–186 (2021).
41. Donovan, M. *et al.* Social isolation alters behavior, the gut-immune-brain axis, and neurochemical circuits in male and female prairie voles. *Neurobiol Stress* **13**, 100278 (2020).
42. Molet, J., Maras, P. M., Avishai-Eliner, S. & Baram, T. Z. Naturalistic Rodent Models of Chronic Early-Life Stress. *Dev Psychobiol* **56**, 1675–1688 (2014).
43. Ivy, A. S., Brunson, K. L., Sandman, C. & Baram, T. Z. Dysfunctional nurturing behavior in rat dams with limited access to nesting material: a clinically relevant model for early-life stress. *Neuroscience* **154**, 1132–1142 (2008).
44. Bales, K. L. *et al.* Are behavioral effects of early experience mediated by oxytocin? *Article* **2**, (2011).
45. Martin, M. Cutadapt removes adapter sequences from high-throughput sequencing reads. *EMBnet.journal* (2011) doi:10.14806/ej.17.1.200.
46. Ewels, P., Magnusson, M., Lundin, S. & Käller, M. MultiQC: Summarize analysis results for multiple tools and samples in a single report. *Bioinformatics* **32**, 3047–3048 (2016).
47. Bray, N. L., Pimentel, H., Melsted, P. & Pachter, L. Near-optimal probabilistic RNA-seq quantification. *Nature Biotechnology* (2016) doi:10.1038/nbt.3519.

48. Arneson, A. *et al.* A mammalian methylation array for profiling methylation levels at conserved sequences. *Nat Commun* **13**, 783 (2022).
49. Zhou, W., Triche, T. J., Jr, Laird, P. W. & Shen, H. SeSAMe: reducing artifactual detection of DNA methylation by Infinium BeadChips in genomic deletions. *Nucleic Acids Research* **46**, e123 (2018).
50. Ding, W., Kaur, D., Horvath, S. & Zhou, W. Comparative epigenome analysis using Infinium DNA methylation BeadChips. *Briefings in Bioinformatics* **24**, bbac617 (2023).
51. Lu, A. T. *et al.* Universal DNA methylation age across mammalian tissues. 2021.01.18.426733 Preprint at https://doi.org/10.1101/2021.01.18.426733 (2021).
52. Marini, F. & Binder, H. Development of Applications for Interactive and Reproducible Research: a Case Study. *Genomics and Computational Biology* (2016) doi:10.18547/gcb.2017.vol3.iss1.e39.
53. Team, R. C. R: A Language and Environment for Statistical Computing. (2018).
54. Love, M. I., Huber, W. & Anders, S. Moderated estimation of fold change and dispersion for RNA-seq data with DESeq2. *Genome Biology* (2014) doi:10.1186/s13059-014-0550-8.
55. Wu, T. *et al.* clusterProfiler 4.0: A universal enrichment tool for interpreting omics data. *The Innovation* **2**, 100141 (2021).
56. Durinck, S. *et al.* BioMart and Bioconductor: a powerful link between biological databases and microarray data analysis. *Bioinformatics* **21**, 3439–3440 (2005).
57. Corson, J., Aldridge, A., Wilmoth, K. & Erisir, A. A Survey of Oral Cavity Afferents to the Rat Nucleus Tractus Solitarii. *J Comp Neurol* **520**, 495–527 (2012).
58. Schindelin, J. *et al.* Fiji - an Open Source platform for biological image analysis. *Nat Methods* **9**, 10.1038/nmeth.2019 (2012).
59. Ferreira, T. A. *et al.* Neuronal morphometry directly from bitmap images. *Nat Methods* **11**, 982–984 (2014).
60. DeFelipe, J. Estimation of the number of synapses in the cerebral cortex: Methodological considerations. *Cerebral Cortex* **9**, 722–732 (1999).
61. Erisir, A. & Harris, J. L. Decline of the critical period of visual plasticity is concurrent with the reduction of NR2B subunit of the synaptic NMDA receptor in layer 4. *Journal of Neuroscience* (2003) doi:10.1523/jneurosci.23-12-05208.2003.
62. King, L. B., Walum, H., Inoue, K., Eyrich, N. W. & Young, L. J. Variation in the Oxytocin Receptor Gene Predicts Brain Region–Specific Expression and Social Attachment. *Biological Psychiatry* **80**, 160–169 (2016).
63. Wickham, H. ggplot2: Elegant Graphics for Data Analysis. (2016).
64. Rogers, F. D. & Bales, K. L. Revisiting paternal absence: Female alloparental replacement of fathers recovers partner preference formation in female, but not male prairie voles (Microtus ochrogaster). *Developmental Psychobiology* **62**, 573–590 (2020).
65. Rogers, F. D., Freeman, S. M., Anderson, M., Palumbo, M. C. & Bales, K. L. Compositional variation in early-life parenting structures alters oxytocin and vasopressin 1a receptor development in prairie voles (Microtus ochrogaster). *Journal of Neuroendocrinology* **33**, e13001 (2021).
66. Faust, T. E., Gunner, G. & Schafer, D. P. Mechanisms governing activity-dependent synaptic pruning in the developing mammalian CNS. *Nat Rev Neurosci* **22**, 657–673 (2021).
67. Kopec, A. M., Smith, C. J., Ayre, N. R., Sweat, S. C. & Bilbo, S. D. Microglial dopamine receptor elimination defines sex-specific nucleus accumbens development and social behavior in adolescent rats. *Nature Communications* (2018) doi:10.1038/s41467-018-06118-z.
68. Kenkel, W. M., Perkeybile, A. M. & Carter, C. S. The Neurobiological Causes and Effects of Alloparenting. *Developmental neurobiology* **77**, 214 (2017).

69. Bester-Meredith, J. K. & Marler, C. A. Vasopressin and the transmission of paternal behavior across generations in mated, cross-fostered Peromyscus mice. *Behavioral Neuroscience* **117**, 455 (2003).
70. Becker, E. A. *et al.* Transmission of paternal retrieval behavior from fathers to sons in a biparental rodent. *Dev Psychobiol* **63**, e22164 (2021).
71. Ahern, T. H., Olsen, S., Tudino, R. & Beery, A. K. Natural variation in the oxytocin receptor gene and rearing interact to influence reproductive and nonreproductive social behavior and receptor binding. *Psychoneuroendocrinology* **128**, 105209 (2021).
72. Braun, K. & Champagne, F. A. Paternal Influences on Offspring Development: Behavioural and Epigenetic Pathways. *Journal of Neuroendocrinology* **26**, 697–706 (2014).
73. Braun, K., Seidel, K., Weigel, S., Roski, C. & Poeggel, G. Paternal Deprivation Alters Region- and Age-Specific Interneuron Expression Patterns in the Biparental Rodent, Octodon degus. *Cerebral Cortex* **21**, 1532–1546 (2011).
74. Wang, Z. & Novak, M. A. Alloparental care and the influence of father presence on juvenile prairie voles, Microtus ochrogaster. *Animal Behaviour* **47**, 281–288 (1994).
75. Leithead, A. B., Yohn, C. N. & Becker, E. A. Early paternal retrieval experience influences the degree of maternal retrieval behavior in adult California mice offspring. *Behavioural Processes* **193**, 104506 (2021).
76. Roberts, R. L., Miller, A. K., Taymans, S. E. & Carter, C. S. Role of social and endocrine factors in alloparental behavior of prairie voles (Microtus ochrogaster). *Can. J. Zool.* **76**, 1862–1868 (1998).
77. Ahern, T. & Young, L. The impact of early life family structure on adult social attachment, alloparental behavior, and the neuropeptide systems regulating affiliative behaviors in the monogamous prairie vole (Microtus ochrogaster). *Frontiers in Behavioral Neuroscience* **3**, (2009).
78. Perkeybile, A. M., Delaney-Busch, N., Hartman, S., Grimm, K. J. & Bales, K. L. Intergenerational transmission of alloparental behavior and oxytocin and vasopressin receptor distribution in the prairie vole. *Frontiers in Behavioral Neuroscience* (2015) doi:10.3389/fnbeh.2015.00191.

Chapter 4: Examine epigenetic consequences of adolescent experience using epigenetic age in humans

This chapter is published in *Development and Psychopathology*

Allen, J., Danoff, J., Costello, M., Loeb, E., Davis, A., Hunt, G., . . . Connelly, J. (2022). Adolescent peer struggles predict accelerated epigenetic aging in midlife. *Development and Psychopathology,* 1-14. doi:10.1017/S0954579422000153

Abstract

This study examined struggles to establish autonomy and relatedness with peers in adolescence and early adulthood as predictors of advanced epigenetic aging assessed at age 30. Participants (*N* = 154; 67 male and 87 female) were observed repeatedly, along with close friends and romantic partners, from ages 13 through 29. Observed difficulty establishing close friendships characterized by mutual autonomy and relatedness from ages 13 to 18, an interview-assessed attachment state of mind lacking autonomy and valuing of attachment at 24, and self-reported difficulties in social integration across adolescence and adulthood were all linked to greater epigenetic age at 30, after accounting for chronological age, gender, race, and income. Analyses assessing the unique and combined effects of these factors, along with lifetime history of cigarette smoking, indicated that each of these factors, except for adult social integration, contributed uniquely to explaining epigenetic age acceleration. Results are interpreted as evidence that the adolescent preoccupation with peer relationships may be highly functional given the relevance of such relationships to long-term physical outcomes.

Introduction

This study examined peer relationship difficulties as predictors of epigenetic aging. Identifying significant biomarkers of the aging process *prior* to the actual onset of disease is fundamental to establishing meaningful approaches to prevention of diseases of aging[1]. Until recently, the long period of onset of classic aging symptoms has made such examination impractical in all but a few cases. Recent advances in epigenetic research, however, are now making it possible to assess markers of aging that can be tracked well prior to the onset of any actual disease. Early epigenetic aging algorithms—yielding measures of epigenetic age based on patterns of methylation within the epigenome—were found to yield estimates that correlated strongly with chronological age and added value in predicting future mortality[2]. By covarying out actual chronological age, these measures also produce an indicator of epigenetic age *acceleration.* This measure reflects the degree to which an individual's epigenome suggests that they have already aged faster (or slower) than their chronological age would indicate (and is distinct from other indices that seek to capture not lifetime aging but rather the current pace of aging[3]).

Further research, though, found that these early measures were often driven more by naturally unfolding biological processes than by external environmental factors[4]. This in turn led to the development of second and third generation 'epigenetic clocks' that were specifically designed to correlate with actual levels of physiological deterioration and also to be sensitive to environmental factors. The present study used a third generation epigenetic aging measure, DNAmGrimAge, which was designed to capture aspects of epigenetic aging that were most strongly correlated with actual indicators of physiological deterioration[5]. DNAmGrimAge has been linked to a broad range of health indicators, including early mortality, time-to-heart disease, and time-to-cancer, and it has been found to outperform other existing epigenetic clocks (e.g.,

DNAmAge) when it comes to predicting many such health outcomes. Further, its link to mortality has been found to be robust across White, African American, and Hispanic individuals[5].

Although not yet well-studied, there is good reason to believe that epigenetic age acceleration will be linked to maladaptive social relationships earlier in life, in part due to the stress that relationship difficulties create. Social baseline theory, for example, suggests that the human brain is tuned to a default position of expecting to be in the presence of others who can act as potential support figures in times of threat or stress[6]; the *absence* of supportive others is then viewed as decreasing the individual's sense of relative safety. Theories regarding the role of social safety note the significant stress that occurs-- and the adverse physiological effects that follow-- when individuals perceive the social environment to be potentially threatening, for example in the face of interpersonal conflict[7,8]. Attachment theory has also long noted the importance of felt security in human functioning across the lifespan[9,10], and variations in attachment have been associated with physiological risk factors such as altered immune function[11] and cortisol responses[12].

Peer relationship struggles in adolescence seem likely to create the type of intense stress that could lead to loss of a sense of safety. Indeed, the combination of hormonal changes, neural development, and social demands in adolescence may make adolescent-era social stressors particularly powerful[13–15].

One way to view and assess adolescent relationship stressors is in terms of the critical dialectical challenge that adolescents face: They must learn how to establish peer relationships that allow for autonomy and independence (including the ability to resist peer pressure) while still providing a strong sense of connection[16]. Mastering this challenge has been identified as a fundamental marker of social competence with long-term implications for adult relationships and functioning[17–19]. Given the importance of establishing autonomy in adolescence, it is unsurprising that its absence in key relationships has been linked to higher levels of future hostile conflict[20]-- precisely the kind of threat to social safety known to influence physical health outcomes. Similarly, failure to establish strong, connected relationships in adolescence seems likely to be inherently lonely and stressful, as well as indicative of difficulties that are likely to cascade forward to future social interactions, creating ongoing stress[21]. Adult attachment theory has found support for the idea that expectations regarding the availability of relationships that are autonomous yet connected can also become internalized[10,22]. In sum, mastering this challenge in adolescence appears to reflect the essence of what it takes to become socially integrated and to establish social relationships as sources of safety vs. as sources of conflict and threat.

Prior to and during adolescence, struggles establishing and maintaining positive connections with peers have been linked to higher levels of inflammation in adulthood[23–25]. Similarly, poor social integration in early adulthood has also been linked to markers of greater inflammation[26] while poor close friendship quality has been found to predict lower self-reported health quality in adulthood[27]. In addition, over-involvement in romantic relationships in adolescence—a potential marker of autonomy difficulties—has in turn been linked to higher levels of adult blood pressure[28]. Whether and how these adolescent struggles with issues of autonomy and connection have been linked to more fundamental aging processes, however, has not been examined.

Evidence that chronic social stress is linked to long-term physical dysfunction suggests that social difficulties in adolescence are likely to predict such dysfunction[29–31]. Exposure to stress has been found to potentially alter the epigenetic landscape across the lifespan, in part via its effects on the hypothalamic-pituitary axis and the glucocorticoid signaling system[32]. Stress exposure also appears linked to lasting changes in DNA methylation, forming a sort of 'molecular scar' from this exposure[33]. Direct links between traumatic and threat-related experiences and accelerated epigenetic aging from a range of studies further support the existence of a stress-epigenetic aging connection[34–37]. No research to date, however, has examined adolescent-era social relationship difficulties in relation to epigenetic aging processes.

This study assessed adolescent relationship difficulties via multiple methods. Self-reports of the degree to which an individual does or does not feel integrated into and motivated to participate in their social network are particularly useful for assessing the role of the individual's perceptions of relationship quality. Direct observations of the extent to which close relationships are meeting the developmental need to establish autonomy and relatedness provide a more objective perspective. Finally, interview techniques can assess implicit internalized representations of relationships and allow for consideration of aspects expectations of relationships of which individuals may or may not be fully conscious. This study used the Adult Attachment Interview (AAI), which uses an individual's description of early relationships to assess the individual's *current* state of mind regarding close relationships. In particular, the AAI captures the degree to which an individual possesses, at present, an internalized sense of themselves as both autonomous and valuing of close relationships. This internalized sense—referred to as a "secure state of mind regarding attachment"[38]—captures the fundamental sense of safety that comes with expectations of relationships as likely to be both autonomous and valuable.

A mediational 'chains of risk' perspective suggests that early stressors, such as those that arise from struggles to establish autonomy and relatedness with peers, may predict future health outcomes by cascading forward to influence future relationship struggles both with peers and with romantic partners, which in turn have been robustly linked to poor health outcomes[17,21,39,40]. Hence, this study considered adolescent-era relationship factors as potentially acting via similar mediating factors in adulthood. For example, we would expect potential links from difficulties in social integration in adolescence to difficulties in social integration in adulthood to accelerated aging, with similar pathways expected for observed autonomy and relatedness and for attachment states of mind. Alternatively, more direct, unmediated links may also exist, as struggles at a critical point in development, especially in the socially sensitive period of adolescence, could well have long-term effects on physiology[41]. Cumulative lifetime stress has been previously shown to predict epigenetic aging[33] and evidence of such socially linked weathering effects on health increasingly appear in the literature[23,28,31]. Ultimately, both direct and mediated paths from relationship struggles to health outcomes appear plausible and warrant examination.

Several specific non-relational mediators were also considered given their historical links to health outcomes. A lifetime history of cigarette smoking was considered, given that one important limit to research on predictors of epigenetic aging is the possibility that markers of social stress are correlated with smoking behavior, which has been strongly related to aging[42,43]. Smoking was primarily considered as a potential covariate, but the possibility that it would mediate the effects of social difficulties that predict lifetime cigarette use was also considered. Similarly, gender, racial/ethnic minority group membership, and adolescent family income were included as covariates in all analyses given their well-established links to markers of health and aging[44–46].

This seventeen-year, multi-method, prospective exploratory study utilized a diverse community sample to examine both direct and mediated pathways from adolescent struggles with processes of autonomy and relatedness to adult patterns of accelerated epigenetic aging. This study assessed struggles to establish autonomy and relatedness with peers from multiple vantage points, including self-reports and direct behavioral observations.

This study considered both pathways from relationship struggles to epigenetic age acceleration via four primary hypotheses:

Hypothesis 1: Observed struggles establishing autonomy and relatedness in relationships with close friends across adolescence will predict epigenetic age acceleration, with links potentially mediated by similar struggles with romantic partners in adulthood.

Hypothesis 2: An internalized lack of autonomy and valuing of relationships in adolescent states of mind regarding attachment will predict epigenetic age acceleration, with links potentially mediated by similar struggles in adulthood.

Hypothesis 3: Self-reported struggles in social integration with peers in adolescence will predict epigenetic age acceleration, with links potentially mediated by similar struggles in adulthood.

Hypothesis 4: Multiple social predictors of epigenetic age acceleration will contribute unique variance to epigenetic age acceleration after considering smoking history, but will also have some of their effects mediated via this history.

Material and Methods

Participants

This report is drawn from a larger longitudinal investigation of adolescent social development in familial and peer contexts. The final sample of participants (*N* = 154 (67 male and 87 female)) was a subset of the original sample of 184 adolescents first assessed at age 13 and for whom epigenetic data was able to be obtained at age 30 (M = 29.7, *SD* = 2.16). This reflected an 84% retention rate across the 17 years of the study. The final sample was racially/ethnically and socioeconomically diverse: 86 (56%) adolescents identified themselves as White, 48 (31%) as Black/African American, 2 (1%) as Asian, 1 (1%) as Hispanic, 1 (1%) as American Indian, and 14 (9%) as from other or mixed racial/ethnic groups. Adolescents' parents reported a median family income at baseline in the $40,000 - $59,999 range (M = $43,900, *SD* = $22,500).

Adolescents were initially recruited from the 7th and 8th grades of a public middle school drawing from suburban and urban populations in the Southeastern United States. Students were recruited via an initial mailing to all parents of students in the school along with follow-up contact efforts at school lunches. Families of adolescents who indicated they were interested in the study were contacted by telephone. Of all students eligible for participation, 63% agreed to participate either as target participants or as peers providing collateral information. All participants provided informed assent before each interview session, and parents provided informed consent. Interviews took place in private offices within a university academic building.

Participants were first assessed annually over a six-year period across adolescence from age 13.35 (*SD* = .64) to age 18.38 (*SD* = 1.04). For the adult follow-up self-report assessments, data were obtained from participants annually from ages 22.8 (*SD* = .96) to age 28.6 (*SD* = 1.02). In adolescence, participants also nominated the same-gender person they currently identified as "the peer to whom they were closest" to be included in the study. In adolescence, close peers came in during a visit along with the target participant and participated in observational assessments, as described below. Close friends in adolescence reported that they had known participants for an average of 4.3 to 5.7 years (*SD* = 3.1 to 3.8) across the various assessment periods. Participants could select a different person at each assessment, given that friendships change over time. Participants selected the same close friend approximately 40% of the time across any one-year period. Only 13% of participants selected the same close friend at age 18 as they had at age 13, indicating that participants' interactions generally reflected a range of different relationships.

Romantic partner observations in adulthood were obtained for participants who were in a relationship for at least three months' duration and in which the romantic partner was willing to come into our offices for an observational assessment. Romantic relationship assessments were obtained whenever a participant was in such a relationship and willing to participate at some point during three three-year windows. The result was that assessments were obtained at participant ages 23.8 (*SD* = 1.12), 27.4 (*SD* = 1.43), and 30.31 (*SD* = 1.24). Approximately 50% of participants had the same romantic partner from age 24 to 27, and 70% had the same partner from age 27 to 30.

Procedure

In the initial introduction and throughout all sessions, confidentiality was assured to all study participants and adolescents were told that their parents would not be informed of any of the answers they provided. Informed assent was obtained from adolescents and informed consent was obtained from adolescents' parents and from adult participants. Transportation and childcare were provided if necessary. Adolescent/adult participants, their parents, their peers, and their romantic partners were all paid for participation.

Attrition Analyses

Initial attrition analyses compared the 154 participants in the final sample to the 30 who were excluded because they lacked epigenetic data. Attrition analyses revealed no differences between these groups on any measures in the study. Among the participants with epigenetic data, analyses also compared the 113 who had romantic partner observational data to the 41 who did not. These analyses also revealed no differences between these groups on any measures in the study.

Measures

Epigenetic Age (Age 30). The DNAmGrimAge measure was developed by combining DNA methylation markers of a range of physiological risk and stress factors. Unlike other epigenetic clocks, increased DNAmGrimAge does not directly indicate the number of years of increased aging, but instead captures and sums levels of methylation across a range of DNA sites that are indicative of increased mortality and morbidity risk[5]. At the research arm of the local university medical center, trained technicians drew eight and a half milliliters of whole blood from participants into a PAXgene Blood DNA Tube (PreAnalytiX, Hombrechtikon, Switzerland). Samples were stored at -20°C for short-term storage (up to 3 months) then transferred to -80°C for long-term storage. DNA was extracted using the PAXgene Blood DNA kit (PreAnalytiX, Hombrechtikon, Switzerland) according to manufacturer instructions. DNA concentration was determined by Quant-iT™ PicoGreen® dsDNA reagent (Thermofisher Scientific, Waltham, MA, USA) per manufacturers instruction. Florescence was detected using a Tecan Infinite M200 Pro microplate reader (Tecan, Switzerland). 500 ng of DNA was bisulfite treated using a Zymo EZ DNA Methylation kit (Zymo Research, Irvine, CA) using PCR conditions for Illumina's Infinium Methylation assay (95°C for 30 seconds, 50°C for 60 minutes×16 cycles). DNA methylation was assayed using the Illumina Infinium MethylationEPIC BeadChips. Briefly, a total of 4 µL of bisulfite converted DNA was hybridized to Illumina BeadChips using the manufacturer's protocols. Samples were denatured and amplified overnight for 20 to 24 hours. Fragmentation, precipitation, and resuspension of the samples followed overnight incubation, before hybridization to EPIC BeadChips for 16 to 24 hours. BeadChips were then washed to remove any unhybridized DNA and labeled with nucleotides to extend the primers to the DNA sample. Following the Infinium HD Methylation protocol, the BeadChips were imaged using the Illumina iScan system (Illumina).

Raw .idat files were read and preprocessed using the *minfi* R package[47,48]. The data set was preprocessed using noob for background subtraction and dye-bias normalization. All methylation values with detection P > 0.01 were set to missing (median sample: 669 probes, range: 255 to 4026), and probes with >1% missing values (n = 5,788) were removed from further analysis. All samples were checked and confirmed to ensure that predicted sex matched reported sex. Additionally, samples were checked for excessive missing data (>5%) and unusual cell mixture estimates, which was estimated using the Houseman method as implemented in *minfi*[49,50].

All samples passed these quality controls. Principal components analysis, as implemented in the *shinyMethyl* R package, was used to examine batch effects[51]. The first seven principal components were examined using plots and potential batch effects were tested using linear models. Principal component 2, which accounted for 2.15% of the total variance, was associated with position on the array ($F_{(7, 245)}$ = 14.93, p = 3.366e-16, adjusted R^2 = 0.2789). Principal component 4, which accounted for 1.56% of the total variance, was associated with both bisulfite conversion plate and array number (bisulfite conversion plate: $F_{(2, 250)}$ = 19.03, p = 2.307e-8, adjusted R^2 = 0.1252; array number: $F_{(31, 221)}$ = 7.98, p < 2.2e-16, adjusted R^2 = 0.462). Bisulfite conversion plate and array number were associated with each other, as samples on the same array originated from the same bisulfite conversion plate. Because samples were randomized across plates and arrays, and proportions of variance explained by PC2 and PC4 were low, no batch correction method was used. The *ewastools* R package was used to assess Illumina quality control metrics and call genotypes and donor IDs to ensure the identity of repeated samples from the same individual[52]. All samples passed Illumina quality controls.

To determine assay variability, we included one set of five technical replicates and an additional ten sets of two technical replicates. After quality control filters and normalization procedures were applied, the 5,000 CpGs with the most variable M values were used as input for calculating Pearson's correlation coefficients among all pairwise combinations of samples. Pearson's correlations of unrelated samples (different individuals) were below 0.8. Pearson's correlations of technical replicates ranged from 0.987-0.996, indicating high agreement between technical replicates.

Unnormalized betas were filtered to include CpGs specified by Horvath as necessary for calculation of various clocks. The betas were uploaded to Horvath's online DNA methylation age calculator (https://dnamage.genetics.ucla.edu), which provides measures of Horvath's multi-tissue age estimator[2], DNA methylation GrimAge[5], and cell type abundance. A sample annotation file was included. The options to normalize data and apply advanced analysis were selected. Technical replicates were used to determine measurement error of DNAmAge, the output of Horvath's multi-tissue age estimator. The absolute difference of DNAmAge between technical replicate pairs was taken, as was the highest absolute difference in the set of five technical replicates. The median of the absolute difference was 2.02 years (range: 0.44-5.73 years), comparable to previous reports of measurement error being approximately 2.41 years[53]. Variability of DNAmAge in technical replicates did not differ by any demographic feature, including sex, race, or age.

Attachment Interview and Q-sets[54,55] (Ages 14 and 24). This structured interview probes individuals' descriptions of their childhood relationships with parents in both abstract terms, and with requests for specific supporting memories. Although the interview utilizes descriptions of past relationships, it does so to yield a marker of the individual's *current* state of mind regarding themselves in close relationships. It yields an overall rating of security defined as a state of mind of being 'autonomous yet valuing of attachment relationships.' For example, participants were asked to list five words describing their early childhood relationships with each parent, and then to describe specific episodes that reflected those words. Other questions focused upon specific instances of upset, separation, loss, trauma, and rejection. Finally, the interviewer asked participants to provide more integrative descriptions of changes in relationships with parents and the current state of those relationships. The interview consisted of 18 questions and lasted one hour on average. Slight adaptations to the adult version were made to make the questions more natural and easily understood for an adolescent population at age 14[56]. These adaptations were not used for the adult interviews at age 24. Interviews were audiotaped and transcribed for coding.

The AAI Q-set[55] was designed to closely parallel the Adult Attachment Interview Classification System[38], but to yield continuous measures of qualities of attachment states of mind. Each rater read a transcript and provided a Q-sort description by assigning 100 items into nine

categories ranging from most to least characteristic of the interview, using a forced distribution. All interviews were blindly rated by at least two raters with extensive training in both the Q-sort and with formal workshop training and certification for coding using the Adult Attachment Interview Classification System. Q-sorts were then compared with a dimensional prototype sort for *secure vs. anxious interview strategies*, reflecting the overall degree of coherence of discourse, the integration of episodic and semantic attachment memories, and a clear objective valuing of attachment. The individual correlation of the 100 items of an individual's Q-sort with a prototype sort for a maximally secure transcript was then used as that participant's scale security score (ranging from -1.00 to 1.00). Inter-rater reliability, assessed via the intraclass correlation coefficient, for the final security scale score was .82 at age 14 and .71 at age 24, which is considered in the good to excellent range for this statistic[57]. Although this system was designed to yield continuous measures of qualities of attachment organization, rather than to replicate classifications from the Main and colleagues (2002) system, prior work has compared the scores obtained to a subsample (N = 76) of adolescent AAI's that were classified by an independent coder with well-established reliability in classifying AAI's. This was done by converting the Q-sort scales described above into classifications using an algorithm described by Kobak (1993). Using this approach, an 84% match for security vs. insecurity was obtained between the Q-sort method and the classification method (kappa = .68). Prior research in adolescent samples has also indicated that security assessed via this interview is relatively stable over a two-year period (i.e., r = .61)[58] and has expected relations to theoretically predictable outcomes including depression, aggression, and romantic behavior within adolescence[59–61].

Autonomy and Relatedness in Romantic Partner Interactions (Ages 24, 28, 30). Each adult participant-romantic partner dyad participated in an 8-minute videotaped task in which they were asked to discuss an issue in their relationship that they had separately identified as an area of disagreement. The discussion began with target participants playing a recording they had made separately describing the problem and their perspective on it. Typical topics of discussion included money, jealousy, moving, friends, and career issues. Researchers then coded interactions using the Autonomy-Relatedness Coding Manual for Romantic Partner Dyads, a coding system derived from the peer autonomy and relatedness coding system described above[62]. Specifically, participants' interactions were coded for expressions of reasoning and confidence (i.e., autonomy) as well as warmth and collaboration (i.e., relatedness). As above, scores were averaged across partners and assessment to yield final scores for capacity to establish romantic relationships characterized by autonomy and relatedness. Inter-rated reliability ranged from good to excellent (e.g., ICC's ranging from .69 to .90) across ages. When participants did not have a romantic partner, these data were considered missing and handled via the FIML procedures.

Adolescent Social Integration (Ages 13 – 18). Social integration in adolescence was assessed annually from age 13 to 18 via a six-item social integration scale created for this study. The scale used the format of Susan Harter's Self-Perception Scale for Adolescents to reduce social desirability biases[63]. Items focused on the extent to which participants perceived themselves to be integrated socially, for example, as '[setting] an example that other kids follow' and '[having] a lot of ideas that other kids listen to;' as well as the extent to which participants desired such integration, for example, 'getting a lot of ideas about how to be from friends' and '[finding it important] that other teens like them.' Scores across the six waves were then summed and averaged to yield the final social integration score for adolescence. Internal consistency of aggregated scale scores was good across the six assessment waves (Cronbach's α= .75). Construct validity for the scale is indicated by its modest links to the adolescent-era attachment instrument measuring autonomy and valuing of relationships (r = .24, p < .01) and to ratings by a close friend summed from ages 13 to 18 (r = .26, p < .001) of the degree to which the participant

was viewed as socially accepted using the Social Acceptance scale from the Adolescent Self-Perception Profile modified to obtain ratings of one's friend (vs. oneself, as in the original scale)[63].

Adult Social Integration (Ages 23 - 29). Social integration in adulthood was assessed annually from age 23 to 29 via the four-item social integration scale from the Social Provisions Scale[64]. The scale includes items such as "I feel part of a group of people who share my attitudes and beliefs." Scores across the seven waves were then summed and averaged to yield the final social integration score for adulthood. Internal consistency of aggregated scale scores was good across the seven assessment waves (Cronbach's $\alpha = .89$).

Lifetime History of Cigarette Smoking (Multiple waves, ages 13 - 30). Information regarding lifetime cigarette use was derived from two sets of data. First, level of smoking was assessed annually each year from age 13 to 18 in terms of number of packs smoked per day. At age 30, data was also obtained regarding year at which smoking began, year at which smoking ceased (if applicable) and average amount smoked in terms of number of packs per day. These two types of data were then harmonized such that where data were inconsistent, the higher level of reported smoking was used. The final score is calculated in terms of 'pack years,' reflecting the product of the number of years smoked X the average number of packs of cigarettes smoked each year (e.g., if an adult participant reported smoking 1 pack/day for 2 years, but the adolescent data suggested more, than the adolescent data were used).

Analytic Plan

For all primary analyses, linear regressions were conducted using SAS PROC CALIS (version 9.4, SAS Institute, Cary, NC). To best address any potential biases due to attrition in longitudinal analyses, full information maximum likelihood (FIML) methods were used with analyses including all variables that were linked to future missing data (i.e., where data were not missing completely at random). Because these procedures have been found to yield the least biased estimates when all available data are used for longitudinal analyses (vs. listwise deletion of missing data), the entire original sample of 184 adolescents was utilized for these analyses. Analyses began by entering effects of blood cell counts, as these can be correlated with (and potentially confound) epigenetic age measures, and Lu and colleagues have found stronger predictions to physiological outcomes when accounting for this potential confound[5]. In this analysis and all further analyses, the blood cell counts were estimated using the Horvath method for naïve CD8+ T cells, CD8+ CD28- CD45RA- T cells, plasmablasts (B cells) and naïve CD4+ T cells[65]. The Houseman method was used to estimate natural killer cells, monocytes, and granulocytes[49]. Chronological age was entered next, followed by participant demographic characteristics. By examining predictors of epigenetic age after accounting for blood cell counts and chronological age, the result is a prediction of epigenetic age acceleration (e.g., the extent to which a participant is epigenetically aging faster than their chronological age would indicate). Following entry of these variables, the primary predictor variables for each hypothesis were entered as described below.

Results

Preliminary analyses

Means and standard deviations for all variables used in the study are presented in Table 4.1. For descriptive purposes, intercorrelations among primary constructs are presented in Table 4.2.

We also examined possible moderating effects of gender, racial/ethnic minority group membership, and adolescent family income on the relation of social relationship qualities to epigenetic aging. Moderating effects were assessed by creating interaction terms based on the product of the centered main effect variables. No moderating effects were found for any of the analyses reported below.

Table 4.1
Means and Standard Deviations of Primary Measures and Demographic Variables

	Mean	s.d.
Blood Cell Counts		
Naïve CD8+ T cells	285.8	44.3
CD8+ CD28- CD45 RA- T cells	3.28	3.13
Plasmablasts	1.94	0.191
Naïve CD4+ T cells	770.3	95.9
Natural Killer cells	0.194	0.032
Monocytes	0.058	0.269
Granulocytes	0.634	0.104
Demographic Factors		
Chronological Age	29.7	2.176
DNAmGrimAge	37.6	4.95
DNAmAge	29.8	4.41
Lifetime Cigarette Use	2.49	4.17
Social Relationship Characteristics		
Observed Autonomy & Relatedness with Close Peer (Ages 13-18)	2.36	0.34
Observed Autonomy & Relatedness with Romantic Partner (Ages 24, 27)	2.27	0.49
Autonomy & Valuing of Attachment (Age 14)	0.25	0.42
Autonomy & Valuing of Attachment (Age 24)	0.026	0.46
Adolescent Social Integration (Ages 13-18)	7.11	2.06
Adult Social Integration (Ages 23-29)	13.8	1.68

Primary analyses

Hypothesis 1: Observed struggles establishing autonomy and relatedness in interactions with a close friend in adolescence will predict epigenetic age acceleration, with findings potentially mediated by similar struggles with romantic partners in adulthood.

As shown in Table 4.3, when measures of autonomy and relatedness were added to the model following the relevant covariates, this step added significant variance to the overall model, with observed autonomy and relatedness in adolescence linked to epigenetic aging, such that lower levels of autonomy and relatedness in adolescence were linked to greater epigenetic age acceleration (β = .22, p < .001). Follow-up bootstrap mediational analyses, using the PROCESS macro in SAS[66] indicated that the mediated pathway from autonomy and relatedness with close peers through autonomy and relatedness with romantic partners to epigenetic age acceleration was not significant (Indirect effect = -.025, 95% CI [-.095, .027]).

Hypothesis 2: An internalized lack of autonomy and valuing of relationships in adolescent states of mind regarding attachment will predict epigenetic age acceleration, with findings potentially mediated by similar struggles in adulthood.

Table 4.2

Intercorrelations Among Primary Constructs

	2.	3.	4.	5.	6.	7.	8.	9.
1. Epigenetic Age (DNAmGrimAge) (30)	.39***	-.22**	-.24**	-.11	-.31***	-.23**	-.17*	.50***
2. Chronological Age (30)	--	.14	.06	.09	.01	-.02	-.03	.20*
3. Observed Autonomy & Relatedness with Close Peer (13-18)		--	.39***	.30***	.20*	.06	.30***	-.01
4. Observed Autonomy & Relatedness with Romantic Partner (24, 27, 30)			--	.34***	.27**	.15	.22*	-.12
5. Autonomy & Valuing of Attachment (14)				--	.46***	.23**	.26***	-.10
6. Autonomy & Valuing of Attachment (24)					--	.23**	.27***	-.20*
7. Adolescent Social Integration (13-18)						--	.20**	-.22**
8. Adult Social Integration (23-29)							--	-.07
9. Lifetime Cigarette Use								--

Note: Participant age(s) at time of assessment are in parentheses. ***$p < .001$. **$p < .01$. *$p < .05$.

Following the procedure described above, analyses next examined prediction of epigenetic age acceleration from attachment states of mind reflecting an internalized sense of autonomy and valuing of attachment at ages 14 and 24. As shown in Table 4.4, predictions were found from attachment states of mind at age 24, but not from these states of mind at age 14. Attachment states of mind indicative of both lack of autonomy and lack of valuing of attachment at 24 were predictive of greater epigenetic age acceleration at age 30 ($\beta = -.24$, $p < .001$). Follow-up bootstrap mediational analyses found evidence of a mediated pathway in which age 14 attachment states of mind predicted epigenetic age acceleration via age 24 attachment states of mind (Indirect effect = -.116, 95% CI [-.211, -.050]).

Hypothesis 3: *Observed struggles in social integration with peers in adolescence will predict epigenetic age acceleration, with findings potentially mediated by similar struggles in adulthood.*

Analyses next examined prediction of epigenetic age acceleration from self-reported social integration in adolescence and adulthood. As shown in Table 4.5, predictions were found from measures of social integration at both time periods, such that lower levels of social integration were predictive of greater epigenetic age acceleration (β's = -.16 and -.12 from adolescence and adulthood respectively, p's < .01 and .05). Follow-up bootstrap mediational analyses revealed no evidence of a mediated pathway from social integration in adolescence thru social integration in adulthood in predicting epigenetic age acceleration (Indirect effect = -.026, 95% CI [-.062, -.0002]).

Table 4.3
Predicting Epigenetic Age Acceleration from Observed Behaviors Displaying Autonomy and Relatedness

		DNAmGrimAge		
	β	95% C.I.	ΔR^2	R^2
Step I. Blood Cell Counts				
Naïve CD8+ T cells	-.43***	[-.59, -.27]		
CD8+ CD28- CD45 RA- T cells	.18*	[.01, .33]		
Plasmablasts	-.21	[-.43, .01]		
Naïve CD4+ T cells	.40***	[.24, .56]		
Natural Killer cells	-.11	[-.27, .05]		
Monocytes	.04	[-.10, .18]		
Granulocytes	.38**	[.14, .62]		
Statistics for Step			.25***	.25***
Step II. Chronological Age				
Statistics for Step	.45***	[.33,.57]	.17***	.42***
Step III. Demographic Characteristics				
Gender (Male = 1, Female = 2)	-.20***	[-.36, -.08]		
Racial/Ethnic Minority Membership	.15*	[.01, .29]		
Family of Origin Income	-.04	[-.18, .10]		
Statistics for Step			.10***	.52***
Step IV. Social Relationship Characteristics				
Observed Autonomy & Relatedness with Close Peer (Ages 13-18)	-.22***	[-.36, -.08]		
Observed Autonomy & Relatedness with Romantic Partner (Ages 24, 27)	-.09	[-.25, .07]		
Statistics for Step			.05***	.57***

Note. *** $p < .001$. ** $p < .01$. * $p < .05$. β weights are from final model.

Hypothesis 4: Identified social predictors of age acceleration identified above will contribute unique variance to epigenetic age acceleration after considering smoking history, but will have some of their effects mediated via this history.

We next used a path analytic approach to examine the potential predictors of epigenetic age acceleration simultaneously, along with a measure of lifetime cigarette smoking history to assess their unique, conjoint, and mediated predictions of epigenetic age acceleration. We began by entering potential mediated pathways from each adolescent-era predictor to aging via its corresponding marker in adulthood. Modification indices were then used to identify any additional links between predictor variables that would significantly improve model fit. Because intercorrelations among cell count measures led to problems with model convergence when included, these were instead handled by first regressing them out of the epigenetic age measure prior to employing path analyses. The result is the same in either case in terms of what is being predicted by substantive factors (i.e., epigenetic age after accounting for cell counts). The effect of cell counts thus do not appear in the final model in Figure 4.1, as they were taken into account at the prior stage.

Table 4.4
Predicting Epigenetic Age Acceleration from Autonomy & Relatedness in Attachment States of Mind

		DNAmGrimAge		
	β	**95% C.I.**	**ΔR^2**	**R^2**
Step I. Blood Cell Counts				
Naïve CD8+ T cells	-.46***	[-.61, -.30]		
CD8+ CD28- CD45 RA- T cells	.13	[-.02, .28]		
Plasmablasts	-.20	[-.42, .01]		
Naïve CD4+ T cells	.41***	[.24, .57]		
Natural Killer cells	-.08	[-.24, .07]		
Monocytes	.06	[-.07, .20]		
Granulocytes	.37**	[.13, .62]		
Statistics for Step			.25***	.25***
Step II. Chronological Age				
Statistics for Step	.41***	[.30, .52]	.17***	.42***
Step III. Demographic Characteristics				
Gender	-.14*	[-.26, -.01]		
Racial/Ethnic Minority Membership	.23**	[.09, .36]		
Family of Origin Income	-.09	[-.22, .04]		
Statistics for Step			.10***	.52***
Step IV. Social Relationship Characteristics				
Autonomy & Valuing of Attachment (Age 14)	.09	[-.04, .23]		
Autonomy & Valuing of Attachment (Age 24)	-.24***	[-.37, -.11]		
Statistics for Step			.04**	.56***

Note. *** $p < .001$. ** $p < .01$. * $p < .05$. β weights are from final model.

The final model fit the data well (χ^2 (12) = 12.41, p = .41, GFI = .99, AGFI = .92, RMSE = .01) and accounted for 50.2% of the variance in epigenetic age as shown in Figure 4.1. For clarity, nonsignificant predictive links and covariances among predictors are omitted in the Figure.

Unique predictions of epigenetic age acceleration were found from each of the previously identified predictors as well as from lifetime cigarette smoking history. Results of a regression model that also includes cell count data is presented in Table 4.6. These results indicated that the final block of five psychosocial predictors combined to predict 7.7% ($p < .001$) of the variance in epigenetic age after accounting for cell counts, demographic factors, chronological age, and lifetime history of cigarette smoking.

Post-hoc analyses

For comparative purposes, the model in Table 4.6 was also tested using the original Horvath measure of DNAmAge as the dependent variable. In this model, not shown, the block of 5 psychosocial predictors was significant (χ^2 (5) = 12.35, p = .03), but only observed autonomy and relatedness with a close peer in adolescence was related to epigenetic age acceleration (β = -.19, p = .01).

Discussion

Table 4.5
Predicting Epigenetic Age Acceleration from Self-reported Social Integration

		DNAmGrimAge		
	β	95% C.I.	ΔR^2	R^2
Step I. Blood Cell Counts				
Naïve CD8+ T cells	-.45***	[-.60, -.29]		
CD8+ CD28- CD45 RA- T cells	.16*	[.02, .31]		
Plasmablasts	-.22*	[-.44, -.01]		
Naïve CD4+ T cells	.39***	[.22, .55]		
Natural Killer cells	-.12	[-.27, .03]		
Monocytes	.01	[-.12, .13]		
Granulocytes	.36**	[.12, .60]		
Statistics for Step	-.19**	[-.31, .07]		.25***
Step II. Chronological Age				
Statistics for Step			.17***	.42***
	.41***	[.30, .52]		
Step III. Demographic Characteristics				
Gender	-.19**	[-.31, -.07]		
Racial/Ethnic Minority Membership	.25***	[.12, .38]		
Family of Origin Income	-.07	[-.14, .12]		
Statistics for Step			.10***	.52***
Step IV. Social Relationship Characteristics				
Adolescent Social Integration (Ages 13-18)	-.16**	[-.27, -.05]		
Adult Social Integration (Ages 23-29)	-.12*	[-.23, -.01]		
Statistics for Step			.04***	.56***

Note. *** $p < .001$. ** $p < .01$. * $p < .05$. β weights are from final model.

The results of this study revealed a clear link between inability to establish social relationships characterized by autonomy and relatedness in adolescence and accelerations in epigenetic aging processes observable by age 30. Social relationship qualities were measured via direct observations, a coded interview, and self-reports, and evidence from each approach revealed links to epigenetic age acceleration. Further, analyses suggested that when considered jointly, the different markers appeared to capture at least somewhat unique aspects of relationship quality, in that several contributed uniquely to explaining epigenetic aging, even over and above a measure of lifetime cigarette use. When considered together, measures of struggles to establish social relationships characterized by autonomy and relatedness accounted for just under 8% of the variance in epigenetic age acceleration over and above variance accounted for by cigarette smoking and demographic factors. The combined variance accounted for by the relationship measures was comparable to the variance accounted for by lifetime history of cigarette smoking, providing an indicator of the substantial magnitude of the effects of observed.

Before considering the specific predictions observed, it is worth reflecting upon the potential mechanisms that can account for these broad findings. It should first be emphasized, however, that longitudinal predictions of this sort are *not* sufficient to support causal hypotheses. Further, given that epigenetic techniques have only recently been developed, we did not assess epigenetic aging at baseline data collection which additionally limits our ability to assess potential causal hypotheses.

Although causal relationships cannot be clearly established, these findings are highly consistent with the idea that social relationship difficulties can serve as both chronic and acute

Figure 4.1. Predictors of Epigenetic Aging

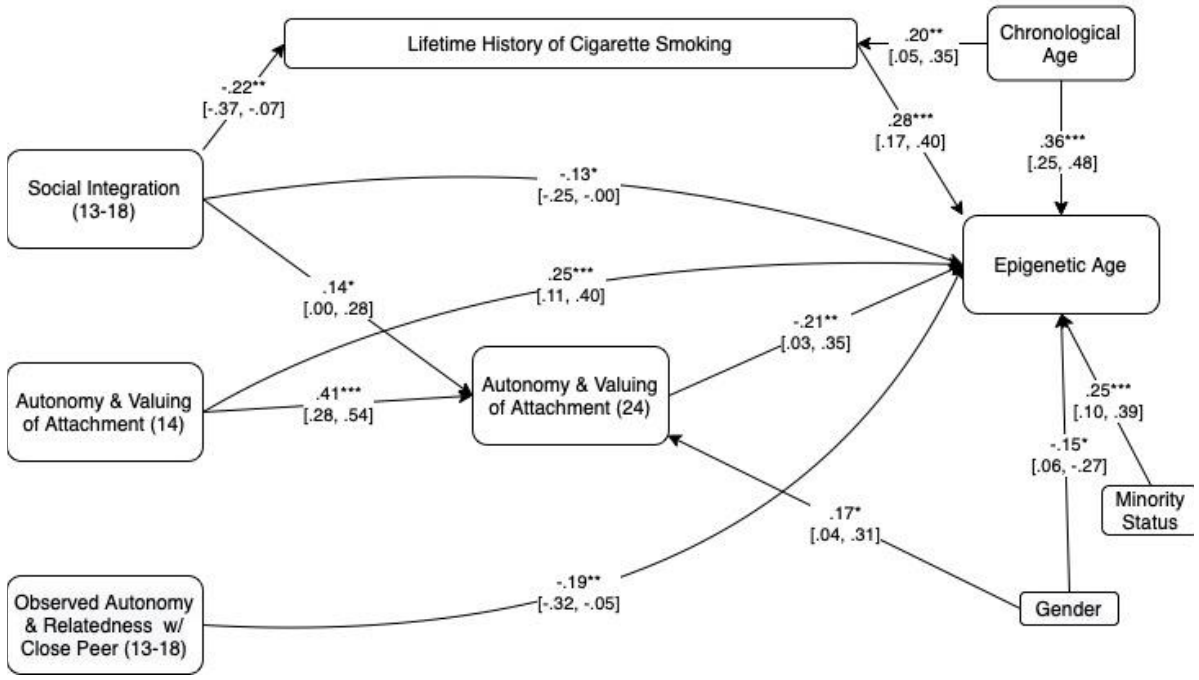

Figure 3.1 presents standardized estimates based on a path model in which all predictor variables were used to predict epigenetic age (residualized after accounting for effects of cell counts). Links across time between predictors were included where indicated via modification indices to improve model fit. For clarity, non-significant paths, variables that had no significant predictive or mediated relationships. and covariances among predictor variables are omitted. 95% confidence intervals are presented in brackets. *** $p < .001$. ** $p < .01$. * $p < .05$.

stressors and may act similarly to other stressors that have been linked to epigenetic aging[34–36]. Previously observed links between the glucocorticoid system and epigenetic changes appear as potentially viable routes of action for these linkages[32], although research in this area is still in very early stages. At first glance, the stress created by maladaptive autonomy and connection processes with close others may seem quite distinct from the kinds of acute stress, typically involving significant trauma, previously linked to epigenetic aging. A developmental perspective can shed further light on these findings, however. Given the centrality of the developmental task of establishing autonomy and relatedness with peers in adolescence[67], struggles with this process may be particularly threatening during this period. Also, because adolescence is the first point in the lifespan in which truly adult-like relationships can begin to form, these relationships take on outsized importance as the first templates for future social relationships[68]. Further, while acute stressors may be more severe, relationship difficulties are often chronic, creating a continuous source of stress on the organism. Difficulties managing the balancing of autonomy and relatedness with peers have previously been linked to a range of problematic psychosocial outcomes, from depressive symptoms and long-term career difficulties, to ongoing difficulties with peer relationships more broadly[69–71]. Notably, both autonomy threats and connection threats in adolescence have now also been linked to indicators of deleterious physical changes well into adulthood[23,72,73].

A link to epigenetic age acceleration was not found when assessing predictions from autonomy and relatedness in romantic interactions at ages 24 and 28. One possibility is that,

Table 4.6
Conjoint Prediction of Epigenetic Age Acceleration from Relationship Factors and Lifetime Cigarette Use History

		DNAmGrimAge		
	β	95% C.I.	ΔR^2	R^2
Step I. Blood Cell Counts				
Naïve CD8+ T cells	-.35***	[-.49, -.20]		
CD8+ CD28- CD45 RA- T cells	.13	[-.00, .26]		
Plasmablasts	-.22*	[-.41, -.02]		
Naïve CD4+ T cells	.32***	[.17, .47]		
Natural Killer cells	-.07	[-.21, .06]		
Monocytes	.08	[-.04, .19]		
Granulocytes	.37***	[.15, .58]		
Statistics for Step			.25***	.25***
Step II. Chronological Age				
Statistics for Step	.36***	[.25, .47]	.17***	.42***
Step III. Demographic Characteristics				
Gender	-.16**	[-.27, -.05]		
Racial/Ethnic Minority Membership	.24***	[.11, .36]		
Family of Origin Income	-.04	[-.16, .07]		
Statistics for Step			.10***	.52***
Step IV. Lifetime Cigarette Use	.24***	[.13, .35]		
Statistics for Step			.07***	.59***
Step IV. Social Relationship Characteristics				
Observed Autonomy & Relatedness with close peer (Ages 13-18)	-.18**	[-.29, -.07]		
Autonomy & Valuing of Attachment (Age 14)	.17*	[.05, .30]		
Autonomy & Valuing of Attachment (Age 24)	-.17**	[-.28, -.05]		
Adolescent Social Integration (Ages 13-18)	-.13*	[-.23, -.03]		
Adult Social Integration (Ages 23-29)	-.05	[-.15, .05]		
Statistics for Step			.08***	.67***

Note. *** $p < .001$. ** $p < .01$. * $p < .05$. β weights are from final model.

beyond adolescence, autonomy and connection have already become well-established in most relationships; hence potential threats to autonomy and connection may come to feel less acute and intense. From this vantage point, adolescence may represent a particularly vulnerable period in the lifespan regarding issues of autonomy and relatedness. Given evidence that relationship stressors in adolescence can forecast adult physiological difficulties even if those stressors do not continue[23,28,31], the possibility of such long-term weathering effects seems quite real. This also makes biological sense as aging effects are cumulative and we would expect that adult epigenetic age would be more influenced by events that happened in the past and have had time to exert their influence on aging. It is also quite possible, of course, that the lack of findings in adulthood simply reflects the smaller sample size of romantic partner observations or the overlapping variance between the adolescent and adult measures, particularly given that the adult measures were significantly related to epigenetic age in univariate correlations.

Findings regarding an internalized expectation of autonomy and connection in attachment states of mind were also linked to epigenetic aging, though with a different temporal pattern than observed displays of autonomy and relatedness. Attachment states of mind at 24 were predictive

of epigenetic aging whereas those at 14 were not. From a developmental perspective, however, this pattern is actually more consistent with a perspective emphasizing the role of adolescent peer relationships than it might first appear. Attachment states of mind at 14 are believed to almost entirely reflect experiences within the family of origin[74]. Although there is considerable stability in these states of mind over time, relative decreases in an overall state of autonomy and valuing of attachment from 14 to 24 have been found to be strongly predicted by intervening *peer* difficulties[75]. Hence, the temporal pattern of findings—with attachment states of mind becoming linked to epigenetic aging at some point between 14 and 24—also points in the direction of adolescent peer experiences as a key long-term predictor of epigenetic aging. This may also be the reason for the apparent suppressor effect observed in final models in which attachment states of mind at 14 showed a positive link to aging (in contrast to the negative, though non-significant, link seen in simple correlations). Further supporting this post-hoc interpretation, in the final path model, although not hypothesized, it was found that adolescent social integration was also predictive of a secure state of mind reflecting autonomy and valuing of attachment at 24.

Lower levels of self-perceived social integration were also related to accelerated epigenetic aging across both time periods. Although self-reports are problematic for many purposes, in this case, self-perception may be useful as a proxy for the likely stress felt by perceived absence of strong social support. Hence in accord with social baseline theory, it may be the *perceived* absence of membership in a group of supportive others that is most threatening[6].

Several limitations to these findings should also be kept in mind. In addition to the lack of baseline epigenetic data, the study also lacked information about stressors that may have occurred prior to adolescence and which may have affected both future social relationships and epigenetic aging. In particular, experiences of childhood maltreatment, which have previously been linked to epigenetic aging[36], could easily have influenced future relationship development as well. Of course, it is also possible that prior childhood experiences had later effects that were observable precisely *because* they were mediated via intervening relationship experiences of the type measured in this study. Also, given that this study assessed a community sample in which rates of severe abuse experiences were relatively rare, this factor alone would seem unlikely to account for the magnitude and range of the effects observed.

A second limitation is that these findings were only partially replicated when using the original epigenetic clock measure[2]. This may be explained by the differences in the clocks. DNAmGrimAge estimates epigenetic age using DNA methylation estimators of serum protein levels of proteins which are markers of biological deterioration and which have been related to stress. Horvath's clock estimates epigenetic age only on the basis of an algorithm which captures biological age and is less sensitive to environmental stressors. Although this is not surprising given that this original measure is considered less sensitive to environmental influences, it nonetheless adds an important cautionary note and indicates a clear need for future work to assess the replicability of these findings. The difference in findings between these two epigenetic clocks also makes clear the need for further research to explore just which epigenetic mechanisms are implicated in potential social stressor effects as well as how these mechanisms may translate into actual diseases of aging. Our lack of knowledge in this area should also make clear that no single measure is sufficient to quantify all aspects of biological aging[76]. A third limitation is that, given the composition of our sample, our examination of potential effects of genetic ancestry was, of necessity, somewhat crude, even though such ancestry differences have the potential to confound results[77]. However, given that the epigenetic aging measure used has been found robust across ancestry groups and that ancestry was considered as a covariate (and not found to be a significant moderator), this limitation is unlikely to have altered results. Finally, it should be noted that the final full model presented in Figure 1 is clearly exploratory in nature, including both hypothesized as well as non-hypothesized pathways between variables.

Given these limitations, this is nonetheless among the first studies to demonstrate long-term linkages between struggles in key aspects of social relationships, beginning as early as

adolescence, and epigenetic aging. These linkages were observed from adolescence to epigenetic age acceleration at age 30, across multiple methods, and from a domain of social functioning previously identified as central to social development. Given previous findings on links from adolescent social experiences to other physical health outcomes, it is becoming increasingly apparent that the adolescent preoccupation with peer relationships, rather than being a quirk of this stage of the lifespan, may reflect a fundamental and biologically adaptive attunement to a domain with long-term consequences for health and for societal efforts to enhance health. For example, these findings may suggest new entry points for pediatricians assessing potential behaviorally-linked risks to future physical health beyond the usual focus on factors such as obesity, cigarette smoking, etc. Similarly, intervention approaches that directly target the quality of adolescents' social relationships[78] might now warrant consideration not just for their immediate effects on adolescent well-being, but for their potential long-term implications for healthy aging. Finally, these findings suggest that parents trying to assess how their adolescent is faring might give greater weight to the quality of their ongoing peer relationships. Overall, then, these findings add growing urgency to calls to place a greater priority on processes of lifelong social connection and disconnection as precursors to key health outcomes[79].

References

1. Koss, K. J. *et al.* Parental job loss and adolescent epigenetic aging. in (2021).
2. Horvath, S. DNA methylation age of human tissues and cell types. *Genome Biology* (2013) doi:10.1186/gb-2013-14-10-r115.
3. Belsky, D. W. *et al.* Quantification of the pace of biological aging in humans through a blood test, the DunedinPoAm DNA methylation algorithm. *eLife* **9**, e54870 (2020).
4. Palma-Gudiel, H., Fañanás, L., Horvath, S. & Zannas, A. S. Psychosocial stress and epigenetic aging. *Int Rev Neurobiol* **150**, 107–128 (2020).
5. Lu, A. T. *et al.* DNA methylation GrimAge strongly predicts lifespan and healthspan. *Aging (Albany NY)* **11**, 303–327 (2019).
6. Coan, J. A. & Sbarra, D. A. Social Baseline Theory: The Social Regulation of Risk and Effort. *Curr Opin Psychol* **1**, 87–91 (2015).
7. Brosschot, J. F., Verkuil, B. & Thayer, J. F. Exposed to events that never happen: Generalized unsafety, the default stress response, and prolonged autonomic activity. *Neurosci Biobehav Rev* **74**, 287–296 (2017).
8. Slavich, G. M. Social Safety Theory: A Biologically Based Evolutionary Perspective on Life Stress, Health, and Behavior. *Annual Review of Clinical Psychology* **16**, 265–295 (2020).
9. Bowlby, J. Attachment and loss: Volume III: Loss, sadness and depression. in *Attachment and Loss: Volume III: Loss, Sadness and Depression* 1–462 (London: The Hogarth press and the institute of psycho-analysis, 1980).
10. Main, M., Kaplan, N. & Cassidy, J. Security in infancy, childhood, and adulthood: A move to the level of representation. *Monographs of the Society for Research in Child Development* **50**, 66–104 (1985).
11. Picardi, A. *et al.* Attachment style and immunity: A 1-year longitudinal study. *Biological Psychology* **92**, 353–358 (2013).
12. Pietromonaco, P. R., DeBuse, C. J. & Powers, S. I. Does Attachment Get Under the Skin? Adult Romantic Attachment and Cortisol Responses to Stress. *Curr Dir Psychol Sci* **22**, 63–68 (2013).
13. Albert, D., Chein, J. & Steinberg, L. The Teenage Brain: Peer Influences on Adolescent Decision Making. *Curr Dir Psychol Sci* **22**, 114–120 (2013).
14. Charles, S. T., Reynolds, C. A. & Gatz, M. Age-related differences and change in positive and negative affect over 23 years. *J Pers Soc Psychol* **80**, 136–151 (2001).

15. Steinberg, L. & Monahan, K. C. Age Differences in Resistance to Peer Influence. *Dev Psychol* **43**, 1531–1543 (2007).
16. Allen, J. P. & Loeb, E. L. The Autonomy-Connection Challenge in Adolescent Peer Relationships. *Child Dev Perspect* **9**, 101–105 (2015).
17. Allen, J. P., Narr, R. K., Kansky, J. & Szwedo, D. E. Adolescent Peer Relationship Qualities as Predictors of Long-Term Romantic Life Satisfaction. *Child Dev* **91**, 327–340 (2020).
18. Loeb, E. L., Davis, A., Costello, M. & Allen, J. P. Autonomy and relatedness in early adolescent friendships as predictors of short- and long-term academic success. *Soc Dev* **29**, 818–836 (2020).
19. Oudekerk, B. A. *et al.* Maternal and Paternal Psychological Control as Moderators of the Link between Peer Attitudes and Adolescents' Risky Sexual Behavior. *J Early Adolesc* **34**, 413–435 (2014).
20. Allen, J. P., Hauser, S. T., O'Connor, T. G., Bell, K. L. & Eickholt, C. The connection of observed hostile family conflict to adolescents' developing autonomy and relatedness with parents. *Development and Psychopathology* **8**, 425–442 (1996).
21. Oudekerk, B. A., Allen, J. P., Hessel, E. T. & Molloy, L. E. The Cascading Development of Autonomy and Relatedness From Adolescence to Adulthood. *Child Dev* **86**, 472–485 (2015).
22. Thompson, R. A. Internal Working Models as Developing Representations. in *Attachment: The Fundamental Questions* 128 (Guilford, 2021).
23. Allen, J. P., Loeb, E., Tan, J., Narr, R. & Uchino, B. N. The Body Remembers: Adolescent Conflict Struggles Predict Adult Interleukin-6 Levels. *Dev Psychopathol* **30**, 1435–1445 (2018).
24. Copeland, W. E. *et al.* Childhood bullying involvement predicts low-grade systemic inflammation into adulthood. *Proc Natl Acad Sci U S A* **111**, 7570–7575 (2014).
25. Takizawa, R., Danese, A., Maughan, B. & Arseneault, L. Bullying victimization in childhood predicts inflammation and obesity at mid-life: a five-decade birth cohort study. *Psychol Med* **45**, 2705–2715 (2015).
26. Ford, J. *et al.* Social Integration and Quality of Social Relationships as Protective Factors for Inflammation in a Nationally Representative Sample of Black Women. *J Urban Health* **96**, 35–43 (2019).
27. Allen, J. P., Uchino, B. N. & Hafen, C. A. Running With the Pack: Teen Peer-Relationship Qualities as Predictors of Adult Physical Health. *Psychol Sci* **26**, 1574–1583 (2015).
28. Allen, J. P., Loeb, E. L., Tan, J., Davis, A. A. & Uchino, B. Adolescent relational roots of adult blood pressure: A 14-year prospective study. *Development and Psychopathology* 1–11 (2021) doi:10.1017/S0954579421000419.
29. Fiorito, G. *et al.* Social adversity and epigenetic aging: a multi-cohort study on socioeconomic differences in peripheral blood DNA methylation. *Sci Rep* **7**, 16266 (2017).
30. Hertzman, C. The biological embedding of early experience and its effects on health in adulthood. *Ann N Y Acad Sci* **896**, 85–95 (1999).
31. Miller, G. E., Chen, E. & Parker, K. J. Psychological stress in childhood and susceptibility to the chronic diseases of aging: moving toward a model of behavioral and biological mechanisms. *Psychol Bull* **137**, 959–997 (2011).
32. Gassen, N. C., Chrousos, G. P., Binder, E. B. & Zannas, A. S. Life stress, glucocorticoid signaling, and the aging epigenome: Implications for aging-related diseases. *Neurosci Biobehav Rev* **74**, 356–365 (2017).
33. Zannas, A. S. *et al.* Lifetime stress accelerates epigenetic aging in an urban, African American cohort: relevance of glucocorticoid signaling. *Genome Biology* **16**, 266 (2015).
34. Brody, G. H., Yu, T., Chen, E., Beach, S. R. H. & Miller, G. E. Family-centered prevention ameliorates the longitudinal association between risky family processes and epigenetic aging. *Journal of Child Psychology and Psychiatry* **57**, 566–574 (2016).

35. Brody, G. H., Miller, G. E., Yu, T., Beach, S. R. H. & Chen, E. Supportive Family Environments Ameliorate the Link Between Racial Discrimination and Epigenetic Aging: A Replication Across Two Longitudinal Cohorts. *Psychol Sci* **27**, 530–541 (2016).
36. Jovanovic, T. *et al.* Exposure to Violence Accelerates Epigenetic Aging in Children. *Sci Rep* **7**, 8962 (2017).
37. Sumner, J. A., Colich, N. L., Uddin, M., Armstrong, D. & McLaughlin, K. A. Early Experiences of Threat, but Not Deprivation, Are Associated With Accelerated Biological Aging in Children and Adolescents. *Biological Psychiatry* **85**, 268–278 (2019).
38. Main, M., Goldwyn, R. & Hesse, E. Adult Attachment scoring and classification systems, Version 7.1. (2002).
39. Ben-Shlomo, Y. & Kuh, D. A life course approach to chronic disease epidemiology: conceptual models, empirical challenges and interdisciplinary perspectives. *Int J Epidemiol* **31**, 285–293 (2002).
40. Holt-Lunstad, J., Smith, T. B. & Layton, J. B. Social relationships and mortality risk: A meta-analytic review. *PLoS Medicine* (2010) doi:10.1371/journal.pmed.1000316.
41. Blakemore, S.-J. & Mills, K. L. Is Adolescence a Sensitive Period of Sociocultural Processing? *Annual Review of Psychology* **65**, 187–207 (2014).
42. Joehanes, R. *et al.* Epigenetic Signatures of Cigarette Smoking. *Circ Cardiovasc Genet* **9**, 436–447 (2016).
43. Norman, R. E. *et al.* The Long-Term Health Consequences of Child Physical Abuse, Emotional Abuse, and Neglect: A Systematic Review and Meta-Analysis. *PLOS Medicine* **9**, e1001349 (2012).
44. Annandale, E. Health and Gender. in *The Wiley Blackwell Companion to Medical Sociology* 237–257 (John Wiley & Sons, Ltd, 2021). doi:10.1002/9781119633808.ch12.
45. Khullar, D. & Chokshi, D. A. Health, Income, & Poverty: Where We Are & What Could Help. *Health Affairs Health Policy Brief* (2018) doi:doi:10.1377/hpb20180817.901935.
46. Nguyen, A. B., Moser, R. & Chou, W.-Y. Race and health profiles in the United States: an examination of the social gradient through the 2009 CHIS adult survey. *Public Health* **128**, 1076–1086 (2014).
47. Aryee, M. J. *et al.* Minfi: A flexible and comprehensive Bioconductor package for the analysis of Infinium DNA methylation microarrays. *Bioinformatics* **30**, 1363–9 (2014).
48. Fortin, J. P., Triche, T. J. & Hansen, K. D. Preprocessing, normalization and integration of the Illumina HumanMethylationEPIC array with minfi. *Bioinformatics* (2017) doi:10.1093/bioinformatics/btw691.
49. Houseman, E. A. *et al.* DNA methylation arrays as surrogate measures of cell mixture distribution. *BMC Bioinformatics* (2012) doi:10.1186/1471-2105-13-86.
50. Jaffe, A. E. & Irizarry, R. A. Accounting for cellular heterogeneity is critical in epigenome-wide association studies. *Genome Biology* (2014) doi:10.1186/gb-2014-15-2-r31.
51. Fortin, J. P., Fertig, E. & Hansen, K. shinyMethyl: Interactive quality control of Illumina 450k DNA methylation arrays in R. *F1000Research* (2014) doi:10.12688/f1000research.4680.2.
52. Heiss, J. A. & Just, A. C. Identifying mislabeled and contaminated DNA methylation microarray data: An extended quality control toolset with examples from GEO. *Clinical Epigenetics* **10**, 73 (2018).
53. McEwen, L. M. *et al.* Systematic evaluation of DNA methylation age estimation with common preprocessing methods and the Infinium MethylationEPIC BeadChip array. *Clinical Epigenetics* (2018) doi:10.1186/s13148-018-0556-2.
54. George, C., Kaplan, N. & Main, M. Adult Attachment Interview (3rd ed.). (1996).
55. Kobak, R. R., Cole, H. E., Ferenz-Gillies, R., Fleming, W. S. & Gamble, W. Attachment and Emotion Regulation during Mother-Teen Problem Solving: A Control Theory Analysis. *Child Development* **64**, 231–245 (1993).

56. Ward, M. J. & Carlson, E. A. Associations among Adult Attachment Representations, Maternal Sensitivity, and Infant-Mother Attachment in a Sample of Adolescent Mothers. *Child Development* **66**, 69–79 (1995).
57. Cicchetti, D. V. & Sparrow, S. A. Developing criteria for establishing interrater reliability of specific items: applications to assessment of adaptive behavior. *Am J Ment Defic* **86**, 127–137 (1981).
58. Allen, J. P., McElhaney, K. B., Kuperminc, G. P. & Jodl, K. M. Stability and Change in Attachment Security Across Adolescence. *Child Development* **75**, 1792–1805 (2004).
59. Chango, J. M., McElhaney, K. B. & Allen, J. P. Attachment organization and patterns of conflict resolution in friendships predicting adolescents' depressive symptoms over time. *Attach Hum Dev* **11**, 331–346 (2009).
60. Miga, E. M., Hare, A., Allen, J. P. & Manning, N. The relation of insecure attachment states of mind and romantic attachment styles to adolescent aggression in romantic relationships. *Attach Hum Dev* **12**, 463–481 (2010).
61. van Hoof, M.-J., van Lang, N. D. J., Speekenbrink, S., van IJzendoorn, M. H. & Vermeiren, R. R. J. M. Adult Attachment Interview differentiates adolescents with Childhood Sexual Abuse from those with clinical depression and non-clinical controls. *Attach Hum Dev* **17**, 354–375 (2015).
62. Allen, J. P. *et al.* Autonomy and relatedness coding manual for adolescent romantic partner dyads.
63. Harter, S. Manual for the self-perception profile for adolescents. (1988).
64. Cutrona, C. E. & Russell, D. W. The provisions of social relationships and adaptation to stress. *Advances in personal relationships* **1**, 37–67 (1987).
65. Horvath, S. & Levine, A. J. HIV-1 Infection Accelerates Age According to the Epigenetic Clock. *The Journal of Infectious Diseases* **212**, 1563–1573 (2015).
66. Hayes, A. F. *Introduction to Mediation, Moderation, and Conditional Process Analysis, Second Edition: A Regression-Based Approach*. (Guilford Publications, 2017).
67. Steinberg, L. *Adolescence*. (McGraw Hill).
68. Roisman, G. I., Masten, A. S., Coatsworth, J. D. & Tellegen, A. Salient and Emerging Developmental Tasks in the Transition to Adulthood. *Child Development* **75**, 123–133 (2004).
69. Chango, J. M., Allen, J. P., Szwedo, D. & Schad, M. M. Early Adolescent Peer Foundations of Late Adolescent and Young Adult Psychological Adjustment. *Journal of Research on Adolescence* **25**, 685–699 (2015).
70. Henrich, C. C., Blatt, S. J., Kuperminc, G. P., Zohar, A. & Leadbeater, B. J. Levels of Interpersonal Concerns and Social Functioning in Early Adolescent Boys and Girls. *Journal of Personality Assessment* **76**, 48–67 (2001).
71. Pakaslahti, L., Karjalainen, A. & Keltikangas-Järvinen, L. Relationships between adolescent prosocial problem-solving strategies, prosocial behaviour, and social acceptance. *International Journal of Behavioral Development* **26**, 137–144 (2002).
72. Loeb, E. L. *et al.* The developmental precursors of blunted cardiovascular responses to stress. *Developmental Psychobiology* **63**, 247–261 (2021).
73. Yang, Y. C. *et al.* Social relationships and physiological determinants of longevity across the human life span. *Proc Natl Acad Sci U S A* **113**, 578–583 (2016).
74. Booth-LaForce, C. The Adult Attachment Interview: Psychometrics, stability and change from infancy, and developmental origins: Abstract. *Monographs of the Society for Research in Child Development* **79**, vii–viii (2014).
75. Allen, J. P., Grande, L., Tan, J. & Loeb, E. Parent and Peer Predictors of Change in Attachment Security From Adolescence to Adulthood. *Child Development* **89**, 1120–1132 (2018).

76. Hägg, S., Belsky, D. W. & Cohen, A. A. Developments in molecular epidemiology of aging. *Emerging Topics in Life Sciences* **3**, 411–421 (2019).
77. Philibert, R. *et al.* Array-Based Epigenetic Aging Indices May Be Racially Biased. *Genes* **11**, 685 (2020).
78. Allen, J. P., Narr, R. K., Nagel, A. G., Costello, M. A. & Guskin, K. The Connection Project: Changing the peer environment to improve outcomes for marginalized adolescents. *Development and Psychopathology* **33**, 647–657 (2021).
79. Holt-Lunstad, J., Robles, T. F. & Sbarra, D. A. Advancing social connection as a public health priority in the United States. *American Psychologist* **72**, 517–530 (2017).

Chapter 5: Overall Significance and Conclusion

Summary of Results

The experiments in this dissertation aim to understand mechanisms by which early life experiences impact behavioral and health outcomes in both animal models and humans. Over three aims, I show that early life social experience impacts epigenetic, neurodevelopmental, and behavior outcomes with significant implications for health throughout the lifespan. These studies advance our understanding of how genes interact with the environment during development and impact ontogeny of social behaviors. Chapters 2 and 3 of this dissertation use prairie voles as an animal model. Prairie voles are an excellent model for these studies because of their human-like social behaviors. The third aim of this dissertation translates some of the findings of Chapter 3 to humans using a longitudinal study.

In Chapter 2, I show that early life experience in the form of parental care impacts epigenetic regulation of the oxytocin receptor gene, *Oxtr*, in prairie vole brain tissue[1]. The results of this study show that in two regions of *Oxtr*, both of which are extensively studied in human neuropsychological studies[2], DNA methylation is reduced in offspring raised with higher care parents. However, only DNA methylation in the MT2 region is predictive of *Oxtr* gene expression, suggesting that studies in human should focus on this region of the gene. Further, using network analysis, I show that specific sites at the 3' end of MT2 are particularly sensitive to early life experience and related to *Oxtr* gene expression. Finally, I identify and characterize a novel transcript of *Oxtr* which is present in prairie vole brain tissue and under genetic control. This study extends our previous findings examining *Oxtr* gene regulation in prairie voles and clarifies the epigenetic regulation of the gene, which we hope will be used by others to inform future studies in humans that examine neuropsychological impacts of *Oxtr* methylation[3].

In Chapter 3, I show that early nurture slows development, measured by epigenetic age in brain tissue. I then show that early life experience leads to widespread transcriptional changes in prairie vole brain tissue in male offspring only. In males, high care parenting leads to increased expression of genes related to synaptic transmission and neurodevelopment and decreased expression of genes related to metabolism in neuroimmune processes. Using a natural parenting paradigm, I then show that while total parental care impacts epigenetic and neuroanatomical outcomes including epigenetic aging, excitatory synapse density and microglia cell density, male offspring are highly sensitive to parental care composition. Specifically, male offspring raised with more care by fathers have increased excitatory synapse density, with more synapses characterized by small terminal areas and shorter synaptic zones. These results may indicate that paternal care leads to increased synapse formation from a specific input into nucleus accumbens core characterized by small terminal areas and short synaptic zones, though I have not identified which input this may be. Finally, I show that parental care composition has opposing effects on pup retrieval behavior in offspring. This study adds to the literature on early life experience by differentiating the impact of different features of parental care. Namely, we show that total parental care impacts neurological and social behavioral outcomes in both male and female prairie voles, but parental care composition particularly impacts neurodevelopmental processes in male prairie voles only. Importantly, this finding is allowed for by using an appropriate human-like model system that displays biparental care.

In Chapter 4, I use the longitudinal KLIFF/VIDA study to examine how adolescent social experience impacts epigenetic age. We find that an epigenetic estimator of mortality risk, DNAmGrimAge, is accelerated by peer struggles during adolescence, even after accounting for demographic and lifestyle factors[4,5]. In fact, the effect of combined social experiences during adolescence on epigenetic age acceleration is comparable to lifetime history of cigarette smoking. These results provide evidence that peer social relationships during adolescence have long lasting impacts on healthspan and lifespan and add to our understanding of physiological impacts

of social experiences. Further, these results are consistent with results from Chapter 3 which show that reduced early life social experience is also associated with increased epigenetic age.

Mechanisms of Paternal Impact on Male Offspring

These results indicate that in prairie voles, paternal care has a specific impact on gene expression, neuroanatomy, and behavior in male offspring. These results are consistent with previous work in other monogamous rodents which indicate male-specific impacts of paternal care[6–10]. I identify neurobiological mechanisms which may mediate these paternal care effects: namely, increased expression of transcriptional programs related to synaptic transmission and increased excitatory synapse density in nucleus accumbens. Further research is necessary to conclusively connect these neurobiological effects with behavioral effects by completing neuroanatomical, neurogenetic, and behavioral experiments in the same animals. Additionally, cross-fostering experiments would be helpful in separating genetic and rearing effects, which would significantly expand upon these results.

The upstream mechanism connecting paternal care and neurobiological changes is unknown. Based on the literature examining paternal effects in other monogamous rodents, possible molecular mediators of paternal care include gonadal hormones[11] and stress hormones[12]. It is likely that the effects of paternal care are greatest in the first week of life and future studies identifying mechanisms relating paternal care and future neurobiological outcomes should focus on this critical period. Nonetheless, these results identify neurobiological outcomes associated with paternal care in this biparental species which might be used to examine upstream mechanisms.

In understanding how paternal care impacts neurodevelopment, one might consider paternal care to be a form of environmental enrichment. Not only does paternal care lead to increased overall care towards pups, but a greater qualitative diversity of parental behaviors. Environmental enrichment has been noted to influence many of the phenotypes investigated in these studies including heightening the oxytocin system[13–15], neuroanatomical variation[16], and promoting social behavior[13,15,17]. In fact, environmental enrichment counteracts the impact of low parental care on some of these outcomes[15,18,19]. Though it is tempting to understand paternal care as a form of environmental enrichment, evidence suggests that paternal care is uniquely important in the development of male offspring. For example, if one expects that biparental care creates an enriching environment simply by the presence of two caregivers, then it should not matter who the caregivers are. However, male prairie vole offspring display reduced species-typical social behavior (pair bonding) when raised by their mother and older sister, even though the total quantity of parental care in this condition is equal to that of biparental care[6]. This suggests that there is a unique aspect of paternal care which may not be able to be replaced by other forms of environmental enrichment.

Epigenetic Age and Implications for Healthspan

In two chapters of this dissertation, I examine how epigenetic age is impacted by early life social experience. Epigenetic age uses DNA methylation from several genomic sites to predict biological age[20]. Many different epigenetic clocks exist which may work in specific or all tissue types and predict specific features of aging. Using the universal mammalian clock[21], I show that increased parenting early in life leads to reduced epigenetic age in brain tissue as juveniles in prairie voles. This is consistent with previous literature indicating that prairie voles raised by higher care parents reach developmental milestones including eye opening, leaving the nest, and eating solid food, later than prairie voles raised by lower care parents[22]. In Chapter 4, I use the GrimAge clock, which estimates mortality risk, to show that experiencing peer struggles during adolescence is associated with increased GrimAge in mid-adulthood[4,5]. These results are consistent with previous literature indicating that social support is highly predictive of longevity[23] and work from

another group connecting early life social experiences to epigenetic age later in life[24]. These results further our understanding of the physiological impact of social experience and the importance of social support in individual and public health outcomes.

Conclusions

Across three studies, I examine how early life social experiences impact physiological and psychological outcomes at the level of gene expression and epigenetic regulation, neuroanatomical structures, and behavioral processes. Specifically, I show that in prairie voles, increased duration of total parental care leads to increased expression of the oxytocin receptor gene which may be mediated by reduced DNA methylation at critical CpG sites, reduced epigenetic age, increased density of excitatory synapses and microglia cells, and reduced attack behavior in an alloparenting test in both sexes. I additionally show that total parental care impacts transcriptional programs in the nucleus accumbens of male prairie voles. Further, by differentiating total parental care from the composition of that care, I show that in males only, increased care by fathers leads to increased excitatory synapse density, more small-area terminals and shorter synaptic zones, and increased pup retrieval behavior in an alloparenting test. These results improve our understanding of sex differences in the response to the early environment and indicate a specific role for male parents in raising male offspring, a phenomenon which has previously been reported in prairie voles and other monogamous rodent species. Additionally, I show that in humans, peer social struggles lead to increased epigenetic age, with effect size equivalent to lifetime history of cigarette smoking. These results have significant implications for health-related interventions and suggest that strong social relationships are critical for extending lifespan and healthspan. Further, given the congruence of the epigenetic age data in prairie voles and humans presented in this dissertation, these results establish that prairie voles would be an excellent model to study the impacts of social experience on epigenetic age and other aging outcomes at the mechanistic level. Overall these studies will inform future research on mechanisms by which early life experience impacts physiological and behavioral outcomes.

References

1. Danoff, J. S. *et al.* Genetic, epigenetic, and environmental factors controlling oxytocin receptor gene expression. *Clin Epigenetics* **13**, 23 (2021).
2. Danoff, J. S., Connelly, J. J., Morris, J. P. & Perkeybile, A. M. An epigenetic rheostat of experience: DNA methylation of OXTR as a mechanism of early life allostasis. *Comprehensive Psychoneuroendocrinology* **8**, 100098 (2021).
3. Perkeybile, A. M. *et al.* Early nurture epigenetically tunes the oxytocin receptor. *Psychoneuroendocrinology* **99**, 128–136 (2019).
4. Lu, A. T. *et al.* DNA methylation GrimAge strongly predicts lifespan and healthspan. *Aging (Albany NY)* **11**, 303–327 (2019).
5. Allen, J. P. *et al.* Adolescent peer struggles predict accelerated epigenetic aging in midlife. *Development and Psychopathology* 1–14 (2022) doi:10.1017/S0954579422000153.
6. Rogers, F. D. & Bales, K. L. Revisiting paternal absence: Female alloparental replacement of fathers recovers partner preference formation in female, but not male prairie voles (Microtus ochrogaster). *Developmental Psychobiology* **62**, 573–590 (2020).
7. Rogers, F. D., Freeman, S. M., Anderson, M., Palumbo, M. C. & Bales, K. L. Compositional variation in early-life parenting structures alters oxytocin and vasopressin 1a receptor development in prairie voles (Microtus ochrogaster). *Journal of Neuroendocrinology* **33**, e13001 (2021).
8. Bester-Meredith, J. K. & Marler, C. A. Vasopressin and the transmission of paternal behavior across generations in mated, cross-fostered Peromyscus mice. *Behavioral Neuroscience* **117**, 455 (2003).

9. Becker, E. A. *et al.* Transmission of paternal retrieval behavior from fathers to sons in a biparental rodent. *Dev Psychobiol* **63**, e22164 (2021).
10. Wang, Z. & Novak, M. A. Alloparental care and the influence of father presence on juvenile prairie voles, Microtus ochrogaster. *Animal Behaviour* **47**, 281–288 (1994).
11. Chary, M. C., Cruz, J. P., Bardi, M. & Becker, E. A. Paternal retrievals increase testosterone levels in both male and female California mouse (Peromyscus californicus) offspring. *Hormones and Behavior* **73**, 23–29 (2015).
12. Wang, J., Tai, F., Yan, X. & Yu, P. Paternal deprivation alters play-fighting, serum corticosterone and the expression of hypothalamic vasopressin and oxytocin in juvenile male mandarin voles. *J Comp Physiol A* **198**, 787–796 (2012).
13. Neal, S., Kent, M., Bardi, M. & Lambert, K. G. Enriched Environment Exposure Enhances Social Interactions and Oxytocin Responsiveness in Male Long-Evans Rats. *Frontiers in Behavioral Neuroscience* **12**, (2018).
14. Prounis, G. S., Thomas, K. & Ophir, A. G. Developmental trajectories and influences of environmental complexity on oxytocin receptor and vasopressin 1A receptor expression in male and female prairie voles. *Journal of Comparative Neurology* **526**, 1820–1842 (2018).
15. Champagne, F. A. & Meaney, M. J. Transgenerational effects of social environment on variations in maternal care and behavioral response to novelty. *Behav Neurosci* **121**, 1353–1363 (2007).
16. Kempermann, G. Environmental enrichment, new neurons and the neurobiology of individuality. *Nature Reviews Neuroscience* **20**, 235–245 (2019).
17. Torquet, N. *et al.* Social interactions impact on the dopaminergic system and drive individuality. *Nature Communications* **9**, 1–11 (2018).
18. Bredy, T. W., Humpartzoomian, R. A., Cain, D. P. & Meaney, M. J. Partial reversal of the effect of maternal care on cognitive function through environmental enrichment. *Neuroscience* **118**, 571–576 (2003).
19. Bredy, T. W., Zhang, T. Y., Grant, R. J., Diorio, J. & Meaney, M. J. Peripubertal environmental enrichment reverses the effects of maternal care on hippocampal development and glutamate receptor subunit expression. *European Journal of Neuroscience* **20**, 1355–1362 (2004).
20. Field, A. E. *et al.* DNA Methylation Clocks in Aging: Categories, Causes, and Consequences. *Mol Cell* **71**, 882–895 (2018).
21. Consortium, M. M. *et al.* Universal DNA methylation age across mammalian tissues. 2021.01.18.426733 Preprint at https://doi.org/10.1101/2021.01.18.426733 (2021).
22. Perkeybile, A. M., Griffin, L. L. & Bales, K. L. Natural variation in early parental care correlates with social behaviors in adolescent prairie voles (Microtus ochrogaster). *Frontiers in Behavioral Neuroscience* (2013) doi:10.3389/fnbeh.2013.00021.
23. Holt-Lunstad, J., Smith, T. B. & Layton, J. B. Social relationships and mortality risk: A meta-analytic review. *PLoS Medicine* (2010) doi:10.1371/journal.pmed.1000316.
24. Hamlat, E. J., Prather, A. A., Horvath, S., Belsky, J. & Epel, E. S. Early life adversity, pubertal timing, and epigenetic age acceleration in adulthood. *Developmental Psychobiology* **63**, 890–902 (2021).

Appendix A: Tables Related to Chapter 2

Table A.1: RT-PCR primers and conditions

Gene	Primers	PCR conditions	Efficiency
Cd47	F: 5′-GGAACCCCTTAACGCATTTAAAGA-3′	Step 1: 95°C/10 min, 1 cycle	E: 97.6%
	R: 5′-TGGGCCAACACATCTTCCATAG-3′	Step 2: 95°C/15s, 61.0°C/60s, 35 cycles	R^2: 0.989
C1qa	F: 5′-AGGGAGGCCGGGTCTCAA-3′	Step 1: 95°C/10 min, 1 cycle	E: 100.9%
	R: 5′-CTCAGGCTTTGGGGGTTTC-3′	Step 2: 95°C/15s, 61.0°C/60s, 35 cycles	R^2: 0.995
Skap2	F: 5′-TATGGCTGGTGGGTAGGAGAAA-3′	Step 1: 95°C/10 min, 1 cycle	E: 101.3%
	R: 5′-TCCATCCTCCCCCTGGTCT-3′	Step 2: 95°C/15s, 59.5°C/60s, 35 cycles	R^2: 0.995
Pgk1	F (TSL402_F): 5′-TTGCCCGTTGACTTTGTCAC-3′	Step 1: 95°C/10 min, 1 cycle	E: 93.5%
	R (TSL402_R): 5′-GCCACAGCCTCAGCATATTTC-3′	Step 2: 95°C/15s, 65.3°C/60s, 35 cycles	R^2: 0.998

Table A.2: Differential gene expression in male and female offspring (MAN1 relative to MAN0).

Female Offspring

row	baseMean	log2FoldChange	lfcSE	stat	pvalue	padj	sig	gene_name
ENSMOCG00000004642	480.51	-5.20	1.06	-4.88	1.05E-06	0.01	TRUE	NA
ENSMOCG00000015262	154.94	-0.70	0.15	-4.57	4.84E-06	0.03	TRUE	Ak8
ENSMOCG00000000123	65.08	-3.86	0.89	-4.32	1.59E-05	0.07	TRUE	NA

Male Offspring

row	baseMean	log2FoldChange	lfcSE	stat	pvalue	padj	sig	gene_name
ENSMOCG00000002407	3288.97	0.17	0.03	5.11	3.24E-07	0.003	TRUE	Zdhhc17
ENSMOCG00000015396	744.37	0.37	0.08	4.91	9.06E-07	0.005	TRUE	Exoc6b
ENSMOCG00000004975	266.15	0.54	0.11	4.73	2.29E-06	0.006	TRUE	Ssh1
ENSMOCG00000015467	812.92	-0.59	0.13	-4.68	2.91E-06	0.006	TRUE	NA
ENSMOCG00000020416	2660.56	0.24	0.05	4.71	2.44E-06	0.006	TRUE	Lrrtm2
ENSMOCG00000005941	887.36	0.34	0.07	4.58	4.62E-06	0.008	TRUE	Wnk3
ENSMOCG00000006852	3464.23	0.30	0.07	4.55	5.29E-06	0.008	TRUE	Tspyl4
ENSMOCG00000022372	1298.93	0.25	0.06	4.53	5.99E-06	0.008	TRUE	Sfmbt1
ENSMOCG00000016949	219.30	-0.44	0.10	-4.47	7.81E-06	0.009	TRUE	Cth
ENSMOCG00000008139	1125.97	0.25	0.06	4.37	1.26E-05	0.013	TRUE	Itsn2
ENSMOCG00000010854	434.06	-0.52	0.12	-4.30	1.68E-05	0.016	TRUE	Thyn1
ENSMOCG00000015568	1239.41	0.37	0.09	4.27	1.96E-05	0.017	TRUE	Etnk1
ENSMOCG00000012511	317.12	-0.49	0.11	-4.24	2.22E-05	0.018	TRUE	Phospho2
ENSMOCG00000002006	825.61	-0.46	0.11	-4.22	2.46E-05	0.018	TRUE	Ttc5
ENSMOCG00000000914	909.57	-0.33	0.08	-4.17	3.05E-05	0.019	TRUE	NA
ENSMOCG00000014781	1203.47	0.34	0.08	4.14	3.47E-05	0.019	TRUE	Plxnc1
ENSMOCG00000016314	386.94	-0.86	0.21	-4.13	3.69E-05	0.019	TRUE	NA
ENSMOCG00000019426	766.46	0.26	0.06	4.13	3.57E-05	0.019	TRUE	Tbc1d30
ENSMOCG00000021616	3258.37	0.29	0.07	4.12	3.75E-05	0.019	TRUE	Klhdc10
ENSMOCG00000023006	554.57	0.48	0.11	4.18	2.95E-05	0.019	TRUE	Slc9a7

ENSMOCG00000017563	452.68	0.39	0.10	4.10	4.05E-05	0.020	TRUE	Irs1
ENSMOCG00000000362	2399.30	0.26	0.06	3.95	7.73E-05	0.030	TRUE	Dmxl1
ENSMOCG00000011439	701.41	-0.37	0.09	-3.95	7.70E-05	0.030	TRUE	Llph
ENSMOCG00000015464	228.20	-0.54	0.14	-3.97	7.13E-05	0.030	TRUE	Lfng
ENSMOCG00000017246	371.68	0.43	0.11	3.95	7.83E-05	0.030	TRUE	Mtx3
ENSMOCG00000018532	611.74	0.61	0.15	3.96	7.61E-05	0.030	TRUE	Csrnp3
ENSMOCG00000022302	863.48	-0.31	0.08	-3.98	6.83E-05	0.030	TRUE	Amn1
ENSMOCG00000013595	1340.46	0.33	0.08	3.90	9.51E-05	0.034	TRUE	Sesn3
ENSMOCG00000013936	620.38	0.52	0.13	3.89	1.01E-04	0.034	TRUE	Pgap1
ENSMOCG00000014082	559.27	-0.26	0.07	-3.88	1.04E-04	0.034	TRUE	Rpusd1
ENSMOCG00000018034	1475.53	0.31	0.08	3.88	1.03E-04	0.034	TRUE	Cdh8
ENSMOCG00000020334	607.75	0.55	0.14	3.86	1.13E-04	0.036	TRUE	Tnrc6b
ENSMOCG00000013858	3062.87	-0.38	0.10	-3.85	1.20E-04	0.038	TRUE	Glo1
ENSMOCG00000003169	598.73	0.37	0.10	3.81	1.39E-04	0.039	TRUE	Nfat5
ENSMOCG00000013274	420.58	-0.80	0.21	-3.81	1.40E-04	0.039	TRUE	Rnase4
ENSMOCG00000016739	491.30	-0.32	0.08	-3.82	1.32E-04	0.039	TRUE	Neu4
ENSMOCG00000017719	454.57	0.49	0.13	3.82	1.34E-04	0.039	TRUE	Lnpep
ENSMOCG00000016414	1286.09	-0.36	0.09	-3.78	1.57E-04	0.042	TRUE	Ezr
ENSMOCG00000010442	776.94	0.31	0.08	3.77	1.62E-04	0.043	TRUE	NA
ENSMOCG00000006901	722.66	-0.74	0.20	-3.77	1.66E-04	0.043	TRUE	C1qa
ENSMOCG00000014172	1977.75	0.25	0.07	3.75	1.74E-04	0.044	TRUE	Fam169a
ENSMOCG00000003748	2009.89	0.36	0.10	3.73	1.90E-04	0.045	TRUE	Gsk3b
ENSMOCG00000008224	826.88	-0.39	0.11	-3.74	1.87E-04	0.045	TRUE	C1qc
ENSMOCG00000014143	466.54	0.35	0.09	3.73	1.95E-04	0.045	TRUE	NA
ENSMOCG00000003884	2248.23	0.37	0.10	3.71	2.05E-04	0.047	TRUE	Aff4
ENSMOCG00000021860	932.59	0.29	0.08	3.70	2.14E-04	0.048	TRUE	Tspyl5
ENSMOCG00000018124	1706.45	-0.35	0.09	-3.68	2.31E-04	0.051	TRUE	Ech1
ENSMOCG00000022870	572.20	0.30	0.08	3.67	2.40E-04	0.051	TRUE	Zfp236

ENSMOCG00000000277	295.95	-0.33	0.09	-3.64	2.70E-04	0.051	TRUE	Rbks
ENSMOCG00000002807	271.26	0.38	0.10	3.64	2.76E-04	0.051	TRUE	Csnk1g1
ENSMOCG00000003347	1958.15	0.26	0.07	3.64	2.72E-04	0.051	TRUE	Jmjd1c
ENSMOCG00000005014	624.00	-0.24	0.07	-3.67	2.45E-04	0.051	TRUE	Cep57
ENSMOCG00000007538	322.19	0.51	0.14	3.64	2.69E-04	0.051	TRUE	Tmtc3
ENSMOCG00000008367	1440.37	-0.21	0.06	-3.65	2.64E-04	0.051	TRUE	Nop53
ENSMOCG00000009823	386.99	-0.26	0.07	-3.63	2.80E-04	0.051	TRUE	Smarcd2
ENSMOCG00000016626	2403.87	0.27	0.07	3.66	2.57E-04	0.051	TRUE	Pcnx
ENSMOCG00000016745	444.81	0.33	0.09	3.61	3.03E-04	0.052	TRUE	NA
ENSMOCG00000017223	644.57	-0.32	0.09	-3.62	3.00E-04	0.052	TRUE	Gadd45gip1
ENSMOCG00000019393	1474.16	-0.25	0.07	-3.62	2.94E-04	0.052	TRUE	NA
ENSMOCG00000021899	5927.46	0.23	0.06	3.62	2.90E-04	0.052	TRUE	Trip12
ENSMOCG00000003236	341.34	-0.36	0.10	-3.58	3.47E-04	0.058	TRUE	Nubp1
ENSMOCG00000000679	14885.11	-0.66	0.18	-3.57	3.63E-04	0.060	TRUE	NA
ENSMOCG00000000167	767.54	-0.23	0.07	-3.55	3.88E-04	0.061	TRUE	Tpgs1
ENSMOCG00000011054	1506.55	0.19	0.05	3.54	3.99E-04	0.061	TRUE	Wapl
ENSMOCG00000011324	2684.29	-0.40	0.11	-3.55	3.88E-04	0.061	TRUE	NA
ENSMOCG00000011846	1464.84	0.31	0.09	3.54	4.00E-04	0.061	TRUE	Tle4
ENSMOCG00000016261	3952.50	-0.19	0.05	-3.56	3.77E-04	0.061	TRUE	Cltb
ENSMOCG00000017068	517.56	-0.29	0.08	-3.54	4.07E-04	0.061	TRUE	Amdhd2
ENSMOCG00000003628	649.95	-0.32	0.09	-3.49	4.79E-04	0.065	TRUE	Ccdc115
ENSMOCG00000004257	1327.67	0.36	0.10	3.52	4.40E-04	0.065	TRUE	Myo9a
ENSMOCG00000005005	404.18	0.47	0.13	3.50	4.61E-04	0.065	TRUE	Slc7a14
ENSMOCG00000007289	1090.95	0.39	0.11	3.48	5.08E-04	0.065	TRUE	Taok1
ENSMOCG00000010045	745.88	0.34	0.10	3.48	5.06E-04	0.065	TRUE	Dgki
ENSMOCG00000011339	1178.17	-0.26	0.08	-3.50	4.73E-04	0.065	TRUE	Ptges2
ENSMOCG00000011494	410.60	0.29	0.08	3.50	4.57E-04	0.065	TRUE	Smcr8
ENSMOCG00000012085	284.48	-0.38	0.11	-3.48	5.09E-04	0.065	TRUE	Acads

ENSMOCG00000012219	329.17	-0.40	0.11	-3.51	4.46E-04	0.065	TRUE	Slc25a26
ENSMOCG00000015070	1825.79	-0.34	0.10	-3.48	4.96E-04	0.065	TRUE	Ndufa13
ENSMOCG00000015177	468.95	-0.28	0.08	-3.48	5.09E-04	0.065	TRUE	Wdr73
ENSMOCG00000017661	3640.02	0.15	0.04	3.50	4.69E-04	0.065	TRUE	Zfp638
ENSMOCG00000020892	348.21	0.42	0.12	3.50	4.58E-04	0.065	TRUE	Tbc1d8
ENSMOCG00000019122	999.54	0.24	0.07	3.47	5.27E-04	0.066	TRUE	Slf2
ENSMOCG00000016094	1863.18	-0.20	0.06	-3.46	5.37E-04	0.067	TRUE	Cwc15
ENSMOCG00000018478	1377.20	-0.63	0.18	-3.46	5.50E-04	0.067	TRUE	Hopx
ENSMOCG00000018523	666.17	-0.27	0.08	-3.45	5.58E-04	0.067	TRUE	Blvrb
ENSMOCG00000013255	267.89	0.44	0.13	3.45	5.69E-04	0.068	TRUE	NA
ENSMOCG00000005122	205.28	-0.44	0.13	-3.44	5.86E-04	0.069	TRUE	Ppp1r3g
ENSMOCG00000011713	1212.40	0.38	0.11	3.43	6.13E-04	0.071	TRUE	Xpr1
ENSMOCG00000017060	488.31	-0.50	0.15	-3.42	6.18E-04	0.071	TRUE	Skap2
ENSMOCG00000019618	729.87	0.44	0.13	3.41	6.39E-04	0.073	TRUE	NA
ENSMOCG00000004441	270.76	-0.58	0.17	-3.39	7.06E-04	0.074	TRUE	NA
ENSMOCG00000005519	1206.21	-0.33	0.10	-3.38	7.16E-04	0.074	TRUE	Mrps7
ENSMOCG00000008839	1602.40	0.16	0.05	3.41	6.61E-04	0.074	TRUE	Pura
ENSMOCG00000012435	2277.52	-0.22	0.06	-3.38	7.23E-04	0.074	TRUE	NA
ENSMOCG00000013336	389.48	0.50	0.15	3.39	6.87E-04	0.074	TRUE	NA
ENSMOCG00000013494	438.41	0.34	0.10	3.38	7.22E-04	0.074	TRUE	NA
ENSMOCG00000015205	954.14	0.34	0.10	3.41	6.52E-04	0.074	TRUE	NA
ENSMOCG00000016300	212.79	-0.46	0.14	-3.39	7.08E-04	0.074	TRUE	Lamb3
ENSMOCG00000019107	792.19	0.50	0.15	3.39	7.09E-04	0.074	TRUE	Zkscan16
ENSMOCG00000021198	2759.91	0.20	0.06	3.39	6.98E-04	0.074	TRUE	Setd5
ENSMOCG00000021683	900.15	-0.24	0.07	-3.40	6.76E-04	0.074	TRUE	NA
ENSMOCG00000020635	1092.60	0.26	0.08	3.37	7.39E-04	0.075	TRUE	Larp4
ENSMOCG00000002992	861.34	-0.28	0.08	-3.35	8.04E-04	0.076	TRUE	Mrpl9
ENSMOCG00000009609	4586.15	0.38	0.11	3.35	8.10E-04	0.076	TRUE	Usp9x

ENSMOCG00000011900	373.06	0.36	0.11	3.34	8.52E-04	0.076	TRUE	NA
ENSMOCG00000012691	2719.68	0.34	0.10	3.34	8.52E-04	0.076	TRUE	Nsd1
ENSMOCG00000014836	582.13	-0.29	0.09	-3.37	7.59E-04	0.076	TRUE	Mrpl28
ENSMOCG00000015085	682.11	0.37	0.11	3.34	8.34E-04	0.076	TRUE	Map3k2
ENSMOCG00000015256	666.63	-0.29	0.09	-3.36	7.65E-04	0.076	TRUE	Parl
ENSMOCG00000016460	1108.31	0.30	0.09	3.33	8.68E-04	0.076	TRUE	Cep350
ENSMOCG00000017115	438.96	-0.50	0.15	-3.35	7.95E-04	0.076	TRUE	Bud31
ENSMOCG00000018312	636.16	-0.20	0.06	-3.36	7.90E-04	0.076	TRUE	Ube2e2
ENSMOCG00000019479	1229.33	0.21	0.06	3.33	8.66E-04	0.076	TRUE	Rbm27
ENSMOCG00000020195	1987.00	0.23	0.07	3.36	7.81E-04	0.076	TRUE	Cd47
ENSMOCG00000020861	1274.37	-0.20	0.06	-3.33	8.57E-04	0.076	TRUE	Lsm4
ENSMOCG00000021843	1026.22	0.35	0.10	3.36	7.82E-04	0.076	TRUE	Pdpk1
ENSMOCG00000022377	349.80	-0.34	0.10	-3.34	8.35E-04	0.076	TRUE	Lmf1
ENSMOCG00000022819	3441.78	0.19	0.06	3.34	8.33E-04	0.076	TRUE	Rnft2
ENSMOCG00000000635	3171.95	0.33	0.10	3.24	0.001	0.077	TRUE	Ube3a
ENSMOCG00000000658	1846.20	-0.18	0.05	-3.24	0.001	0.077	TRUE	Ranbp1
ENSMOCG00000002234	1807.33	-0.46	0.14	-3.26	0.001	0.077	TRUE	S100a16
ENSMOCG00000003005	875.51	-0.23	0.07	-3.24	0.001	0.077	TRUE	Arfrp1
ENSMOCG00000003160	6578.17	0.29	0.09	3.25	0.001	0.077	TRUE	Prepl
ENSMOCG00000003369	606.65	-0.40	0.12	-3.31	0.001	0.077	TRUE	NA
ENSMOCG00000006000	18430.30	-0.31	0.09	-3.31	0.001	0.077	TRUE	Ttyh1
ENSMOCG00000006707	638.36	0.48	0.15	3.27	0.001	0.077	TRUE	Dgkh
ENSMOCG00000007179	1230.05	-0.52	0.16	-3.27	0.001	0.077	TRUE	C1qb
ENSMOCG00000007803	692.05	0.29	0.09	3.31	0.001	0.077	TRUE	Bcorl1
ENSMOCG00000009338	587.19	0.35	0.11	3.28	0.001	0.077	TRUE	Trpm3
ENSMOCG00000009371	1204.09	-0.17	0.05	-3.26	0.001	0.077	TRUE	Trir
ENSMOCG00000009834	1286.50	0.25	0.08	3.29	0.001	0.077	TRUE	Coro7
ENSMOCG00000010741	720.93	-0.38	0.12	-3.26	0.001	0.077	TRUE	Nenf

ENSMOCG00000010784	1133.40	0.15	0.05	3.26	0.001	0.077	TRUE	Ireb2
ENSMOCG00000011060	607.54	0.35	0.11	3.27	0.001	0.077	TRUE	Trip11
ENSMOCG00000011142	199.76	-0.49	0.15	-3.31	0.001	0.077	TRUE	Rgs10
ENSMOCG00000012518	611.49	0.39	0.12	3.24	0.001	0.077	TRUE	NA
ENSMOCG00000013270	1028.86	-0.35	0.11	-3.25	0.001	0.077	TRUE	Rhoc
ENSMOCG00000013275	4630.55	-0.17	0.05	-3.24	0.001	0.077	TRUE	Cyc1
ENSMOCG00000013388	13702.33	-0.11	0.03	-3.29	0.001	0.077	TRUE	Mrfap1
ENSMOCG00000013685	1331.68	-0.25	0.08	-3.28	0.001	0.077	TRUE	Mrpl51
ENSMOCG00000014526	659.27	-0.19	0.06	-3.24	0.001	0.077	TRUE	Akt1s1
ENSMOCG00000014871	298.56	0.33	0.10	3.30	0.001	0.077	TRUE	Prkdc
ENSMOCG00000015614	1429.13	-0.27	0.08	-3.24	0.001	0.077	TRUE	Grpel1
ENSMOCG00000015701	2931.55	0.26	0.08	3.25	0.001	0.077	TRUE	Cds2
ENSMOCG00000016083	2122.73	0.27	0.08	3.24	0.001	0.077	TRUE	Spen
ENSMOCG00000016297	266.29	0.31	0.09	3.31	0.001	0.077	TRUE	Lcor
ENSMOCG00000016467	1472.29	0.36	0.11	3.27	0.001	0.077	TRUE	St8sia3
ENSMOCG00000016670	428.98	0.22	0.07	3.30	0.001	0.077	TRUE	Pgr
ENSMOCG00000016714	569.84	-0.66	0.20	-3.26	0.001	0.077	TRUE	Tmem106c
ENSMOCG00000017188	907.14	-0.30	0.09	-3.29	0.001	0.077	TRUE	Narfl
ENSMOCG00000017394	531.07	0.25	0.08	3.28	0.001	0.077	TRUE	NA
ENSMOCG00000018006	890.81	-0.35	0.11	-3.26	0.001	0.077	TRUE	Ppif
ENSMOCG00000018243	1764.95	0.28	0.09	3.26	0.001	0.077	TRUE	Heatr5b
ENSMOCG00000018836	3231.91	0.21	0.06	3.32	0.001	0.077	TRUE	Phlpp2
ENSMOCG00000019127	1366.11	0.48	0.15	3.28	0.001	0.077	TRUE	NA
ENSMOCG00000019667	584.04	0.34	0.10	3.27	0.001	0.077	TRUE	Fam120c
ENSMOCG00000019778	383.28	0.38	0.12	3.27	0.001	0.077	TRUE	Mid2
ENSMOCG00000021173	595.44	0.28	0.08	3.25	0.001	0.077	TRUE	Ap5m1
ENSMOCG00000021346	2502.22	0.19	0.06	3.24	0.001	0.077	TRUE	Ankrd12
ENSMOCG00000021419	476.37	0.38	0.11	3.31	0.001	0.077	TRUE	Zfp790

ENSMOCG00000022982	843.17	-0.20	0.06	-3.27	0.001	0.077	TRUE	Ppil1
ENSMOCG00000008324	532.39	0.27	0.08	3.23	0.001	0.077	TRUE	Ldoc1
ENSMOCG00000006127	630.93	0.27	0.08	3.23	0.001	0.078	TRUE	Nin
ENSMOCG00000020278	1006.53	-0.30	0.09	-3.23	0.001	0.078	TRUE	Hes6
ENSMOCG00000021578	376.27	0.32	0.10	3.23	0.001	0.078	TRUE	Cdyl2
ENSMOCG00000009964	417.86	0.32	0.10	3.21	0.001	0.079	TRUE	NA
ENSMOCG00000013414	2263.82	-0.22	0.07	-3.21	0.001	0.079	TRUE	Polr2e
ENSMOCG00000015847	3340.53	0.32	0.10	3.22	0.001	0.079	TRUE	Nlgn3
ENSMOCG00000017539	1606.75	0.29	0.09	3.21	0.001	0.079	TRUE	NA
ENSMOCG00000017806	646.32	-0.25	0.08	-3.21	0.001	0.079	TRUE	Yipf2
ENSMOCG00000019974	950.08	0.53	0.16	3.21	0.001	0.079	TRUE	Vps13a
ENSMOCG00000020304	8416.62	-0.58	0.18	-3.21	0.001	0.079	TRUE	S100b
ENSMOCG00000020922	1340.76	0.33	0.10	3.21	0.001	0.079	TRUE	Atg2b
ENSMOCG00000021143	1202.48	-0.22	0.07	-3.22	0.001	0.079	TRUE	Tex264
ENSMOCG00000022404	1110.23	-0.23	0.07	-3.21	0.001	0.079	TRUE	Vta1
ENSMOCG00000022499	673.30	0.30	0.09	3.22	0.001	0.079	TRUE	Mdga2
ENSMOCG00000006660	840.15	0.35	0.11	3.20	0.001	0.079	TRUE	Mut
ENSMOCG00000010471	435.88	-0.42	0.13	-3.20	0.001	0.079	TRUE	Arpc1b
ENSMOCG00000012039	605.42	-0.32	0.10	-3.20	0.001	0.079	TRUE	Sri
ENSMOCG00000017840	556.85	-0.31	0.10	-3.20	0.001	0.079	TRUE	NA
ENSMOCG00000017896	8625.34	0.38	0.12	3.20	0.001	0.079	TRUE	Lonrf2
ENSMOCG00000018320	516.06	0.34	0.11	3.20	0.001	0.079	TRUE	Sema3c
ENSMOCG00000022121	6662.21	0.20	0.06	3.20	0.001	0.079	TRUE	AI593442
ENSMOCG00000022928	225.75	0.27	0.09	3.19	0.001	0.079	TRUE	Asb7
ENSMOCG00000004236	1600.70	-0.40	0.13	-3.18	0.001	0.081	TRUE	Acaa2
ENSMOCG00000017726	1511.76	-0.32	0.10	-3.18	0.001	0.081	TRUE	Smdt1
ENSMOCG00000019569	5339.62	-0.32	0.10	-3.18	0.001	0.081	TRUE	NA
ENSMOCG00000021976	2199.44	-0.89	0.28	-3.18	0.001	0.081	TRUE	NA

ENSMOCG00000007220	582.75	-0.27	0.08	-3.17	0.002	0.082	TRUE	NA
ENSMOCG00000018113	313.22	0.39	0.12	3.17	0.002	0.082	TRUE	Brwd3
ENSMOCG00000021439	523.22	-0.66	0.21	-3.16	0.002	0.084	TRUE	Dusp19
ENSMOCG00000010859	1609.58	-0.32	0.10	-3.15	0.002	0.086	TRUE	Timm13
ENSMOCG00000021486	505.14	0.35	0.11	3.15	0.002	0.086	TRUE	Mgat4a
ENSMOCG00000012367	685.36	0.31	0.10	3.15	0.002	0.087	TRUE	Fam126b
ENSMOCG00000001630	688.13	-0.30	0.09	-3.14	0.002	0.087	TRUE	NA
ENSMOCG00000002060	1596.78	0.22	0.07	3.14	0.002	0.087	TRUE	Lhfpl4
ENSMOCG00000005661	3484.70	-0.42	0.13	-3.14	0.002	0.087	TRUE	Rpl10a
ENSMOCG00000012958	200.88	0.39	0.12	3.14	0.002	0.087	TRUE	Pcdh11x
ENSMOCG00000014847	392.43	0.22	0.07	3.14	0.002	0.087	TRUE	Ccdc112
ENSMOCG00000015545	529.19	0.22	0.07	3.15	0.002	0.087	TRUE	Zfp654
ENSMOCG00000019631	827.94	-0.34	0.11	-3.14	0.002	0.087	TRUE	Tmem11
ENSMOCG00000020087	768.53	-0.36	0.11	-3.14	0.002	0.087	TRUE	Ctbs
ENSMOCG00000022048	4272.28	0.27	0.09	3.14	0.002	0.087	TRUE	Ankrd17
ENSMOCG00000004746	215.22	-0.63	0.20	-3.13	0.002	0.087	TRUE	Ccdc167
ENSMOCG00000022652	2068.25	-0.25	0.08	-3.13	0.002	0.087	TRUE	NA
ENSMOCG00000002192	282.38	0.35	0.11	3.12	0.002	0.089	TRUE	Creb1
ENSMOCG00000002256	5017.86	0.21	0.07	3.12	0.002	0.089	TRUE	Usp34
ENSMOCG00000002880	284.76	0.48	0.15	3.11	0.002	0.089	TRUE	Nhsl2
ENSMOCG00000005630	1579.80	-0.28	0.09	-3.11	0.002	0.089	TRUE	Snta1
ENSMOCG00000006739	1257.89	0.41	0.13	3.11	0.002	0.089	TRUE	Slc38a1
ENSMOCG00000006999	198.21	-0.46	0.15	-3.12	0.002	0.089	TRUE	Tmem176a
ENSMOCG00000013911	3776.39	-0.35	0.11	-3.11	0.002	0.089	TRUE	Gatm
ENSMOCG00000020783	730.29	0.47	0.15	3.12	0.002	0.089	TRUE	Plxna4
ENSMOCG00000021063	471.72	0.50	0.16	3.11	0.002	0.089	TRUE	NA
ENSMOCG00000005375	996.77	0.70	0.22	3.11	0.002	0.089	TRUE	Grin2b
ENSMOCG00000005759	390.48	0.35	0.11	3.11	0.002	0.090	TRUE	NA

ENSMOCG00000021755	1834.21	0.25	0.08	3.11	0.002	0.090	TRUE	Togaram1
ENSMOCG00000009075	709.09	0.46	0.15	3.10	0.002	0.090	TRUE	Grik3
ENSMOCG00000007034	2320.87	0.26	0.09	3.10	0.002	0.091	TRUE	Pnmal1
ENSMOCG00000017689	2290.36	0.18	0.06	3.10	0.002	0.091	TRUE	AW549877
ENSMOCG00000018380	2669.31	0.21	0.07	3.10	0.002	0.091	TRUE	Mcm3ap
ENSMOCG00000022273	240.76	-0.43	0.14	-3.10	0.002	0.091	TRUE	Cenpx
ENSMOCG00000000550	865.44	-0.23	0.07	-3.08	0.002	0.091	TRUE	Upf3a
ENSMOCG00000000587	1255.73	0.36	0.12	3.08	0.002	0.091	TRUE	Frmpd4
ENSMOCG00000001464	3097.46	-0.19	0.06	-3.09	0.002	0.091	TRUE	Psmc3
ENSMOCG00000001969	760.50	0.22	0.07	3.09	0.002	0.091	TRUE	Champ1
ENSMOCG00000003627	2398.94	0.17	0.06	3.08	0.002	0.091	TRUE	Tsc1
ENSMOCG00000003658	636.07	0.27	0.09	3.09	0.002	0.091	TRUE	Spast
ENSMOCG00000005201	11583.49	0.29	0.09	3.09	0.002	0.091	TRUE	Faim2
ENSMOCG00000005386	434.64	-0.41	0.13	-3.08	0.002	0.091	TRUE	NA
ENSMOCG00000007365	665.54	-0.31	0.10	-3.08	0.002	0.091	TRUE	Urm1
ENSMOCG00000012157	191.41	-0.48	0.16	-3.08	0.002	0.091	TRUE	Mapkapk3
ENSMOCG00000012337	1021.20	-0.41	0.13	-3.09	0.002	0.091	TRUE	Hebp1
ENSMOCG00000014778	1963.79	0.33	0.11	3.09	0.002	0.091	TRUE	Pde1a
ENSMOCG00000019979	973.25	-0.26	0.08	-3.08	0.002	0.091	TRUE	NA
ENSMOCG00000020090	235.45	0.44	0.14	3.09	0.002	0.091	TRUE	Zc3h12c
ENSMOCG00000021376	1971.31	0.48	0.16	3.08	0.002	0.091	TRUE	Slc24a2
ENSMOCG00000011714	1495.63	0.36	0.12	3.07	0.002	0.092	TRUE	Mga
ENSMOCG00000019551	1467.46	0.18	0.06	3.07	0.002	0.092	TRUE	NA
ENSMOCG00000004770	354.02	-0.51	0.17	-3.07	0.002	0.093	TRUE	Akr1c19
ENSMOCG00000020041	438.53	0.29	0.10	3.07	0.002	0.093	TRUE	Bbx
ENSMOCG00000003715	334.99	0.31	0.10	3.06	0.002	0.093	TRUE	Slc41a2
ENSMOCG00000014165	549.05	0.21	0.07	3.06	0.002	0.093	TRUE	Cdc73
ENSMOCG00000008492	6149.58	0.20	0.06	3.06	0.002	0.094	TRUE	Kif21a

ENSMOCG00000016642	2291.98	0.37	0.12	3.06	0.002	0.094	TRUE	Disp2
ENSMOCG00000013135	1279.65	-0.42	0.14	-3.05	0.002	0.095	TRUE	Commd3
ENSMOCG00000013679	2997.67	-0.43	0.14	-3.05	0.002	0.095	TRUE	NA
ENSMOCG00000001215	746.61	0.33	0.11	3.04	0.002	0.096	TRUE	NA
ENSMOCG00000001486	11243.78	-0.19	0.06	-3.03	0.002	0.096	TRUE	NA
ENSMOCG00000001493	361.86	-0.32	0.10	-3.04	0.002	0.096	TRUE	Psph
ENSMOCG00000001765	830.73	0.17	0.06	3.03	0.002	0.096	TRUE	Flcn
ENSMOCG00000003056	366.59	-0.44	0.14	-3.05	0.002	0.096	TRUE	2010111I01Rik
ENSMOCG00000005179	702.82	0.38	0.13	3.03	0.002	0.096	TRUE	Csmd3
ENSMOCG00000005728	691.82	-0.40	0.13	-3.03	0.002	0.096	TRUE	Commd10
ENSMOCG00000005839	2248.74	-0.33	0.11	-3.02	0.002	0.096	TRUE	Hexb
ENSMOCG00000006075	369.10	-0.31	0.10	-3.02	0.002	0.096	TRUE	NA
ENSMOCG00000008385	331.94	-2.10	0.69	-3.03	0.002	0.096	TRUE	NA
ENSMOCG00000011698	536.76	-0.24	0.08	-3.03	0.002	0.096	TRUE	NA
ENSMOCG00000013725	336.05	-0.27	0.09	-3.04	0.002	0.096	TRUE	Mfng
ENSMOCG00000015064	7152.36	0.26	0.09	3.03	0.002	0.096	TRUE	Ptprn2
ENSMOCG00000015655	3118.61	-0.26	0.09	-3.04	0.002	0.096	TRUE	Snn
ENSMOCG00000016250	834.72	0.34	0.11	3.03	0.002	0.096	TRUE	Slc6a6
ENSMOCG00000016266	3697.69	0.34	0.11	3.05	0.002	0.096	TRUE	Glg1
ENSMOCG00000017535	855.68	0.21	0.07	3.03	0.002	0.096	TRUE	Kdm6a
ENSMOCG00000017644	654.28	0.31	0.10	3.04	0.002	0.096	TRUE	Axin2
ENSMOCG00000021532	1898.22	-0.13	0.04	-3.03	0.002	0.096	TRUE	Dars
ENSMOCG00000022174	381.44	-0.27	0.09	-3.03	0.002	0.096	TRUE	Sdccag8
ENSMOCG00000011064	370.08	0.32	0.10	3.02	0.003	0.097	TRUE	Mblac2
ENSMOCG00000014558	764.74	-0.31	0.10	-3.02	0.003	0.097	TRUE	Pdzd11
ENSMOCG00000015231	2947.88	0.16	0.05	3.02	0.003	0.097	TRUE	Slc41a1
ENSMOCG00000002054	977.39	0.18	0.06	3.02	0.003	0.097	TRUE	Zc3h6
ENSMOCG00000000300	424.52	0.35	0.12	3.01	0.003	0.097	TRUE	Ago2

ENSMOCG00000004155	1640.21	-0.55	0.18	-3.01	0.003	0.097	TRUE	S100a1
ENSMOCG00000009516	1215.70	0.27	0.09	3.01	0.003	0.097	TRUE	Golgb1
ENSMOCG00000009693	215.70	-0.41	0.14	-3.01	0.003	0.097	TRUE	Ginm1
ENSMOCG00000009899	1165.76	-0.38	0.13	-3.01	0.003	0.097	TRUE	Acsf2
ENSMOCG00000011786	1144.50	-0.41	0.14	-3.01	0.003	0.097	TRUE	NA
ENSMOCG00000021019	621.03	-0.46	0.15	-3.01	0.003	0.097	TRUE	Gstz1
ENSMOCG00000009594	7072.02	0.28	0.09	3.00	0.003	0.098	TRUE	Huwe1
ENSMOCG00000002757	457.09	0.30	0.10	3.00	0.003	0.098	TRUE	Rpgrip1l
ENSMOCG00000005286	892.56	0.37	0.12	3.00	0.003	0.098	TRUE	Cntnap4
ENSMOCG00000014859	747.47	0.27	0.09	3.00	0.003	0.098	TRUE	NA
ENSMOCG00000018194	1417.14	0.39	0.13	3.00	0.003	0.098	TRUE	Kmt2a
ENSMOCG00000022190	2820.92	-0.25	0.08	-3.00	0.003	0.098	TRUE	Tsen34
ENSMOCG00000001428	4107.79	0.23	0.08	2.99	0.003	0.099	TRUE	Ube4b
ENSMOCG00000002379	420.54	-0.25	0.08	-2.99	0.003	0.099	TRUE	Exosc5
ENSMOCG00000003857	373.34	-0.25	0.08	-2.99	0.003	0.099	TRUE	NA
ENSMOCG00000005885	1623.92	0.26	0.09	2.99	0.003	0.099	TRUE	Bclaf1
ENSMOCG00000017042	2601.58	-0.19	0.06	-2.99	0.003	0.099	TRUE	Park7
ENSMOCG00000009737	702.37	-0.26	0.09	-2.99	0.003	0.099	TRUE	NA
ENSMOCG00000022401	1416.43	-0.39	0.13	-2.99	0.003	0.099	TRUE	Acadl
ENSMOCG00000000855	1492.30	0.40	0.13	2.97	0.003	0.099	TRUE	Stxbp5l
ENSMOCG00000001363	482.03	-0.39	0.13	-2.97	0.003	0.099	TRUE	Sdhaf2
ENSMOCG00000002035	5555.49	-0.30	0.10	-2.99	0.003	0.099	TRUE	Klhdc3
ENSMOCG00000002468	1249.49	-0.55	0.18	-2.98	0.003	0.099	TRUE	Rpl36a
ENSMOCG00000002473	364.22	-0.44	0.15	-2.97	0.003	0.099	TRUE	NA
ENSMOCG00000002649	286.90	0.27	0.09	2.96	0.003	0.099	TRUE	NA
ENSMOCG00000002873	587.28	0.52	0.17	2.97	0.003	0.099	TRUE	Dcc
ENSMOCG00000003318	1007.35	0.46	0.15	2.96	0.003	0.099	TRUE	Ptprt
ENSMOCG00000003604	732.39	-0.28	0.10	-2.98	0.003	0.099	TRUE	Mrpl16

ENSMOCG00000006150	1139.99	0.27	0.09	2.97	0.003	0.099	TRUE	Pbrm1
ENSMOCG00000006431	1856.64	0.19	0.06	2.96	0.003	0.099	TRUE	Tnfrsf21
ENSMOCG00000008665	304.60	0.37	0.12	2.97	0.003	0.099	TRUE	Xrn1
ENSMOCG00000008807	2107.07	0.33	0.11	2.97	0.003	0.099	TRUE	Dip2c
ENSMOCG00000009635	225.85	-0.81	0.27	-2.96	0.003	0.099	TRUE	NA
ENSMOCG00000010160	934.73	0.28	0.10	2.97	0.003	0.099	TRUE	Epm2aip1
ENSMOCG00000010333	2378.04	-0.25	0.08	-2.96	0.003	0.099	TRUE	Ppib
ENSMOCG00000010351	622.34	0.44	0.15	2.97	0.003	0.099	TRUE	Nexmif
ENSMOCG00000011394	2463.29	-0.26	0.09	-2.96	0.003	0.099	TRUE	NA
ENSMOCG00000012383	715.33	-0.32	0.11	-2.97	0.003	0.099	TRUE	NA
ENSMOCG00000013292	1795.57	0.22	0.07	2.97	0.003	0.099	TRUE	Crkl
ENSMOCG00000014097	1740.46	0.23	0.08	2.96	0.003	0.099	TRUE	Xpot
ENSMOCG00000014602	413.00	-0.38	0.13	-2.97	0.003	0.099	TRUE	Prdx4
ENSMOCG00000017782	1267.02	-0.19	0.07	-2.96	0.003	0.099	TRUE	NA
ENSMOCG00000018172	944.33	0.43	0.14	2.98	0.003	0.099	TRUE	Slc4a8
ENSMOCG00000019397	370.66	0.35	0.12	2.98	0.003	0.099	TRUE	Tet2
ENSMOCG00000019633	298.56	-0.28	0.10	-2.96	0.003	0.099	TRUE	Gemin7
ENSMOCG00000021212	2511.96	-0.19	0.06	-2.97	0.003	0.099	TRUE	Nelfb
ENSMOCG00000021510	1715.18	0.26	0.09	2.97	0.003	0.099	TRUE	Slc35e2
ENSMOCG00000021864	2830.53	0.13	0.05	2.97	0.003	0.099	TRUE	Cdc27
ENSMOCG00000020728	3678.48	-0.26	0.09	-2.96	0.003	0.099	TRUE	Eif3h

Table A.3: GO terms enriched in genes upregulated in MAN1 males.

ONT	ID	Description	pvalue	p.adjust	qvalue	Count
BP	GO:0007409	axonogenesis	1.89E-07	6.17E-04	5.54E-04	27
BP	GO:0009791	post-embryonic development	5.73E-07	7.67E-04	6.88E-04	12
BP	GO:0048638	regulation of developmental growth	8.02E-07	7.67E-04	6.88E-04	22
BP	GO:0050808	synapse organization	9.97E-07	7.67E-04	6.88E-04	27
BP	GO:0061564	axon development	1.30E-06	7.67E-04	6.88E-04	27
BP	GO:0007611	learning or memory	1.41E-06	7.67E-04	6.88E-04	20
BP	GO:0090066	regulation of anatomical structure size	3.96E-06	0.00184646	0.00165687	26
BP	GO:0050890	cognition	7.29E-06	0.00297096	0.00266591	20
BP	GO:0048639	positive regulation of developmental growth	1.37E-05	0.00494135	0.00443397	14
BP	GO:0050804	modulation of chemical synaptic transmission	1.65E-05	0.00494135	0.00443397	25
BP	GO:0099177	regulation of trans-synaptic signaling	1.71E-05	0.00494135	0.00443397	25
BP	GO:0060560	developmental growth involved in morphogenesis	1.82E-05	0.00494135	0.00443397	17
BP	GO:0007411	axon guidance	2.52E-05	0.0062435	0.00560242	15
BP	GO:0097485	neuron projection guidance	2.68E-05	0.0062435	0.00560242	15
BP	GO:0032535	regulation of cellular component size	3.74E-05	0.00813167	0.00729671	20
BP	GO:0019932	second-messenger-mediated signaling	4.71E-05	0.00957362	0.0085906	14
BP	GO:0050806	positive regulation of synaptic transmission	4.99E-05	0.00957362	0.0085906	13
BP	GO:0007612	learning	5.33E-05	0.00964689	0.00865635	13
BP	GO:0045927	positive regulation of growth	5.74E-05	0.00984314	0.00883245	16
BP	GO:2001223	negative regulation of neuron migration	6.60E-05	0.01075124	0.00964731	4
BP	GO:0050770	regulation of axonogenesis	9.32E-05	0.01446895	0.01298328	13
BP	GO:0008361	regulation of cell size	1.05E-04	0.01555458	0.01395743	13
BP	GO:0044728	DNA methylation or demethylation	1.14E-04	0.01614693	0.01448897	7
BP	GO:0051960	regulation of nervous system development	1.21E-04	0.01642474	0.01473825	23
BP	GO:0014068	positive regulation of phosphatidylinositol 3-kinase signaling	1.29E-04	0.01684902	0.01511896	7

BP	GO:0050772	positive regulation of axonogenesis	1.53E-04	0.01914509	0.01717927	9
BP	GO:0050767	regulation of neurogenesis	1.75E-04	0.02107221	0.01890852	20
BP	GO:0006814	sodium ion transport	1.85E-04	0.02135183	0.01915943	12
BP	GO:0006491	N-glycan processing	0.00018994	0.02135183	0.01915943	4
BP	GO:0048536	spleen development	2.20E-04	0.02387133	0.02142022	5
BP	GO:0051962	positive regulation of nervous system development	2.41E-04	0.02538307	0.02277673	17
BP	GO:0042391	regulation of membrane potential	2.67E-04	0.02672282	0.02397892	19
BP	GO:0014065	phosphatidylinositol 3-kinase signaling	2.71E-04	0.02672282	0.02397892	9
BP	GO:0010720	positive regulation of cell development	2.83E-04	0.02678538	0.02403506	17
BP	GO:0050769	positive regulation of neurogenesis	2.88E-04	0.02678538	0.02403506	15
BP	GO:0006304	DNA modification	3.21E-04	0.02867919	0.02573441	7
BP	GO:0060998	regulation of dendritic spine development	3.26E-04	0.02867919	0.02573441	8
BP	GO:0030516	regulation of axon extension	3.40E-04	0.02917917	0.02618305	9
BP	GO:0048675	axon extension	3.68E-04	0.03073424	0.02757845	10
BP	GO:0008217	regulation of blood pressure	4.18E-04	0.03409289	0.03059223	10
BP	GO:0044030	regulation of DNA methylation	4.29E-04	0.03409289	0.03059223	4
BP	GO:0006936	muscle contraction	4.42E-04	0.03428436	0.03076404	13
BP	GO:0035725	sodium ion transmembrane transport	4.55E-04	0.03452316	0.03097832	9
BP	GO:1990138	neuron projection extension	4.73E-04	0.03503152	0.03143448	12
BP	GO:0051048	negative regulation of secretion	5.05E-04	0.03634705	0.03261494	10
BP	GO:0001508	action potential	5.24E-04	0.03634705	0.03261494	9
BP	GO:0106027	neuron projection organization	5.24E-04	0.03634705	0.03261494	9
BP	GO:0098742	cell-cell adhesion via plasma-membrane adhesion molecules	5.75E-04	0.03779968	0.03391841	11
BP	GO:0060284	regulation of cell development	5.78E-04	0.03779968	0.03391841	22
BP	GO:0019226	transmission of nerve impulse	5.80E-04	0.03779968	0.03391841	7
BP	GO:0035637	multicellular organismal signaling	6.01E-04	0.03841364	0.03446933	9
BP	GO:0048167	regulation of synaptic plasticity	6.13E-04	0.03843766	0.03449088	13
BP	GO:0009100	glycoprotein metabolic process	6.38E-04	0.03920613	0.03518044	15

BP	GO:0050807	regulation of synapse organization	6.49E-04	0.03920613	0.03518044	14
BP	GO:0048266	behavioral response to pain	6.75E-04	0.03998521	0.03587953	4
BP	GO:0072577	endothelial cell apoptotic process	8.05E-04	0.04688861	0.04207409	5
BP	GO:0050803	regulation of synapse structure or activity	8.32E-04	0.04760802	0.04271963	14
BP	GO:0061387	regulation of extent of cell growth	8.89E-04	0.04996388	0.04483358	9
CC	GO:0034703	cation channel complex	3.44E-07	1.06E-04	8.04E-05	16
CC	GO:0034702	ion channel complex	1.67E-06	2.57E-04	1.95E-04	17
CC	GO:0032279	asymmetric synapse	4.49E-06	4.61E-04	3.50E-04	21
CC	GO:0098984	neuron to neuron synapse	1.15E-05	8.89E-04	6.74E-04	21
CC	GO:1990351	transporter complex	2.99E-05	0.00184118	0.00139693	18
CC	GO:0098793	presynapse	4.52E-05	0.00210769	0.00159913	23
CC	GO:0042734	presynaptic membrane	5.18E-05	0.00210769	0.00159913	11
CC	GO:1902495	transmembrane transporter complex	6.15E-05	0.00210769	0.00159913	17
CC	GO:0005901	caveola	6.16E-05	0.00210769	0.00159913	9
CC	GO:0014069	postsynaptic density	1.13E-04	0.00347253	0.00263466	18
CC	GO:0098797	plasma membrane protein complex	1.42E-04	0.00397565	0.00301639	20
CC	GO:0097060	synaptic membrane	1.59E-04	0.00397565	0.00301639	19
CC	GO:0043235	receptor complex	1.79E-04	0.00397565	0.00301639	16
CC	GO:0099572	postsynaptic specialization	2.04E-04	0.00397565	0.00301639	18
CC	GO:0045121	membrane raft	2.07E-04	0.00397565	0.00301639	17
CC	GO:0098857	membrane microdomain	2.07E-04	0.00397565	0.00301639	17
CC	GO:0044853	plasma membrane raft	3.57E-04	0.00611302	0.00463804	9
CC	GO:0099699	integral component of synaptic membrane	3.57E-04	0.00611302	0.00463804	9
CC	GO:0005581	collagen trimer	5.87E-04	0.00952039	0.00722326	6
CC	GO:0098982	GABA-ergic synapse	6.61E-04	0.01005819	0.0076313	7
CC	GO:0099240	intrinsic component of synaptic membrane	7.06E-04	0.01005819	0.0076313	9
CC	GO:0045211	postsynaptic membrane	7.18E-04	0.01005819	0.0076313	14
CC	GO:0034705	potassium channel complex	7.86E-04	0.01053046	0.00798962	7

CC	GO:0099061	integral component of postsynaptic density membrane	0.0012191	0.0151172	0.01146965	5
CC	GO:0099055	integral component of postsynaptic membrane	0.00127578	0.0151172	0.01146965	7
CC	GO:0008076	voltage-gated potassium channel complex	0.00132175	0.0151172	0.01146965	6
CC	GO:0150034	distal axon	0.0013662	0.0151172	0.01146965	16
CC	GO:0034704	calcium channel complex	0.00137429	0.0151172	0.01146965	5
CC	GO:0098839	postsynaptic density membrane	0.00144829	0.01522827	0.01155392	6
CC	GO:0031594	neuromuscular junction	0.00148327	0.01522827	0.01155392	7
CC	GO:0099146	intrinsic component of postsynaptic density membrane	0.00154357	0.01533615	0.01163576	5
CC	GO:0098936	intrinsic component of postsynaptic membrane	0.00171619	0.01612523	0.01223445	7
CC	GO:0099056	integral component of presynaptic membrane	0.0017277	0.01612523	0.01223445	5
CC	GO:0042383	sarcolemma	0.00190344	0.01724297	0.0130825	9
CC	GO:0005604	basement membrane	0.0019766	0.01739404	0.01319712	7
CC	GO:0044309	neuron spine	0.00230704	0.01970374	0.01494952	11
CC	GO:0033017	sarcoplasmic reticulum membrane	0.00236701	0.01970374	0.01494952	3
CC	GO:0098644	complex of collagen trimers	0.00296523	0.02403393	0.0182349	3
CC	GO:0098889	intrinsic component of presynaptic membrane	0.00349681	0.02761586	0.02095257	5
CC	GO:0033270	paranode region of axon	0.00364836	0.02809238	0.02131411	3
CC	GO:0044304	main axon	0.00407023	0.03057635	0.02319874	6
CC	GO:0043083	synaptic cleft	0.00528297	0.03874174	0.02939394	3
CC	GO:0043197	dendritic spine	0.00581563	0.04125755	0.03130272	10
CC	GO:0099634	postsynaptic specialization membrane	0.00606102	0.04125755	0.03130272	6
CC	GO:0043292	contractile fiber	0.00613507	0.04125755	0.03130272	9
CC	GO:0098978	glutamatergic synapse	0.00622246	0.04125755	0.03130272	14
CC	GO:0099060	integral component of postsynaptic specialization membrane	0.00629579	0.04125755	0.03130272	5
CC	GO:0030017	sarcomere	0.0071349	0.04578229	0.03473571	8
CC	GO:0098948	intrinsic component of postsynaptic specialization membrane	0.00732128	0.04601949	0.03491567	5
MF	GO:0046873	metal ion transmembrane transporter activity	2.64E-07	1.41E-04	1.24E-04	22
MF	GO:0005261	cation channel activity	1.32E-06	2.21E-04	1.95E-04	18

MF	GO:0022836	gated channel activity	1.42E-06	2.21E-04	1.95E-04	18
MF	GO:0005244	voltage-gated ion channel activity	2.32E-06	2.21E-04	1.95E-04	14
MF	GO:0022832	voltage-gated channel activity	2.52E-06	2.21E-04	1.95E-04	14
MF	GO:0005216	ion channel activity	2.66E-06	2.21E-04	1.95E-04	20
MF	GO:0022890	inorganic cation transmembrane transporter activity	2.90E-06	2.21E-04	1.95E-04	24
MF	GO:0008324	cation transmembrane transporter activity	4.56E-06	3.04E-04	2.68E-04	25
MF	GO:0015318	inorganic molecular entity transmembrane transporter activity	6.99E-06	3.90E-04	3.44E-04	26
MF	GO:0004888	transmembrane signaling receptor activity	7.32E-06	3.90E-04	3.44E-04	23
MF	GO:0015267	channel activity	8.93E-06	3.97E-04	3.49E-04	20
MF	GO:0022803	passive transmembrane transporter activity	8.93E-06	3.97E-04	3.49E-04	20
MF	GO:0030020	extracellular matrix structural constituent conferring tensile strength	1.01E-05	4.15E-04	3.66E-04	6
MF	GO:0038023	signaling receptor activity	1.39E-05	4.95E-04	4.36E-04	26
MF	GO:0060089	molecular transducer activity	1.39E-05	4.95E-04	4.36E-04	26
MF	GO:0022843	voltage-gated cation channel activity	2.20E-05	7.32E-04	6.45E-04	11
MF	GO:0015081	sodium ion transmembrane transporter activity	3.21E-05	0.00100486	8.85E-04	10
MF	GO:0005201	extracellular matrix structural constituent	2.31E-04	0.00685209	0.00603542	9
MF	GO:0005262	calcium channel activity	2.49E-04	0.00699412	0.00616052	8
MF	GO:0050839	cell adhesion molecule binding	3.84E-04	0.00985441	0.0086799	14
MF	GO:0005516	calmodulin binding	3.88E-04	0.00985441	0.0086799	11
MF	GO:0015079	potassium ion transmembrane transporter activity	6.88E-04	0.01666921	0.01468247	9
MF	GO:0015085	calcium ion transmembrane transporter activity	8.48E-04	0.01964506	0.01730364	8
MF	GO:0019199	transmembrane receptor protein kinase activity	0.00212291	0.04714631	0.04152711	6

Table A.4: GO terms enriched in genes downregulated in MAN1 males.

ONT	ID	Description	pvalue	p.adjust	qvalue	Count
BP	GO:0006119	oxidative phosphorylation	4.57E-18	1.44E-14	1.42E-14	29
BP	GO:0022904	respiratory electron transport chain	8.11E-16	1.28E-12	1.26E-12	24
BP	GO:0022900	electron transport chain	3.93E-15	3.30E-12	3.26E-12	24
BP	GO:0019646	aerobic electron transport chain	4.19E-15	3.30E-12	3.26E-12	19
BP	GO:0045333	cellular respiration	9.22E-15	5.56E-12	5.49E-12	34
BP	GO:0009060	aerobic respiration	1.06E-14	5.56E-12	5.49E-12	30
BP	GO:0002181	cytoplasmic translation	2.95E-14	1.33E-11	1.31E-11	22
BP	GO:0042773	ATP synthesis coupled electron transport	5.47E-14	2.15E-11	2.12E-11	20
BP	GO:0042775	mitochondrial ATP synthesis coupled electron transport	3.42E-13	1.20E-10	1.18E-10	19
BP	GO:0015980	energy derivation by oxidation of organic compounds	1.60E-12	5.02E-10	4.96E-10	37
BP	GO:0033108	mitochondrial respiratory chain complex assembly	7.88E-12	2.26E-09	2.23E-09	21
BP	GO:0046034	ATP metabolic process	9.75E-12	2.56E-09	2.53E-09	33
BP	GO:0010257	NADH dehydrogenase complex assembly	7.81E-11	1.76E-08	1.73E-08	16
BP	GO:0032981	mitochondrial respiratory chain complex I assembly	7.81E-11	1.76E-08	1.73E-08	16
BP	GO:0000028	ribosomal small subunit assembly	7.37E-10	1.55E-07	1.53E-07	9
BP	GO:0006091	generation of precursor metabolites and energy	3.30E-09	6.49E-07	6.42E-07	38
BP	GO:0042255	ribosome assembly	5.93E-08	1.10E-05	1.08E-05	13
BP	GO:0006120	mitochondrial electron transport, NADH to ubiquinone	4.55E-07	7.96E-05	7.87E-05	9
BP	GO:0007005	mitochondrion organization	8.06E-07	1.34E-04	1.32E-04	39
BP	GO:0042274	ribosomal small subunit biogenesis	4.35E-06	6.85E-04	6.77E-04	12
BP	GO:0006839	mitochondrial transport	7.45E-06	0.00111589	0.00110259	21
BP	GO:0006959	humoral immune response	1.16E-05	0.00166637	0.0016465	12
BP	GO:0071826	ribonucleoprotein complex subunit organization	3.95E-05	0.00534046	0.00527677	18
BP	GO:0002082	regulation of oxidative phosphorylation	4.07E-05	0.00534046	0.00527677	6
BP	GO:1990542	mitochondrial transmembrane transport	6.14E-05	0.00772345	0.00763136	12
BP	GO:0022618	ribonucleoprotein complex assembly	7.48E-05	0.00905216	0.00894422	17

BP	GO:0061844	antimicrobial humoral immune response mediated by antimicrobial peptide	1.08E-04	0.01256697	0.01241711	6
BP	GO:0002455	humoral immune response mediated by circulating immunoglobulin	3.58E-04	0.04025931	0.03977924	5
BP	GO:1903715	regulation of aerobic respiration	3.88E-04	0.04210437	0.04160229	6
BP	GO:0042254	ribosome biogenesis	4.65E-04	0.04877668	0.04819505	22
BP	GO:0019730	antimicrobial humoral response	4.83E-04	0.04900448	0.04842013	6
CC	GO:0022626	cytosolic ribosome	5.52E-41	2.24E-38	2.03E-38	41
CC	GO:0005840	ribosome	2.26E-37	4.59E-35	4.16E-35	57
CC	GO:0044391	ribosomal subunit	2.06E-36	2.78E-34	2.52E-34	52
CC	GO:0022625	cytosolic large ribosomal subunit	2.02E-25	2.04E-23	1.85E-23	23
CC	GO:0070469	respirasome	1.82E-23	1.47E-21	1.33E-21	31
CC	GO:0005743	mitochondrial inner membrane	1.23E-22	8.32E-21	7.54E-21	63
CC	GO:0098803	respiratory chain complex	3.51E-21	2.03E-19	1.84E-19	28
CC	GO:0019866	organelle inner membrane	8.40E-21	4.25E-19	3.86E-19	63
CC	GO:0098798	mitochondrial protein-containing complex	5.30E-20	2.27E-18	2.06E-18	47
CC	GO:0022627	cytosolic small ribosomal subunit	5.59E-20	2.27E-18	2.06E-18	19
CC	GO:0015934	large ribosomal subunit	2.17E-19	7.97E-18	7.23E-18	29
CC	GO:0098800	inner mitochondrial membrane protein complex	2.50E-19	8.44E-18	7.66E-18	33
CC	GO:0005746	mitochondrial respirasome	3.71E-19	1.16E-17	1.05E-17	26
CC	GO:0015935	small ribosomal subunit	1.14E-18	3.30E-17	2.99E-17	24
CC	GO:0042788	polysomal ribosome	2.56E-14	6.91E-13	6.27E-13	14
CC	GO:0005747	mitochondrial respiratory chain complex I	4.18E-13	9.40E-12	8.52E-12	17
CC	GO:0030964	NADH dehydrogenase complex	4.18E-13	9.40E-12	8.52E-12	17
CC	GO:0045271	respiratory chain complex I	4.18E-13	9.40E-12	8.52E-12	17
CC	GO:1990204	oxidoreductase complex	1.17E-11	2.50E-10	2.27E-10	22
CC	GO:0005844	polysome	3.57E-10	7.23E-09	6.56E-09	16
CC	GO:0070069	cytochrome complex	2.41E-09	4.64E-08	4.21E-08	11
CC	GO:0045277	respiratory chain complex IV	5.46E-08	1.01E-06	9.12E-07	8

CC	GO:0000313	organellar ribosome	3.44E-05	5.80E-04	5.26E-04	13
CC	GO:0005761	mitochondrial ribosome	3.44E-05	5.80E-04	5.26E-04	13
CC	GO:0005759	mitochondrial matrix	4.14E-05	6.70E-04	6.08E-04	24
CC	GO:0005751	mitochondrial respiratory chain complex IV	4.18E-04	0.00651787	0.00591225	4
CC	GO:0005750	mitochondrial respiratory chain complex III	6.37E-04	0.00921484	0.00835862	4
CC	GO:0045275	respiratory chain complex III	6.37E-04	0.00921484	0.00835862	4
CC	GO:0000153	cytoplasmic ubiquitin ligase complex	0.00175809	0.0245526	0.02227124	4
CC	GO:1902495	transmembrane transporter complex	0.00211883	0.02860414	0.02594632	21
CC	GO:1990351	transporter complex	0.00342721	0.0447748	0.04061444	21
MF	GO:0003735	structural constituent of ribosome	1.96E-41	1.05E-38	1.01E-38	52
MF	GO:0005198	structural molecule activity	8.68E-21	2.32E-18	2.23E-18	59
MF	GO:0015453	oxidoreduction-driven active transmembrane transporter activity	9.73E-20	1.73E-17	1.67E-17	22
MF	GO:0009055	electron transfer activity	1.95E-16	2.60E-14	2.51E-14	22
MF	GO:0015399	primary active transmembrane transporter activity	1.16E-12	1.24E-10	1.20E-10	26
MF	GO:0019843	rRNA binding	1.95E-11	1.74E-09	1.68E-09	18
MF	GO:0004129	cytochrome-c oxidase activity	3.09E-10	2.36E-08	2.27E-08	9
MF	GO:0016655	oxidoreductase activity, acting on NAD(P)H, quinone or similar compound as acceptor	7.23E-10	4.43E-08	4.27E-08	12
MF	GO:0016675	oxidoreductase activity, acting on a heme group of donors	7.47E-10	4.43E-08	4.27E-08	9
MF	GO:0008137	NADH dehydrogenase (ubiquinone) activity	1.68E-09	8.14E-08	7.85E-08	10
MF	GO:0050136	NADH dehydrogenase (quinone) activity	1.68E-09	8.14E-08	7.85E-08	10
MF	GO:0003954	NADH dehydrogenase activity	5.07E-09	2.26E-07	2.18E-07	10
MF	GO:0003955	NAD(P)H dehydrogenase (quinone) activity	8.40E-09	3.45E-07	3.32E-07	10
MF	GO:0015078	proton transmembrane transporter activity	9.80E-09	3.74E-07	3.60E-07	17
MF	GO:0016651	oxidoreductase activity, acting on NAD(P)H	9.63E-07	3.43E-05	3.30E-05	12
MF	GO:0022804	active transmembrane transporter activity	1.21E-06	4.03E-05	3.89E-05	28
MF	GO:0004602	glutathione peroxidase activity	2.77E-06	8.69E-05	8.38E-05	7
MF	GO:0004601	peroxidase activity	4.05E-06	1.20E-04	1.16E-04	9

MF	GO:0016684	oxidoreductase activity, acting on peroxide as acceptor	1.10E-05	3.08E-04	2.97E-04	9
MF	GO:0016209	antioxidant activity	4.25E-05	0.00113452	0.0010936	10
MF	GO:0004857	enzyme inhibitor activity	2.49E-04	0.00633764	0.00610902	8
MF	GO:0022853	active ion transmembrane transporter activity	3.62E-04	0.00879157	0.00847443	16
MF	GO:0016846	carbon-sulfur lyase activity	5.93E-04	0.01376634	0.01326974	4
MF	GO:0000062	fatty-acyl-CoA binding	8.21E-04	0.01825929	0.01760062	5
MF	GO:0044548	S100 protein binding	8.62E-04	0.01841835	0.01775393	4
MF	GO:1901567	fatty acid derivative binding	0.00104313	0.02142419	0.02065134	5
MF	GO:0120227	acyl-CoA binding	0.00161798	0.03126239	0.03013465	5
MF	GO:0016863	intramolecular oxidoreductase activity, transposing C=C bonds	0.00163923	0.03126239	0.03013465	4
MF	GO:0046933	proton-transporting ATP synthase activity, rotational mechanism	0.00216743	0.03858028	0.03718856	4
MF	GO:0055106	ubiquitin-protein transferase regulator activity	0.00216743	0.03858028	0.03718856	4

Table A.5: KEGG pathways enriched in differentially expressed genes in males.				
ID	Description	pvalue	p.adjust	qvalues
mmu00190	Oxidative phosphorylation	1.00E-10	6.30E-09	3.62E-09
mmu03010	Ribosome	1.00E-10	6.30E-09	3.62E-09
mmu04714	Thermogenesis	1.00E-10	6.30E-09	3.62E-09
mmu05012	Parkinson disease	1.00E-10	6.30E-09	3.62E-09
mmu05208	Chemical carcinogenesis - reactive oxygen species	1.00E-10	6.30E-09	3.62E-09
mmu04080	Neuroactive ligand-receptor interaction	1.18E-10	6.30E-09	3.62E-09
mmu05020	Prion disease	2.20E-10	1.00E-08	5.75E-09
mmu05415	Diabetic cardiomyopathy	1.01E-09	4.01E-08	2.30E-08
mmu05171	Coronavirus disease - COVID-19	2.03E-09	7.19E-08	4.13E-08
mmu04020	Calcium signaling pathway	2.66E-09	8.50E-08	4.88E-08
mmu04360	Axon guidance	6.18E-09	1.79E-07	1.03E-07
mmu04932	Non-alcoholic fatty liver disease	1.55E-08	4.11E-07	2.36E-07
mmu04512	ECM-receptor interaction	2.27E-08	5.57E-07	3.20E-07
mmu05033	Nicotine addiction	3.17E-08	7.21E-07	4.14E-07
mmu04713	Circadian entrainment	1.66E-07	3.53E-06	2.03E-06
mmu04514	Cell adhesion molecules	1.96E-07	3.91E-06	2.25E-06
mmu05414	Dilated cardiomyopathy	2.44E-07	4.58E-06	2.63E-06
mmu04742	Taste transduction	1.23E-06	2.18E-05	1.25E-05
mmu04024	cAMP signaling pathway	2.26E-06	3.79E-05	2.18E-05
mmu04725	Cholinergic synapse	2.70E-06	4.30E-05	2.47E-05
mmu03050	Proteasome	4.75E-06	7.22E-05	4.15E-05
mmu05412	Arrhythmogenic right ventricular cardiomyopathy	7.53E-06	1.09E-04	6.27E-05
mmu04727	GABAergic synapse	1.05E-05	1.42E-04	8.13E-05
mmu04151	PI3K-Akt signaling pathway	1.11E-05	1.42E-04	8.13E-05
mmu05204	Chemical carcinogenesis - DNA adducts	1.11E-05	1.42E-04	8.13E-05
mmu05410	Hypertrophic cardiomyopathy	1.20E-05	1.47E-04	8.46E-05

mmu00980	Metabolism of xenobiotics by cytochrome P450	1.43E-05	1.69E-04	9.70E-05
mmu04925	Aldosterone synthesis and secretion	1.58E-05	1.80E-04	1.03E-04
mmu04930	Type II diabetes mellitus	2.16E-05	2.38E-04	1.37E-04
mmu05032	Morphine addiction	2.38E-05	2.54E-04	1.46E-04
mmu04961	Endocrine and other factor-regulated calcium reabsorption	3.09E-05	3.10E-04	1.78E-04
mmu04927	Cortisol synthesis and secretion	3.11E-05	3.10E-04	1.78E-04
mmu04970	Salivary secretion	3.21E-05	3.10E-04	1.78E-04
mmu04010	MAPK signaling pathway	4.98E-05	4.57E-04	2.62E-04
mmu04510	Focal adhesion	5.01E-05	4.57E-04	2.62E-04
mmu04974	Protein digestion and absorption	6.97E-05	6.17E-04	3.54E-04
mmu04960	Aldosterone-regulated sodium reabsorption	1.05E-04	9.04E-04	5.19E-04
mmu04724	Glutamatergic synapse	1.37E-04	0.00114735	6.59E-04
mmu04261	Adrenergic signaling in cardiomyocytes	1.44E-04	0.00115291	6.62E-04
mmu04540	Gap junction	1.45E-04	0.00115291	6.62E-04
mmu04130	SNARE interactions in vesicular transport	1.58E-04	0.00122585	7.04E-04
mmu00260	Glycine, serine and threonine metabolism	1.82E-04	0.00136777	7.85E-04
mmu05205	Proteoglycans in cancer	1.84E-04	0.00136777	7.85E-04
mmu04934	Cushing syndrome	2.19E-04	0.00158626	9.11E-04
mmu04550	Signaling pathways regulating pluripotency of stem cells	2.42E-04	0.00170503	9.79E-04
mmu04915	Estrogen signaling pathway	2.46E-04	0.00170503	9.79E-04
mmu01240	Biosynthesis of cofactors	3.30E-04	0.00224185	0.00128719
mmu04022	cGMP-PKG signaling pathway	3.71E-04	0.00244293	0.00140264
mmu04520	Adherens junction	3.75E-04	0.00244293	0.00140264
mmu04310	Wnt signaling pathway	3.88E-04	0.0024778	0.00142266
mmu04012	ErbB signaling pathway	4.25E-04	0.00265973	0.00152712
mmu00534	Glycosaminoglycan biosynthesis - heparan sulfate / heparin	4.60E-04	0.00282072	0.00161955
mmu04726	Serotonergic synapse	4.82E-04	0.00290061	0.00166542
mmu04270	Vascular smooth muscle contraction	5.32E-04	0.00314534	0.00180594

mmu04929	GnRH secretion	6.24E-04	0.00357301	0.00205149
mmu00982	Drug metabolism - cytochrome P450	6.27E-04	0.00357301	0.00205149
mmu04340	Hedgehog signaling pathway	7.86E-04	0.00439878	0.00252562
mmu00983	Drug metabolism - other enzymes	8.34E-04	0.00458916	0.00263492
mmu05206	MicroRNAs in cancer	8.81E-04	0.00476527	0.00273604
mmu01522	Endocrine resistance	9.04E-04	0.00480376	0.00275814
mmu00280	Valine, leucine and isoleucine degradation	9.68E-04	0.0050616	0.00290618
mmu04940	Type I diabetes mellitus	0.00105217	0.00541358	0.00310827
mmu04935	Growth hormone synthesis, secretion and action	0.00114032	0.00577399	0.00331521
mmu04750	Inflammatory mediator regulation of TRP channels	0.00130132	0.00648626	0.00372417
mmu04911	Insulin secretion	0.00132543	0.00650479	0.00373481
mmu00040	Pentose and glucuronate interconversions	0.00138604	0.00669921	0.00384644
mmu04070	Phosphatidylinositol signaling system	0.00148437	0.00706736	0.00405781
mmu04921	Oxytocin signaling pathway	0.00171247	0.0080335	0.00461254
mmu00340	Histidine metabolism	0.00198738	0.00918802	0.00527542
mmu04213	Longevity regulating pathway - multiple species	0.00217729	0.00992224	0.00569698
mmu04918	Thyroid hormone synthesis	0.00232024	0.01042476	0.00598551
mmu05224	Breast cancer	0.00237823	0.01053689	0.00604989
mmu00330	Arginine and proline metabolism	0.00256237	0.01119718	0.00642901
mmu01521	EGFR tyrosine kinase inhibitor resistance	0.00289272	0.01246997	0.00715979
mmu04211	Longevity regulating pathway	0.00315238	0.01340811	0.00769844
mmu04730	Long-term depression	0.00325513	0.01366299	0.00784478
mmu05031	Amphetamine addiction	0.00338447	0.01384353	0.00794844
mmu04924	Renin secretion	0.00338494	0.01384353	0.00794844
mmu04971	Gastric acid secretion	0.0034707	0.0140146	0.00804666
mmu00760	Nicotinate and nicotinamide metabolism	0.0038877	0.0155022	0.00890078
mmu05200	Pathways in cancer	0.00413123	0.01626992	0.00934158
mmu04015	Rap1 signaling pathway	0.00429889	0.01672374	0.00960215

mmu04350	TGF-beta signaling pathway	0.00477374	0.01795202	0.01030738
mmu04919	Thyroid hormone signaling pathway	0.00479047	0.01795202	0.01030738
mmu05215	Prostate cancer	0.00485998	0.01795202	0.01030738
mmu04978	Mineral absorption	0.00488966	0.01795202	0.01030738
mmu04972	Pancreatic secretion	0.00489601	0.01795202	0.01030738
mmu05320	Autoimmune thyroid disease	0.00565547	0.0199504	0.01145478
mmu05330	Allograft rejection	0.00565547	0.0199504	0.01145478
mmu05332	Graft-versus-host disease	0.00565547	0.0199504	0.01145478
mmu04720	Long-term potentiation	0.00572924	0.0199504	0.01145478
mmu05202	Transcriptional misregulation in cancer	0.00575372	0.0199504	0.01145478
mmu00020	Citrate cycle (TCA cycle)	0.00604874	0.02074782	0.01191262
mmu00910	Nitrogen metabolism	0.00636019	0.02148208	0.01233421
mmu04150	mTOR signaling pathway	0.00639748	0.02148208	0.01233421
mmu05165	Human papillomavirus infection	0.00754114	0.02505859	0.01438771
mmu00071	Fatty acid degradation	0.00770137	0.02530405	0.01452864
mmu04260	Cardiac muscle contraction	0.00777366	0.02530405	0.01452864
mmu04916	Melanogenesis	0.00810563	0.02611814	0.01499606
mmu04926	Relaxin signaling pathway	0.00874761	0.02790487	0.01602194
mmu04146	Peroxisome	0.0088929	0.02808747	0.01612678
mmu00120	Primary bile acid biosynthesis	0.00962464	0.03010058	0.01728263
mmu03040	Spliceosome	0.00991292	0.03070118	0.01762747
mmu05231	Choline metabolism in cancer	0.01041259	0.03166347	0.01817998
mmu00480	Glutathione metabolism	0.0104336	0.03166347	0.01817998
mmu05322	Systemic lupus erythematosus	0.0105214	0.03166347	0.01817998
mmu05150	Staphylococcus aureus infection	0.01112437	0.03295262	0.01892016
mmu05207	Chemical carcinogenesis - receptor activation	0.01115637	0.03295262	0.01892016
mmu03060	Protein export	0.01132934	0.03315652	0.01903724
mmu05030	Cocaine addiction	0.01164018	0.03375653	0.01938174

mmu00520	Amino sugar and nucleotide sugar metabolism	0.01443936	0.0414969	0.02382597
mmu04740	Olfactory transduction	0.01463131	0.0416731	0.02392714
mmu04728	Dopaminergic synapse	0.01665035	0.04700408	0.02698799
mmu04371	Apelin signaling pathway	0.01692437	0.04735855	0.02719151
mmu04976	Bile secretion	0.01776361	0.04927471	0.0282917